Universitat Politecnica de Catalunya

Tesi doctoral

Analysis of night-time climate in plastic-covered greenhouses

Davide Piscia

Terrassa, desembre 2012

Analysis of night-time climate in plastic-covered greenhouses

Davide Piscia

Tesi Doctoral

Presentada al

Departament de Màquines i Motors Tèrmics

E.T.S.E.I.A.T.

Universitat Politecnica de Catalunya

Per a optar al grau de Doctor

Terrassa, desembre 2012

Director de la tesis:

Doctor Juan Ignacio Montero

Ponente de la tesis:

Professor Assensi Oliva Llena

Acta de qualificació de tesi doctoral

Curs acadèmic:

Nom i cognoms

DNI / NIE / Passaport

Programa de doctorat

Unitat estructural responsable del programa

Resolució del Tribunal

Reunit el Tribunal designat a l'efecte, el doctorand / la doctoranda exposa el tema de la seva tesi doctoral titulada _____

_____.

Acabada la lectura i després de donar resposta a les qüestions formulades pels membres titulars del tribunal, aquest atorga la qualificació:

☐ APTA/E ☐ NO APTA/E

(Nom, cognoms i signatura) President/a		(Nom, cognoms i signatura) Secretari/ària
(Nom, cognoms i signatura) Vocal	(Nom, cognoms i signatura) Vocal	(Nom, cognoms i signatura) Vocal

_____, _____ d'/de _____ de _____

El resultat de l'escrutini dels vots emesos pels membres titulars del tribunal, efectuat per l'Escola de Doctorat, a instància de la Comissió de Doctorat de la UPC, atorga la MENCIÓ CUM LAUDE:

☐ SI ☐ NO

(Nom, cognoms i signatura) Presidenta de la Comissió de Doctorat	(Nom, cognoms i signatura) Secretària de la Comissió de Doctorat

Barcelona, _____ d'/de _____ de _____

Ringraziamenti

Desidero ringraziare in primo luogo il dottor Juan Ignacio per il suo inestimabile aiuto e supporto, e per avermi dato l'occasione di svolgere questo lavoro di ricerca. Questi anni mi hanno insegnato il valore della precisione, della metodologia e della scienzia.

Voglio ringraziare il Professore Oliva per la comprensione e l'ospitalitá (nel programma di dottorato da lui diretto).

Ringrazio il Dottor Bailey per l'aiuto nella fase di redazione degli articoli, e per non avermi mai denunciato alle autoritá inglesi per le mie frasi contorte scritte in un ipotetico inglese.

Ringrazio inoltre i colleghi di lavoro che ho trovato e tuttora trovo nel dipartamento di ingegneria dell'orticultura, Pere, Assuncio, le Marte, Montze, Ileana, Jorge, Pepe y Mari Carmen.

Ringrazio l'IRTA e l'INIA che mi hanno fornito i mezzi e i servizi per svolgere in tuttá normalita la ricerca.

Ringrazio la mia famiglia per la pazienza mostrata e la comprensione verso l'ennesima tappa universitaria.

In fine, ringrazio le persone che hanno sopportato tutto il peso delle mie continue critiche e dubbi al riguardo del perché fare un dottorato e non prendere un altro cammino. Parlo di mia moglie, Iris, mia figlia Noa e del prossima bimba che verrá a farci compagnia presto, Erica.

Summary

This work studied night-time greenhouse climate. The focus was on unheated plastic greenhouses and analyses were carried out using CFD models, Energy balance (ES) models and experimental data. The aims were twofold: on the one hand, it was intended to analyse and understand night-time greenhouse climate and propose solutions to the high-humidity issue. On the other hand, the aim was to investigate novel simulation approaches based on the coupling of CFD and ES models as well as the use of optimisation algorithms to study greenhouse climate.

Chapter 1 is an introductory chapter which includes the general context and overall research objectives. **Chapter 2** studies night-time climate in single-layer greenhouses by means of CFD. The model is validated and condensation User Defined Function (UDF) is introduced which accounted for the condensation rate found on the inner face of the greenhouse cover. **Chapter 3** studies a commonly used solution to the issue of low night-time temperature. A thermal screen was analysed by means of CFD simulations. A thorough comparison was made between single-layer and screened greenhouses and detailed information was provided in order to build a framework for taking decisions as to whether to use a screen or not. **Chapter 4** introduces a novel approach to optimizing greenhouse design; the approach relies on two optimization algorithms linked to an ES model which was coupled to a CFD model. The aim of the study was twofold: on the one hand to introduce a method offering a general approach for optimizing greenhouse design and on the other, to attempt to solve one of the issues highlighted in Chapter 2. It was shown that using a highly reflective covering material would have a theoretically significant impact on greenhouse performance. **Chapter 5** introduces a coupled model for studying greenhouse climate. The CFD was used to provide the ventilation rate and convective coefficients for the ES model. This approach was applied to study the effects of different ventilation strategies on humidity under different outside air conditions. Finally **Chapter 6** summarizes the conclusions and proposes themes for future research.

Resumen

Este trabajo analiza el clima nocturno del invernadero. EL objeto del estudio es el invernadero de plástico sin calefacción, cuyo clima se estudia utilizando modelos CFD, modelos basados en los balance de energía (ES) y s datos experimentales. El fin es doble, por un lado se trata de analizar y comprender el clima nocturno del invernadero, y proponer soluciones a los problemas relacionados con las altas tasas de humedad. Por otro lado se investigan nuevos métodos de simulación del clima del invernadero, métodos basados en el uso conjunto o acoplamiento de modelos CFD y ES , y también basados en la técnica de optimización.

El **Capitulo 1** introduce el contexto general y los objetivos que plantea el trabajo. El **Capitulo 2** estudia el clima nocturno en un invernadero de capa sencilla. Para ello desarrolla un modelo CFD que incluye una UDF (User Define Function) para calcular la tasa de condensación. Una vez validado el modelo se analiza el comportamiento del invernadero bajo distintas condiciones de contorno.. El **Capitulo 3** analiza una solución para combatir las bajas temperaturas nocturnas, la pantalla térmica. Los efectos de la pantalla se analizan mediante el uso del CFD. Se lleva a cabo una comparación completa entre el invernadero de capa sencilla y el invernadero con pantalla. El capitulo proporciona información detallada sobre el clima del invernadero y presenta un estudio paramétrico del efecto de la temperatura equivalente del cielo y la cesión de calor desde el suelo en el clima del invernadero con pantalla térmica. EL **Capitulo 4** presenta un nuevo método para optimizar el diseño del invernadero. El método se basa en el acoplamiento de dos algoritmos de optimización que operan con el modelo ES. A su vez el modelo ES está conectado con el modelo CFD. El objetivo es doble, por un lado introducir una nueva manera de optimizar el diseño del invernadero, y por el otro lado tratar de resolver uno de los problemas evidenciados en el capítulo 2. El resultado muestra que un material de cubierta de alto poder de reflexión del infrarrojo lejano aportaría mejorías relevantes al clima del invernadero. El **Capitulo 5** presenta un modelo acoplado para el estudio del clima del invernadero. EL CFD se utiliza para proporcionar las tasas de ventilación y los coeficientes convectivos al modelo ES. Esta técnica se utiliza para estudiar los efectos de diferentes estrategias de ventilación sobre el régimen de humedad con diferentes condiciones externas. Finalmente, el **Capitulo 6** resume las conclusiones y propone algunos temas para futuras investigaciones.

Table of contents

1 Introduction

1.1 Foreword

The present challenge for the greenhouse industry is to provide an environment which is optimal for crop development. A greenhouse provides protection against insects, pests and extreme climate conditions such as heavy rain, strong winds and low temperatures.
According to recent studies (Giacomelli, Castilla, Van Henten, Mears, & Sase, 2008), there are more than 692,350 ha of plastic greenhouses in the world (48,250 ha of glasshouses), of which plastic greenhouses cover about 140,000 ha in Western Europe. Most Western European plastic greenhouses are located in coastal areas of Southern Europe, where the air temperature and solar radiation are higher than in Northern Europe. Under favourable outside air conditions, plastic covered greenhouses are fairly simple and offer little climate control. During hot periods, greenhouse climate is essentially controlled by means of natural ventilation (Baeza, Pèrez-Parra, Montero, Bailey, Lòpez, & Gàzquez, 2007). During cold periods, there is no means of climate control since the majority of plastic greenhouses are unheated.

1.2 The issue of low temperature and high humidity

A lack of available heating devices makes regulating greenhouse climate a significant problem. Indeed, during the cold season, night-time greenhouse climates are typified by low temperatures, high humidity and condensation.
Controlling excessive humidity is one of the most important issues with regard to greenhouse climate during the winter period; high relative humidity (RH) and the presence of free water on plant surfaces have been shown to favour the development of fungal diseases (Baptista, 2012). Growers have been recommended to combine ventilation and heating to reduce relative humidity and thereby prevent condensation, but natural ventilation is difficult to control. However, combining heating and ventilation results in high energy consumption and greenhouse climate heterogeneity (Campen, Kempkes, & Bot, 2009). Moreover, as previously mentioned, most Mediterranean greenhouses are unheated, so other methods must be found to reduce greenhouse humidity.

In greenhouses the humidity regime is the result of the water vapour balance between different sources, such as plant transpiration and soil evaporation, and sinks, such as ventilation, dehumidification and condensation.

One of the terms in the mass balance equation for water vapour that has received least attention is condensation, possibly because it is difficult to measure the condensed water in a greenhouse, but also because most commercial CFD packages do not explicitly include a calculation for condensation rate. Nevertheless, roof condensation is an important sink for air humidity, particularly in unheated greenhouses under clear-night sky conditions, when the cover is usually the coldest part of the greenhouse.

High humidity and low temperatures are intrinsically related; indeed, an indirect way to reduce high humidity is to increase greenhouse temperature. In this respect, one technique commonly used to increase night-time temperature is to use a thermal screen. Since the 1970s, screens of different types have been used to conserve energy in heated greenhouses. During the period 1978 to 1988, scientific literature particularly addressed to the study of thermal screens focused not only on their energy saving effects, but also on how thermal screens affected humidity, although condensation received little attention.

In addition to thermal screens, another possible way to increase greenhouse temperature involved selecting the cover material in order to reduce the heat loss attributable to radiative exchange.

From a heat transfer point of view, one major consideration when not heating a greenhouse is that while convective heat exchange is the most relevant heat transfer process in heated greenhouses, in unheated ones, radiative exchanges tend to prevail. This effect is particularly evident on clear nights when greenhouse air temperatures may be lower than those of the outside air. This effect is caused by the greenhouse cover emitting more infrared radiation than it receives from the sky.

1.3 Models for greenhouse climate simulations

A greenhouse is a complex ecosystem in which several different physical phenomena take place: transpiration, condensation, ventilation, leakage, etc. Greenhouses may be equipped with several devices, including heating, dehumidification and cooling systems. Their performances have to be calculated for the climatic conditions of each season, remembering to allow for continuously changing external conditions. The enormous variety of boundary conditions and design elements makes analysing greenhouse climate a complex task.

Simulation tools are an indispensable support for greenhouse climate studies because they make it possible to take all of these characteristics into account.

The most commonly used simulation techniques are the CFD and energy balance simulation (ES) models.

1.3.1 CFD

CFD solves a set of non-linear partial differential equations using numerical techniques. The partial differential equations represent the fundamental physical laws that govern fluid flow and related phenomena: the conservation of mass, momentum, and energy.

The conservation equation reads:

$$\frac{\partial \varphi}{\partial t} + \nabla \cdot \varphi \vec{v} = \nabla \cdot \left(\Gamma_{\varphi} \nabla \varphi \right) + S_{\varphi} \qquad (1.1)$$

Where $\vec{v}$ is the velocity vector, Γ_{φ} is the diffusion coefficient and S_{φ} is the source term.

A general description of the application of CFD in greenhouse studies is given by Boulard, Kittas, Roy and Wang (2002).

The equations are discretized and linearized according to the numerical schemes used, and the computational domain delimited by their boundary conditions.

This process creates a set of matrixes which are solved iteratively to predict (at discrete points) the distribution of pressure, temperature, and velocity.

Computational fluid dynamics is a simulation technique that can efficiently develop both spatial and temporal field solutions for fluid pressure, temperature and velocity, and has already proven its effectiveness in system design and optimisation within the chemical, aerospace, and hydrodynamic industries.

The CFD technique is extremely useful for simulating situations in which the airflow component plays an important role. It was for this reason that the technique was used to study greenhouse climate. In a greenhouse climate study, the inside environmental conditions are dependent on the performance of the ventilation phenomena. As a consequence, indoor environmental parameters such as temperature, pollution and humidity are also governed by airflow patterns. An understanding of the principles of air motion is therefore necessary in order to correctly study the greenhouse environment.

The main drawback of CFD is the high cost in terms of computational requirements. This limits its application to the simulation of short periods and to the exploration of a limited set of possible scenarios.

1.3.2 Energy balance models

Energy balance simulation is based on the resolution of heat and mass balance equations applied to the whole greenhouse system.

Heat balance of greenhouse air

$$\frac{\rho V c_p \Delta T}{\Delta t} = \sum_i q_i A_i + \Phi(c_p T_{out} - c_p T_{in}) \quad (1.2)$$

Mass Balance of greenhouse air

$$\frac{M_w}{\partial t} = \Gamma_{crop} - \Omega_{\text{cov}} + \Phi(w_{air} - w_{air\_ou}) \quad (1.3)$$

Where ρ is the density, t is the time, T is the temperature, c_p is the heat capacity at constant pressure, Φ is the ventilation rate (Kg s^{-1}) and W (Kg m^{-3}), $\sum_i q_i A_i$ (W) is the sum of the convective contribution, Γ_{crop} (Kg s^{-1}) is the transpiration rate, w_{air} (kg kg^{-1}) is the inside humidity ratio, $w_{air\_outside}$ (kg kg^{-1}) is the outside humidity ratio and M_w is the water vapour mass.

ES, which is also referred to as a perfectly stirred tank in greenhouse literature (Roy, Boulard, Kittas, & Wang, 2002), is based on the assumption of the uniformity/homogeneity of greenhouse variables (such as temperature and humidity). On the one hand, this assumption makes ES computationally fast and straightforward to implement, but on the other, it is the source of certain limitations. ES calculation requires some priori and empirical knowledge of different coefficients such as the ventilation rate and convective coefficients.

Indeed, the ventilation rate for the greenhouse ES model can be computed using Bernoulli equations and values from semi-empirical formulas. The parameters of these semi-empirical equations were either derived through direct determination of the discharge coefficients or by

in situ determination (by regressing an overall coefficient of wind efficiency or ventilation to measure the air exchange rate).

The convective heat transfer is governed by a combination of forced convection, due to wind pressure, and free convection, due to the buoyancy forces caused by differences in temperature between the solid surfaces of the walls, the soil, the plants and the air. As a consequence, the convective coefficients are dependent on the type of greenhouse in question, the outside climate and the ventilation conditions. This strong dependence on several different factors makes it difficult to choose which convective coefficients to use.

1.4 Research objectives

The research objectives can be grouped into two categories. The first relates to the study of night-time greenhouse climate and an assessment of the impact of different humidity control strategies. The specific aims are:

- To study night–time greenhouse climate in terms of temperature, humidity and condensation in order to establish a reference situation
- To study the effects of using a thermal screen in terms of temperature, humidity and condensation
- To study the properties and effects of cover properties in terms of temperature, humidity and condensation
- To study the effects of nocturnal ventilation on greenhouse climate variables

The second category includes objectives related to the use of the ES and CFD techniques:

- To propose an optimization process based on ES and CFD and to apply such a process in order to find the optimal greenhouse cover in terms of far infrared optical properties
- To propose a novel methodology for greenhouse analysis based on coupling the ES and CFD models

1.5 Thesis outlines

The core of the thesis consists of four chapters. **Chapter 2** studies night-time climate by means of the CFD model. This model introduces a condensation UDF which accounts for the rate of condensation forming on the inner face of the greenhouse cover. After model validation by comparison with experimental data, the model was used to determine the transient and

steady-state greenhouse climate under different sky conditions and different soil heat fluxes. **Chapter 3** studies a commonly used solution to the issue of low night-time temperature and the use of a thermal screen was analysed by means of CFD simulations. For this purpose, the CFD model presented in Chapter 2 was modified to incorporate an internal screen. After validating the model through in situ experiments, a thorough comparison was made between a single-layer and screened greenhouse and detailed information was provided in order to build a framework for taking decisions as to whether to use a screen or not. **Chapter 4** introduces a novel approach to optimizing greenhouse design; the approach relies on two optimization algorithms linked to an ES model which was coupled to a CFD model. The aim of the study was twofold: on the one hand to introduce a method offering a general approach for optimizing greenhouse design and on the other hand, to attempt to solve one of the issues highlighted in chapter 2: the influence of the thermal optical properties of the cover on greenhouse climate. Indeed, it was shown that using a highly reflective cover material would have a theoretically significant impact on greenhouse performances. **Chapter 5** introduces a coupled model for the study of greenhouse climate. The CFD was used to provide the ventilation rate and convective coefficients for the ES model. Coupling the ES and CFD models constitutes a novel approach to greenhouse studies than could be used as a general methodology. In Chapter 5 this approach was applied to study the effect of different ventilation strategies on humidity under both clear and overcast sky conditions.

1.6 References

Baeza, E.J. , Pèrez-Parra, J.J., Montero, J.I. , Bailey, B.J. , Lòpez, J.C., & Gàzquez, J.C. (2009). Analysis of the role of sidewall vents on buoyancy-driven natural ventilation in parral-type greenhouses with and without insect screens using computational fluid dynamics. Biosystems Engineering, 104(1), 86-96.

Baptista, F.J.,Bailey, B.J. ,& Meneses,J.F. (2012). Effect of nocturnal ventilation on the occurrence of *Botrytis cinerea* in Mediterranean unheated tomato greenhouses. Crop Protection, 32,144-149.

Boulard, T., Kittas ,C., Roy, J.C., & Wang , S. (2002). SE—Structure and Environment: Convective and Ventilation Transfers in Greenhouses, Part 2: Determination of the Distributed Greenhouse Climate. Biosystems Engineering, 83(2), 129-147.

Campen, J., Kempkes, F., & Bot, G. (2009). Mechanically controlled moisture removal from greenhouses. *Biosystems Engineering, 102*(4), 424-432.

Giacomelli, G., Castilla, N., Van Henten, E. J., Mears, D., & Sase, S. (2008). Innovation in greenhouse engineering. Acta horticulturae, 801, 75-88.

Roy, J.C., Boulard, T., Kittas ,C., & Wang , S. (2002). PA—Precision Agriculture: Convective and Ventilation Transfers in Greenhouses, Part 1: the Greenhouse considered as a Perfectly Stirred Tank. Biosystems Engineering, 83(1), 1-20.

Teitel, M. ,Peiper, UM., & Zvieli, Y. (1996). Shading screens for frost protection. Agricultural and forest meteorology, 81(3-4),273-286.

2 A CFD greenhouse night-time condensation model

The contents of this chapter are published in Biosystem Engineering as a paper entitled: A CFD greenhouse night-time condensation model.
Davide Piscia, J. I. Montero, E. Baeza, B. J. Bailey
Volume 111, Issue 2, February 2012, Pages 141–154
DOI http://dx.doi.org/10.1016/j.biosystemseng.2011.11.006

2.1 Abstract

A computational fluid dynamics (CFD) model for simulating greenhouse night-time climate and condensation is presented. The model was applied to a four-span plastic covered greenhouse. Film condensation was simulated by applying a UDF (user defined function) added to the commercial CFD package. The CFD model was verified by comparing CFD results with experimental measurements. The effect of cover temperature on greenhouse humidity was then determined by the CFD model and compared to experimental results. Root mean square values for the differences between the CFD and experimental values of internal temperature and humidity showed there was good agreement between. The results showed the importance of heat transfer losses by radiation, particularly for low values of soil heat flux. They also showed the roof was the coolest surface in the greenhouse, and therefore the sink for the water vapour produced by the crop. For each configuration (soil heat flux 10, 25, 50 and 100 W m^{-2} and equivalent sky temperature 263 K, 273 K and 276 K), the condensation rate curves and relative humidity evolution are presented. It was observed that all the condensation rate curves had the same characteristic shape and could be represented by a single logistic function. The response of the CFD model to a step-change in the water vapour source (night-time transpiration from the crop) was then analysed. It was observed that the model predicted the same steady-state temperature, relative humidity and condensation rate independent of the time when the water vapour source was enabled. The CFD condensation model is intended to be used for the design of strategies for humidity control, particularly in unheated greenhouses.

2.2 Nomenclature

$A_{cellwall}$ Area of cell face at wall (m^2)

a Asyntotic value of logistic function

b Parameter of logistic function

C_r Condensation rate ($g\ s^{-1}$)

c Parameter of logistic function

c_p Heat capacity at constant pressure ($J\ kg^{-1}\ K^{-1}$)

D binary mass diffusivity ($m^2\ s^{-1}$)

DOM Discrete ordinate model

g Gravitational acceleration ($m\ s^{-2}$)

k Turbulence kinetic energy ($m\ s^{-2}$)

$\dot{m}''$ Mass flux ($kg\ m^{-2}\ s^{-1}$)

$\dot{m}'''$ Volumetric mass source ($kg\ m^{-3}\ s^{-1}$)

N Solid angle (degree)

n Number of measurements

n_i Interface normal direction

p_d Dynamic pressure (Pa)

RH Relative humidity (%)

RMSE Root mean square error

RTE Radiation transfer equation

S Source term

S_{crop} Crop surface (m^2)

SHF Soil heat flux ($W\ m^{-2}$)

T Temperature (K)

T_c *C*over temperature (K)

T_{rate} Transpiration rate ($kg\ m^{-2}\ s^{-1}$)

T_∞ Reference temperature (K)

U Velocity component of the x coordinates ($m\ s^{-1}$)

UDF User define function

u_τ Friction velocity ($m\ s^{-1}$)

V Velocity component of the y coordinates (m s^{-1})

V_{cell} Volume of computational cell (m^3)

V_G Greenhouse volume (m^3)

VPD Vapour pressure deficit (Pa)

W Humidity ratio (kg kg^{-1})

W_{Sat} Humidity ratio at saturation (kg kg^{-1})

W_{Init} Initial humidity ratio (kg kg^{-1})

y_P Distance from point P (centre-cell value) to the wall (m)

$y_{Data,i}$ Experimental value at time i

$y_{Mod,i}$ Simulated value at time i

y^+ Non-dimensional distance indicator

Δt Starting time of condensation (s)

α Location parameter of logistic function

β Scale parameter of logistic function

β_T Coefficient of thermal expansion (K^{-1})

Γ Diffusion coefficient

ε Turbulence kinetic energy dissipation rate (m^2 s^{-3})

ϕ Concentration variable

θ Polar angle (degree)

λ Thermal conductivity (W $m^{-1}K^{-1}$)

μ Turbulent viscosity (kg m^{-1} s^{-1})

$\vec{v}$ Velocity vector (m s^{-1})

v_i Interface normal velocity component (m s^{-1})

ρ Density (kg m^{-3})

τ Shear stress (Pa)

φ Azimuthal angle (degree)

Φ Heat source term (W m^{-3})

∇ Divergence operator

Subscript

int Greenhouse inside air

H_2O Water

out Outside air

w Wall

2.3 Introduction

The control of excessive humidity is one of the most important issues regarding greenhouse climate during winter periods; high relative humidity (RH) and the presence of free water on plant surfaces have been recognised as favourable for the development of fungal diseases (F. J. F. Baptista, 2007). Growers have been recommended to combine ventilation and heating to reduce relative humidity and to avoid condensation, but natural ventilation is difficult to control. As a consequence, combined heating and ventilation results in high energy consumption and greenhouse climate heterogeneity (Campen, Kempkes, & Bot, 2009). Moreover, most Mediterranean greenhouses are unheated, so other methods to reduce greenhouse humidity are needed.

The humidity regime is the result of the water vapour balance between sources, namely plant transpiration and soil evaporation, and sinks, such as ventilation, dehumidification and condensation. In order to correctly manage the water vapour balance, knowledge of each term in the equation is required. In greenhouse analysis, most studies on transpiration have examined day–time conditions and have been based on the Penman-Monteith equation (Stanghellini, 1987); (Montero, Anton, Muñoz, & Lorenzo, 2001). In terms of night-time transpiration, Caird, Richards and Donovan, (2007) provided a list of species showing incomplete stomatal closure at night. Values of night-time leaf conductance were given for a few greenhouse crops such as tomato (*Lycopersicum esculentum*); for greenhouse tomato the night-time leaf conductance ranged from 0.37 to 0.068 cm s^{-1} depending on the cultivar and measurement method. No information was given on the relationships between leaf conductance and climate conditions such as vapour pressure deficit (VPD) or greenhouse temperature, so night-time transpiration could not be accurately estimated from the reported leaf conductance values. The authors therefore concluded that experimental evidence on the subject is very scarce but two studies are relevant. Firstly, Assaf and Ziesling, (1996) conducted a study for a rose crop in a heated greenhouse with forced air (treatment A) and with a dehumidifier and a thermal screen (treatment B), conditions and crop which are different to those of the experimental greenhouse in the present study. Average values of rose evapotranspiration for the whole night were given and a highly significant linear regression between the “heat energy” and night-time transpiration was found; the authors concluded that differences in “thermal convection between the plant and greenhouse cladding” could be a more important factor in regulation of plant transpiration during night hours than the differences in VPD. Secondly, Seginer, Kantz, Levav and Peiper (1990), focussed on night-time

transpiration in greenhouses and investigated how the measured transpiration of different crops depended on the heating and dehumidifying conditions. The latter study can be considered as the one closest to the experimental conditions presented in this article, although this study did not include information on lettuce, which was the crop used for this analysis.

Many studies on ventilation have been conducted, but few have been related to humidity. Boulard et al (2004) studied the effect of ventilation on the humidity level through a theory-based, leaf-boundary layer model validated by experimentation. Their study concluded that greenhouse vent opening and wind speed dominate the relationships between outside and inside humidity, and showed that greenhouse ventilation can be used to directly control air humidity at leaf level. One drawback of this approach is the loss of heat through the vent openings. Baptista, Abreu, Meneses and Bailey (2001) found that nocturnal ventilation reduced the condensation periods by decreasing the RH and reducing the rate of inside air temperature increase in the early morning. Later, Baptista (2007) reported a reduction of disease severity (number of lesions) on tomato leaves caused by *B. Cinerea* by permanent night ventilation; our study also showed that better air circulation during the night contributes to lower humidity inside the greenhouse air and crop canopy

Several dehumidification techniques have been studied and tested for greenhouse applications. A number of authors have studied phase change methods, especially using desiccants to force phase change between water and water vapour in the air, possibly coupled to renewable energy sources.

In the greenhouse, air can be dehumidified by hygroscopic absorption or by condensation at a cooled surface. Campen, Bot and De Zwart (2003) presented a comprehensive study of dehumidification in Central European greenhouses. They discarded the hygroscopic absorption concept due to the cost and environmental risks of the installation. Among the dehumidifying systems based on condensation, Campen and Bot (2001) analysed a low-energy demand dehumidification system consisting of a water to air heat exchanger with buoyancy driven air circulation, and reported an energy saving of 4-7% in a conventional single glass greenhouse.

An arrangement of finned pipes, cooled by a heat pump, placed under the greenhouse gutter has also been tested (Campen & Bot, 2002). This was based on experimental measurements and CFD simulations. It was concluded that the finned pipes could remove 54 g of vapour per hour from air at 20 º C and 80% RH. Campen et al (2009) studied the effect of mechanical ventilation as a way of controlling moisture removal. Their study analysed a new system applied to a greenhouse equipped with a thermal screen. With this system, outside air entered near floor level, with the exchange between outside and greenhouse air controlled

mechanically by an air distribution system, forcing the humid air to pass through the thermal screen. The results showed a more uniform temperature and humidity distribution, as well as more efficient energy consumption compared to classical usage of a thermal screen, based on slightly opening the thermal screen.

The cover is usually the coldest surface within the greenhouse environment, particularly in unheated greenhouses under clear night sky conditions (Montero, Muñoz, Antón, & Iglesias, 2004). This makes roof condensation an important sink of air humidity. One of the terms in the mass balance equation for water vapour that has received less attention is condensation, possibly because it is difficult to measure the condensed water in a greenhouse, but also because most commercial CFD packages do not explicitly include a calculation for condensation rate.

Condensation has been taken into account in heat balance models (both steady and unsteady state), based on the assumption that inside air is instantaneously and homogenously mixed (which in reality does not occur). Garzoli and Blackwell (1981) and (De Halleux, Deltour, Nijskens, Nisen and Coutisse (1984) concluded that the night-time heat transfer coefficient with condensation increased for glass and decreased for polyethylene. The reason is that for materials which are partially or highly transparent to infra-red radiation, such as polyethylene, heat loss due to condensation is more than compensated for by the fact that the wet cover annuls direct far-infrared radiation heat loss from vegetation to the sky. Pieters and Deltour (1997), based on a dynamic climate model for glasshouses, indicated that the simulated yearly fossil heating requirements were underestimated by about 15 % when condensation was not taken into account.

Therefore, in the literature there are two areas which have not been the subject of extensive research; the first is greenhouse CFD simulation with a model which includes condensation and the second is an analysis of humidity in unheated greenhouses, such as those of the Mediterranean areas. A specific CFD simulation model was developed to analyse the night-time greenhouse humidity regimes and condensation. This model is intended to set the basis for humidity control strategies, mainly for Mediterranean plastic covered greenhouses.

The condensation on the inner surface of the greenhouse cover was modelled by the addition of a user defined function (UDF) written in C language, which extends the software capabilities, and the CFD results were compared to experimental data for model validation. The relationship between condensation rate and external boundary conditions (soil heat flux and equivalent sky temperature) were assessed using different CFD simulations.

2.4 Material and Methods

Two methods were used to analyse condensation, one based on a CFD model developed to account for condensation at the greenhouse cover, and the other based on experimental data collected over a period of two winter months.

2.4.1 CFD simulation

2.4.1.1 Numerical method

The CFD model is based on the resolution of the governing equations of momentum, energy and continuity applied to the greenhouse case. Such equations can be written as the convection-diffusion equation:

$$\frac{\partial \rho \phi}{\partial t} + \nabla(\rho \vec{v} \phi) = \nabla(\Gamma \nabla \phi) + S \qquad (2.1)$$

Table 2.1. Continuity, momentum and energy variables

Equation	ϕ	Γ	S
Continuity	1	0	0
Momentum x	U	μ	$-\partial p_d / \partial x$
Momentum y	V	μ	$-\partial p_d / \partial y + \rho g \beta (T - T_\infty)$
Energy	T	λ / c_p	Φ / c_p

In which ρ is the density, t is the time; ∇ is the divergence operator; ϕ is the concentration variable; $\vec{v}$ is the velocity vector; Γ is the diffusion coefficient; *S* is the source term.

To construct the momentum, energy and mass transport equations, the relevant entries for ϕ, Γ and *S* are given in Table 2.1.

In our CFD simulations, turbulence was analysed using the standard *k*–ε model. The variable k accounts for kinetic energy, while the variable ε accounts for the rate of dissipation of energy in unit volume and time. The *k*–ε model is based on two equations, one for *k* and the other for ε. It is the most widely used and validated turbulence model, and in the greenhouse CFD literature it is one of the most used and recommended (T. Boulard & Wang, 2000).

The CFD modelling was carried out using the Ansys Fluent software package (Ansys, 2009). The Fluent enhanced wall treatment was used for the near wall cells. In this approach the whole domain is subdivided in a viscosity-affected region and a fully-turbulent region; this approach can be used with wall y^+ values ranging from 1 to 200, where y^+ is a non-dimensional distance defined by the following equation:

$$y^+ = \frac{\rho u_\tau y_P}{\mu} \tag{2.2}$$

in which $u_\tau = \sqrt{\frac{\tau_w}{\rho_w}}$ is the friction velocity; y_P the distance from point P (centre-cell value) to the wall; μ the dynamic viscosity and τ is the shear stress .

Density was computed through the perfect gas law, which related density to temperature. In this way the buoyancy effect was taken into account.

For the case under investigation, radiation played a fundamental role, and its contribution was added as a source component (S) in the energy equation. The discrete ordinate model (DOM) was used to calculate the radiation component because plastic is a participating media and DOM is recommended for semi-transparent materials (Versteeg & Malalasekera, 1995). DOM solves the general equation of radiation transfer (RTE) for a set of *n* different directions for a finite number of discrete solid angles, each associated with a vector direction fixed in the global Cartesian system (*x,y,z*). It transforms the RTE equation into a transport equation for the radiation intensity in the spatial coordinates. The angular space 4π is discretised into $N_\theta \times N_\varphi$ solid angles of extent ω. The angles θ and φ are the polar and azimuthal angles. For our CFD simulations the following parameters were used, θ divisions 4, φ divisions 4, θ pixels 2 and φ pixels 2. The radiation equations were computed every 10 iterations. Baxevanou, Bartzanas, Fidaros and Kittas (2008) gave a detailed description of DOM applied to CFD greenhouse computation.

The greenhouse roof and walls in the model were meshed as 0.2 mm thick elements. They were modelled as semi-transparent solids; their optical properties for far infrared radiation were: absorptivity 0.69, transmissivity 0.19, and reflectivity 0.12. These values were assumed to be independent of wavelength.

The soil was modelled as a grey media with emissivity 0.98 for the black mulching (Liakatas, Clark, & Monteith, 1986). The heat transfer rate from the soil surface to the greenhouse was set as a boundary condition.

A UDF was added to the CFD package to account for condensation on the inner cover surfaces. The effect of condensation on the flow and species distribution in the vapour phase was

included in the flow analysis through a customised source term applied automatically by the code to the domain cells in contact with the greenhouse cover.
Assumptions of the model:

- The vapour phase contained a binary ideal gas mixture of air and water vapour
- The liquid phase consisted of water only
- Only film-wise condensation occurred
- The thermal resistance of the liquid film could be neglected
- Local thermodynamic equilibrium existed at the liquid-vapour interface

The equations governing the calculation of condensation rate are explained in the Appendix
The crop was considered as a homogeneous and constant vapour source with a production rate of 1.74 x 10^{-6} kg m^{-2} s^{-1}, as will be explained later.
The aerodynamic resistance between the greenhouse air and the lettuce crop was not considered; firstly because no specific aerodynamic resistance coefficients for lettuce were found in scientific literature and, secondly, because the crop height was only approximately 0.03 m which is relatively small considering the global greenhouse height, thus no significant effect on internal air movement would be expected.
During the night ventilators were closed so ventilation was not considered. Infiltration losses could not be measured; nevertheless, during model validation the difference between inside-outside air temperature was between 1 and 2 K (as shown in Fig 2.2) and the outside air speed was close to 2 m s^{-1}, and so no relevant thermally induced or wind induced infiltration loses were expected. Therefore infiltration was neglected in this CFD model.

2.4.1.2 Mesh and boundary conditions

The three-dimensional (3D) domain was divided in 383,226 cells (space discretisation) and the relevant governing equations were resolved for each cell, the mesh was built by using the Ansys Mesh program. The dimensions of the domain were 160 m in the *x*-direction, 50 metre in the *y*-direction and 12 metre in the z-direction (the x axis is oriented from left to right, the y axis from bottom to top and the z axis represents the depth of the domain) , chosen following the recommended domain dimensions (Bournet, Ould Khaoua, & Boulard, 2007). Several simulations were run to check whether the CFD results were independent of the domain dimensions.

The quality of the grid was checked through the skewness and the y^+ parameters. The skewness parameter indicates how ideal a cell shape is, whilst the wall y^+ parameter, is a non-dimensional parameter that indicates whether the mesh refinement close to the boundary condition is appropriate or not. The mesh used gave a maximum skewness parameter of 0.669 (which falls into the "fair" range, according to the Ansys Fluent manual (Ansys, 2009)) and an average value, based on all the mesh cells, of 0.19 ("very good" range). The mesh parameter y^+ was kept under the 300 value (upper limit suggested (Ansys 2009) and the average y^+ of all boundary conditions defined as "wall" was 26.

In the 3D model, the upper domain surface was defined as a non-slip wall (corresponding to the sky) and the bottom domain as a non-slip wall that corresponds to the ground. In later figures, (Figs. 2.2 and 2.3), the air flows in from the left surface (*y-z* plane) and flows out of the domain through the right surface. The domain surfaces parallel to the wind direction (*x-y* plane) were modelled as symmetrical. The mass diffusivity of water vapour was 3.747×10^{-5} m^2 s^{-1} (Ansys, 2009).

Two sets of simulations were conducted. The first set was used to validate the CFD model and the second set was used to study the greenhouse humidity and temperature regimes for a range of boundary conditions, such as equivalent sky temperature and soil heat flux (SHF).

For model validation, transient simulations were made from sunset to sunrise. The boundary conditions were taken as the hourly average values of the greenhouse SHF, outside air temperature and humidity, outside net radiation and wind speed. Hourly averages were used since these were available from the meteorological station. Transient simulations were run with a time step of 60 s; each time-step consisted of 300 iterations.

For the second set of simulations (use of the model), steady state conditions were used for the range of boundary conditions as shown in Table 2.2.

Table 2.2. Boundary and initial conditions used for the steady state CFD simulations

Boundary conditions	Values
Top domain surface	Sky temperature: 263, 273 and 276 K
Bottom domain surface	Greenhouse soil heat flux ranged from 10, 25, 50 to 100 W m^{-2}
Left domain surface (normal to wind direction)	Inlet temperature was set to 276 K, and velocity to 2 m s^{-1} (average values measured during the night used for model validation)

Right domain surface (normal to wind direction)	Outlet boundary condition
Parallel domain surface (parallel to wind direction)	Symmetry
Initial conditions	
Temperature	280 K
Relative humidity	68%

2.4.2 Greenhouse measurements

An experimental greenhouse was equipped with several sensors in order to validate and compare the results obtained from the CFD model. It had four spans, 4.9 m wide, a 45º roof slope and polyethylene plastic film cladding (200 µm thick). The greenhouse was 19.6 m wide, 3.5 m high at the gutter and 4.5m high at the ridge. The greenhouse length was 12 m.

Measurements were taken between 26 January and 1 March 2010. The conditions inside the greenhouse were measured using two air humidity and temperature sensors (Campbell hmp45c, Logan, UT,USA) located 2 m high in the central spans and two thermocouples (diameter 200µm, type T, RS Components Ltd. ,Corby, UK) to measure roof temperature. Thermocouples were placed on the inner side of the cover of the two central spans, mid distance between ridge and gutter; they were fastened by using adhesive transparent tape over the thermocouple wires, though the measuring tip was not covered with the tape. Other sensors were one net radiometer (Hukseflux NR01, Delft, The Netherlands) in a central span at gutter height, one temperature probe (Campbell, Pt100) for soil surface temperature and one heat flux sensor (Hukseflux hfp01sc, Delft, The Netherlands) in the middle of the greenhouse. A pyrgeometer (Hukseflux IR02, Delft, The Netherlands) and a hmp45c relative humidity probe were located externally, near the greenhouse. A datalogger (Campbell CR10X, Logan, UT, USA) recorded measurements every 5 min.

Given the lack of date in the research literature for the lettuce crop, night-time transpiration was measured experimentally. Measurements were made using a weighing lysimeter (Mettler, KCC-150, capacity 150 kg, accuracy 1 g, Columbus, OH, USA). Eight mature lettuce plants were placed on the lysimeter for continuous weighing. Attempts were made to establish a relationship between measured transpiration, VPD and greenhouse air temperature. However, no significant regressions could be found between any of the variables under consideration;

therefore it was decided to take the average transpiration for the same night used for transient validations, which was 0.247 g s^{-1} for the experimental greenhouse. Since the soil crop area was 142 m^2 the transpiration rate per unit area was 1.74 x 10^{-6} kg m^{-2} s^{-1}. So the crop was considered as a constant vapour source with a production rate of 1.74 x 10^{-6} kg m^{-2} s^{-1} produced homogeneously from the volume occupied by the crop to the greenhouse air.

Outside data were taken from a meteorological station approximately 50 m from the experimental greenhouse, with a net radiometer (Kipp & Zonen *NR-Lite* , Delft, The Netherlands*)*, a temperature and humidity probe (Campbell hmp45c, Logan, UT,USA) and a wind anemometer (Campbell 05305-L, Logan, UT,USA) at a height of 10 m. The meteorological station provided hourly averaged values.

2.5 Results

2.5.1 Model validation

The outside and inside air conditions were quite stable over most winter nights except between 14 and 15 February 2010, when the greenhouse air temperature changed by about 4 K (Fig. 2.1a). This night was chosen for the validation process, as it was considered to be more suitable for studying the transient behaviour of the CFD model. The averages of the two air temperature and humidity sensors were compared with the CFD simulated greenhouse air temperature and humidity of the whole greenhouse volume. Additionally the average of the two roof temperature sensors was compared with the CFD simulated temperature of the whole greenhouse roof.

With regard to greenhouse air temperature, the difference between measured and simulated values was always less than 1 K (Fig. 2.1a). Both followed the same tendency after midnight, when there was a gradual drop in temperature until sunrise. The agreement of the transient temperature change was also good.

Figure 2.1b shows the experimental and simulated roof temperatures. The agreement was particularly good during the early part of the night (very stable temperature conditions) but less so afterwards. In all cases, the difference between the measured and predicted values was always less than 2 K. The experimental and simulated roof temperatures (Fig. 2.1b) were always lower than the greenhouse air temperature. The maximum difference between the measured and simulated values was 2.1 K.

The time trend of the measured and CFD predicted humidity ratios are shown in Fig. 2.1c. The maximum difference between both values occurred after midnight, when the experimental values dropped more quickly than those predicted by the CFD model. This difference could be because the vapour source was considered as constant throughout the night for the CFD calculations, given the difficulty in detecting minor weight loses with the lysimeter. In all cases, the maximum difference was approximately 0.0007 kg kg^{-1}, which is approximately 14% of the humidity ratio measured experimentally.

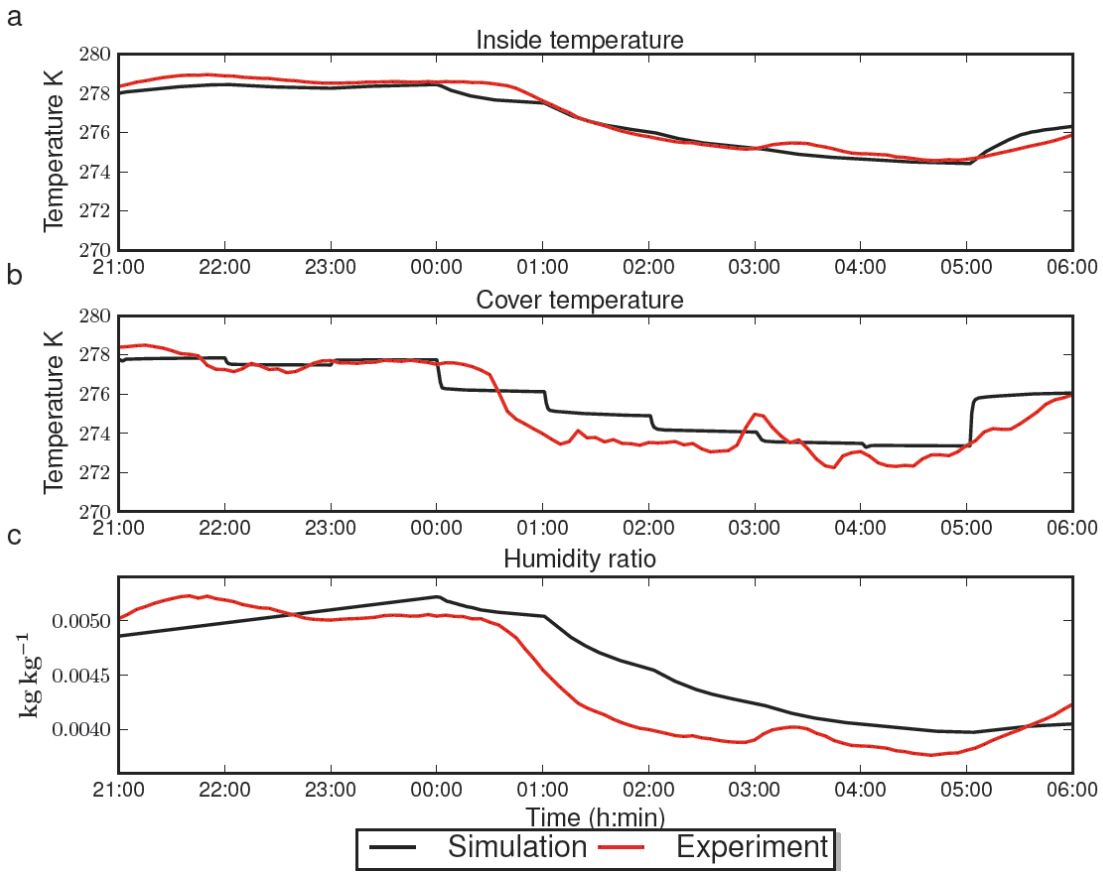

Fig. 2.1. Experimental and CFD simulated values of the greenhouse air temperature. Night 14 - 15 February 2010: a) greenhouse air temperature, b) greenhouse roof temperature and c) greenhouse humidity ratio.

2.5.1.1 Assessment of model accuracy

Model performance was tested from a quantitative point of view using the root mean squared error (RMSE).

The RMSE can be written as: $$\sqrt{\frac{1}{n}\sum_{i=1}^{n}(y_{Mod,i} - y_{Data,i})^2} \quad (2.3)$$

where n is the number of measurements (108 for this case), $y_{Mod,i}$ is the simulated value at period i and $y_{Data,i}$ is the measured value. For the CFD model the RMSE values were:

- inside temperature RMSE 0.367 ^{o}C
- cover temperature RMSE 0.89 ^{o}C
- relative humidity RMSE 6.5 %
- humidity ratio RMSE 0.00029 kg/kg

These values are in agreement with the RMSE values found by Baptista (2006), who developed a model for similar conditions and obtained an inside air temperature RMSE of 1.6 ^{o}C and relative humidity RMSE of 7%. As demonstrated by Baptista (2007), most greenhouse climate models have an RMSE of around 10%.

2.5.2 Steady state CFD simulations

Figures 2.2 and 2.3 show the simulated greenhouse temperature and humidity at 3 AM during the night 14 to 15 February. At this time the soil heat flux was 9.8 W m^{-2}, the outside air temperature was 275.7 K, the outside relative humidity was 71% and the wind speed was 2.3 m s^{-1}. The equivalent sky temperature was calculated as 264.3 K, according to Berdahl, Martin and Sakkal (1983).

Figure 2.2 is a temperature map of a cross section of the simulated greenhouse under clear-sky night conditions, showing a minor thermal inversion; the greenhouse air was slightly cooler than the outside air since the average greenhouse air temperature was 275.0 K. The CFD model also gave the roof as the coolest surface of the greenhouse (approximately 1 K less than the greenhouse air), so this was the area with the highest tendency to produce condensation. Similar observations regarding thermal inversion and roof temperature in unheated greenhouses are widely supported by experimentation as well as simulation, since most of the heat losses are by infrared radiation emission (López Hernández, 2003).

The air temperature was uniform over most of the greenhouse cross section, except that the left area of the cross section was slightly warmer. This was due to the wind impinging on the left span and transferring heat to the first span cover, which became warmer than the other regions of the roof.

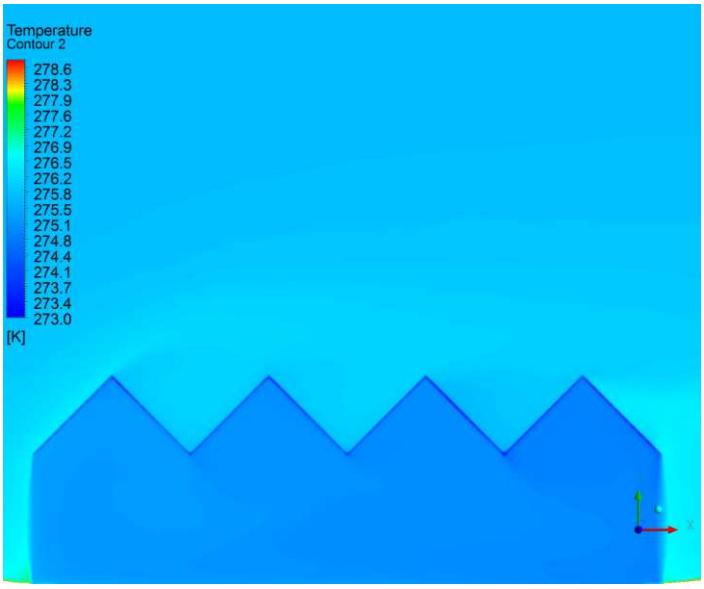

Fig. 2.2. Map of temperature of a greenhouse cross section. Soil heat flux 9.8 W m^{-2}, outside air 275.7 K, equivalent sky temperature 264.3 K. Wind speed 2.3 m s^{-1}

The humidity ratio is shown in Fig. 2.3 for the same set of boundary conditions. The humidity level was slightly higher on the left of the greenhouse cross section. This is in agreement with the temperature distribution shown in Fig 2.2, since warmer air can hold more water vapour. For the same reason the areas with lower water vapour content were those closest to the greenhouse roof since the roof surface had the lowest temperatures.

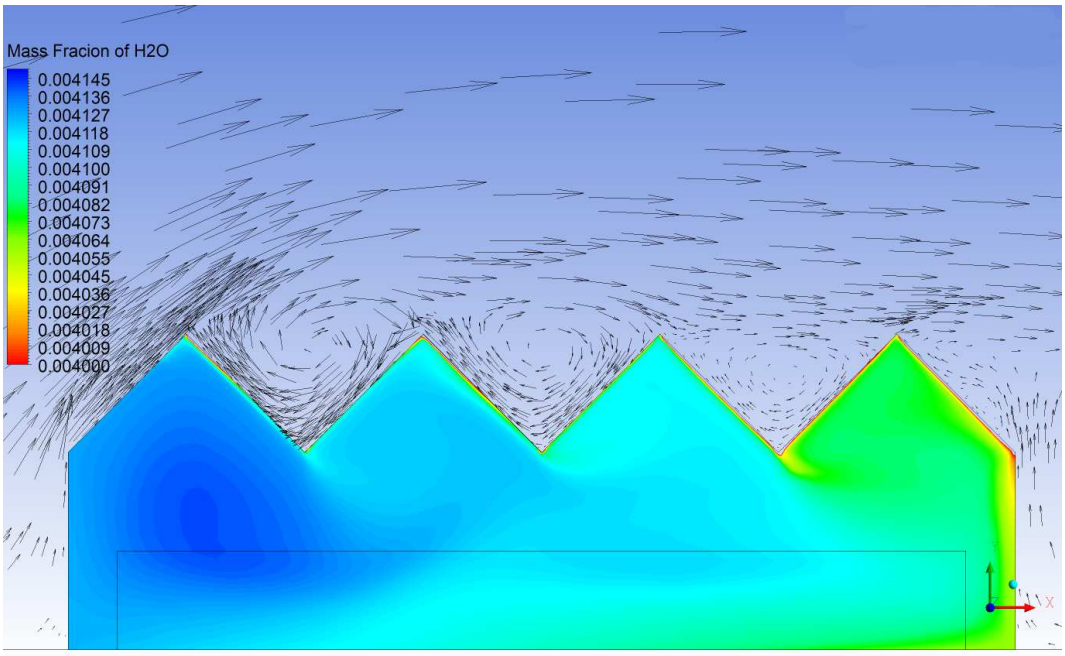

Fig. 2.3. Map of humidity ratio of a greenhouse cross section. Soil heat flux 9.8 W m^{-2}, outside air 275.7 K, equivalent sky temperature 264.3 K. Wind speed 2.3 m s^{-1}. Air velocity vectors around the greenhouse are also shown.

The relationship between greenhouse humidity and roof temperature was investigated (Fig 2.4). Since sky temperature had a major effect on roof temperature, a number of simulations were run for a range of equivalent sky temperatures (263 K, 273 K and 276 K), covering clear to overcast conditions. Four soil heat fluxes were analysed (10, 25, 50 and 100 Wm^{-2}), which covered from unheated to heated greenhouse conditions. This gave twelve combinations of boundary conditions for the simulations.

Figure 2.4a shows a strong correlation between roof temperature and greenhouse humidity ratio for the twelve simulations. The equation of the regression line was $W = 0.34T_c + 4.03$ (R^2 = 0.99). For comparison, the experimental measurements of humidity ratio versus roof temperature are given in Fig. 2.4b. The experimental humidity regression line was $W = 0.36T_c + 3.68$ (R^2 = 0.97, n=105). In spite of the experimental measurements being taken under different conditions to those used in some of the CFD simulations (no greenhouse heating during the experiments), both CFD model and experimental data gave very good statistical indicators and the slope and constant coefficients of both regression lines were very similar. The greenhouse humidity was controlled by the roof temperature: due to the condensation on the roof it acted as the sink of air humidity, so that the greenhouse air reached a given value of water vapour content for each roof temperature.

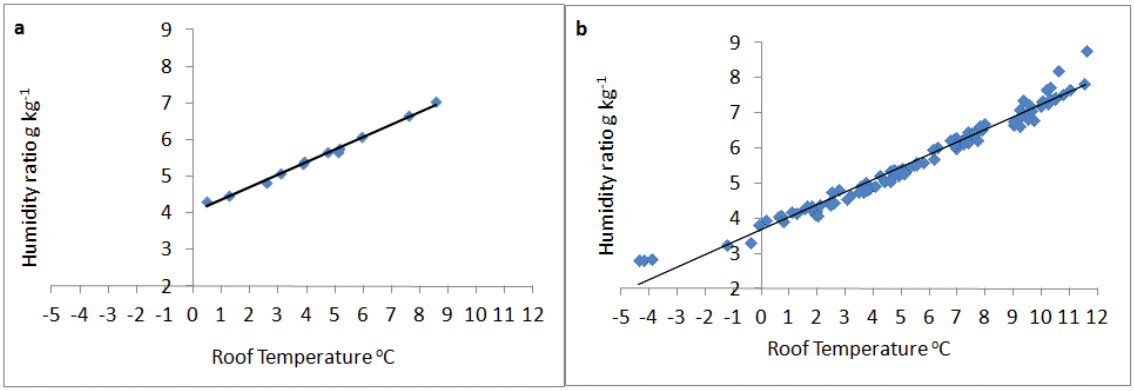

Fig. 2.4. Relationship between greenhouse humidity ratio and roof temperature: a) CFD simulations, b) experimental data.

2.5.3 Transient analysis of the night-time greenhouse climate

2.5.3.1 Condensation rate

The formation of condensation as a function of SHF and equivalent sky temperature was studied by running transient simulations with a time step of one minute. The initial humidity content of the greenhouse air was set to zero; from this point a constant source of water vapour was given to the greenhouse air.

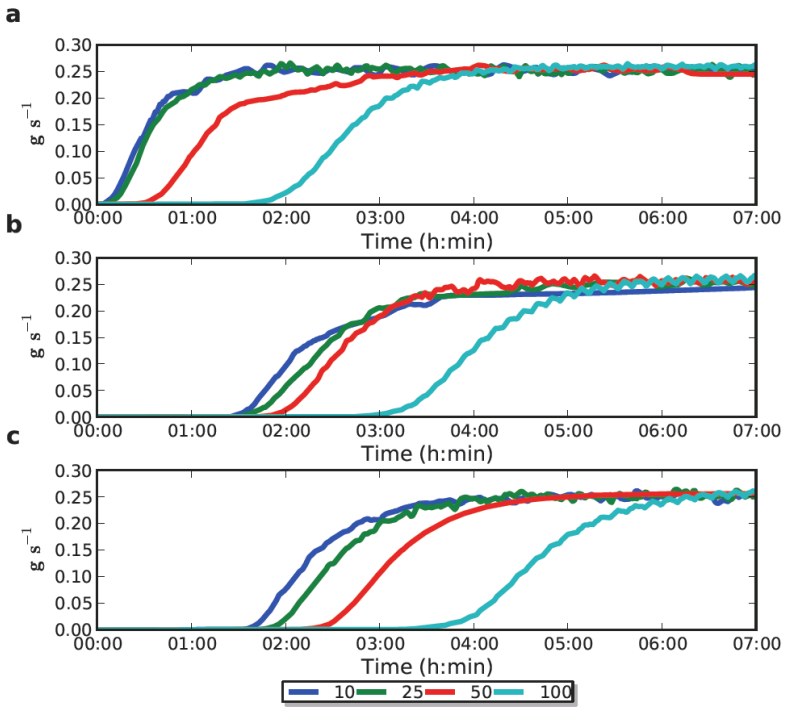

Fig. 2.5. Condensation rate as a function of time for four soil heat fluxes (10, 25, 50 and 100 W m^{-2} and three equivalent sky temperatures a) 263 K, b) 273 K, c) 276 K.

Figure 2.5 shows that, independently of the SHF and sky temperature, the condensation curves had a similar pattern in which three phases can be differentiated:

a) Initial phase, where condensation has not yet begun.
b) Transitional phase (growing phase), where condensation rate increases sharply. (The slope of the condensation rate will be considered later.)
c) The steady phase, where the condensation rate reaches a steady state. Under steady state conditions the source of water vapour (crop transpiration) should equal the sink of vapour (roof condensation).

The main difference between Figs 2.5 a, b *and* c is the duration of the initial phase (zero condensation). The greater the SHF the later condensation starts. This can be explained by the fact that a higher SHF raises the greenhouse air and roof temperature, so condensation takes place at higher moisture content. The onset of condensation is also delayed for higher equivalent sky temperatures, due to the effect of the equivalent sky temperature on the cover temperature. The temperature of the cover is lower on clear nights since the net radiation loss from the greenhouse cover is greater.

Zero condensation phase. In this phase, cover temperature and air moisture content do not fulfil the condensation conditions. This is the situation at the beginning of the night, when the cover temperature is higher than the dew point temperature of the greenhouse air.

The onset of condensation can be determined approximately by assuming uniform conditions in the greenhouse air. With this assumption, condensation will start when the greenhouse humidity reaches the humidity ratio at saturation.

The water vapour in the greenhouse air can be given by the mass balance equation as:

$$(W_{Sat} - W_{Init}) V_G \rho_{air} = T_{rate} \Delta t S_{crop} \quad \text{[Kg]} \qquad (2.4)$$

where W_{Sat} is humidity ratio at saturation, kg kg^{-1}; W_{Init} is initial humidity ratio of the greenhouse air when transpiration started, kg kg^{-1}; V_G is greenhouse volume, m^3; T_{rate} is transpiration rate, kg m^{-2} s^{-1}; S_{crop} is crop surface, m^2; Δt is starting time of condensation, s; ρ_{air} is air density, kg m^{-3}.

If the cover temperature is known, the psychrometric properties of moist air such as

W_{sat} can be determined. For instance the ASAE Handbook, 2001 provides equations to calculate humidity ratio from the dry-bulb temperature and relative humidity (ASAE Handbook, 2001) The cover temperature (T_c) can be accurately measured in the absence of solar radiation. Where the crop transpiration rate and the initial water vapour content in the greenhouse air (W_{Init}) are known, the time needed to reach the required water vapour in the air can be calculated from Eq. 2.4.

Condensation transitional phase. This phase begins with the onset of condensation, and continues until a steady state condensation rate is reached. Condensation curves show a sharply increasing slope at the beginning followed by a slow decrease towards the end of this phase. This shape, which was found in all curves, is characteristics of a logistic function. The general equation of a logistic function is given by

$$f(x) = \frac{a}{1 + be^{cx}} \quad \text{with } a \text{ and } b > 0 \tag{2.5}$$

A logistic curve has a stretched S-shape, initially modelling exponential growth and slowing down over time until the curve finally levels off. In the logistic function, *a* is defined as the limiting value (or asymptotic value) while *b* and *c* are parameters of the function.

When logistic functions are applied to the study of condensation, the parameter *a* is the steady-state condensation rate, which is the same as the constant vapour water source (in this case *a* = 0.247), the independent variable x is the time variable. The term *b* of Eq. 2.5 can be rewritten as $e^{\left(\frac{\alpha}{\beta}\right)}$, hence the term e^{cx} becomes $e^{\left(\frac{t}{-\beta}\right)}$. For each case study, every condensation curve was statistically analysed against a logistic-type function, to find the coefficients which gave the best statistical results, using an R-language based software which used a variant of the Levenberg–Marquardt algorithm:

$$f(t) = \frac{0.247}{(1 + e^{((-t+\alpha)/\beta)})} \tag{2.6}$$

where α is the location parameter which translates the logistic function with time and β is the scale parameter which has the effect of stretching out the graph (Filiben, 2010). For all cases studied there was a strong correlation between simulation results and a logistic function. The minimum coefficient of determination (R^2) was 0.97 for the 263_10 case.

Attempts were made to develop a general curve that could fit all case studies under consideration. Since the starting time of condensation varied from one case to another (see Fig. 2.5), it was decided to take the origin (zero) as the time of onset of condensation for each individual curve. The condensation rate with time ($C_r(t)$, g s^{-1}) for the range of boundary conditions analysed in this study can then be modelled by:

$$C_r(t) = \frac{0.247}{(1 + e^{((-t+65.89)/19.06))}} \qquad [\text{g s}^{-1}] \tag{2.7}$$

where *time* is expressed in minutes. The mean slope coefficient (β) was 19.06 and the mean absolute deviation was 2.8 for all condensation curves, and the mean α coefficient was 65.89 and mean absolute deviation was 13

Steady-state condensation rate phase. This is the final section of the condensation rate curve. At steady state, the condensation rate equals the crop transpiration rate, which in this case and for the whole greenhouse crop was 0.247 g s^{-1}.

Figure 2.6 shows the best-fit logistic function for all case studies under consideration.

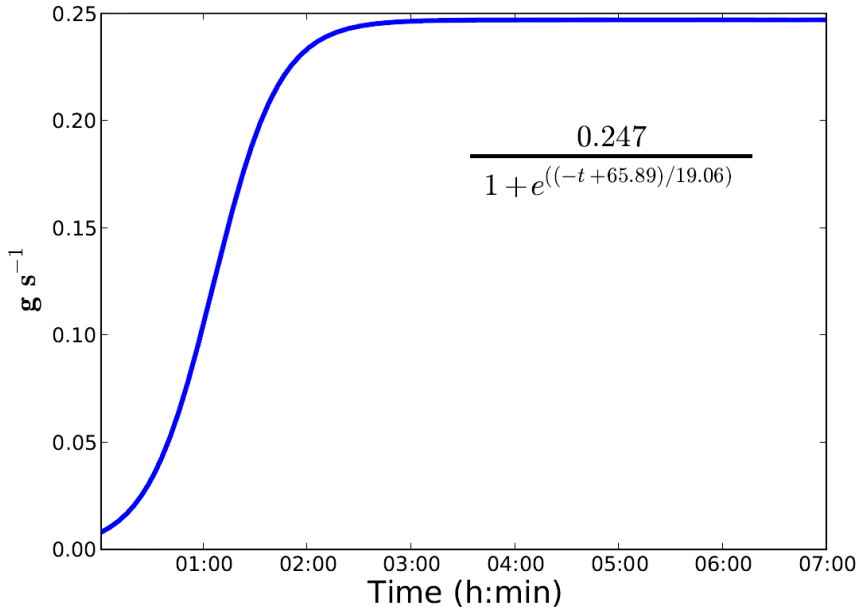

Fig. 2.6. Logistic function for the condensation curve.

2.5.3.2 Time course of Relative Humidity

Relative humidity plays a major role on the development of relevant physiological processes such as transpiration and physiological disorders, as well as for the development of fungal diseases. As with the condensation rate, it was possible to plot the CFD predicted RH values against time for each pair of boundary conditions (SHF and equivalent sky temperature). An initial RH of 76% was used for simulations, the outside air RH at the beginning of the night between 14 and 15 February, which was the night chosen for the transient simulations (see Fig. 2.1).

After an initial phase, a constant RH value was reached for all boundary conditions under consideration, which were: SHF 10 and 25 W m^{-2} (for unheated greenhouses) and SHF 50 and 100 W m^{-2} (for heated greenhouses). For each soil heat flux three equivalent sky temperatures were simulated: 263 K, 273 K and 276 K. The results are shown in Fig. 2.7. The steady state value varied from 70 % to saturation. For a given source of water vapour (night-time transpiration rate), the final RH depended mainly on the SHF: the higher the SHF the higher the greenhouse air temperature and the lower the RH. For each SHF, after an initial phase, the plots for different sky temperatures reached the same steady-state RH. This indicates that the final RH was independent of equivalent sky temperature and a function of crop transpiration rate and SHF only.

In some cases, there was an initial reduction in RH, particularly for SHF = 100 W m^{-2}. This was due to the transient simulation process, since for higher SHF values the increase in temperature was faster than the increase in absolute humidity.

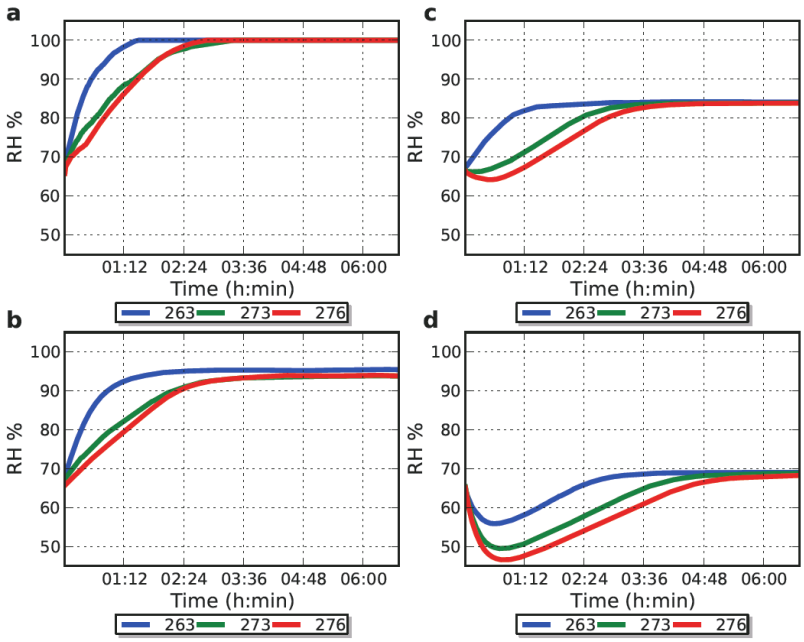

Fig. 2.7. Time course of RH (%) with time (min) Top left: SHF 10 W m^{-2}. Bottom left: soil heat flux 25 W m^{-2}. Top right: soil heat flux 50 W m^{-2}. Bottom right: soil heat flux 100 W m^{-2}.

The simulations shown in Fig. 2.7 are for a constant source of water vapour, which is a model simplification due to the lack of knowledge on the night-time transpiration rate of greenhouse crops. The CFD model presented here allows for the implementation of a variable source of water vapour, since the model requires an updated input of variables such as outside temperature, humidity and wind speed, for each time step.

2.5.3.3 Model response to a step change in transpiration rate

Since the objective of this study was to develop and test a night-time condensation model it was decided to assess its response to a sudden change in one of the model variables. For this purpose, the transient behaviour was simulated with a step-change in transpiration. The idea behind a step change in transpiration was to separate the model response from the initial conditions and see if the steady state solution is independent of the initial conditions. It was not intended to simulate a situation that could take place in practice but to test the model

reaction; in this case a change in the humidity source was chosen since humidity is a key issue in the condensation model.

The CFD simulation was made with the following boundary conditions: 273 K for the equivalent sky temperature and 100 W m^{-2} for the SHF. The wind speed, outside air temperature and humidity were the same as for the previous simulations (Table 2.2). Plant transpiration was considered as zero at the beginning of the simulation, and was then enabled to the previously used vapour source value of 0.247 g s^{-1} for the whole experimental greenhouse after 160 time steps (equivalent to 160 min) during which time the modelled air temperature and RH had reached steady-state (Fig. 2.8).

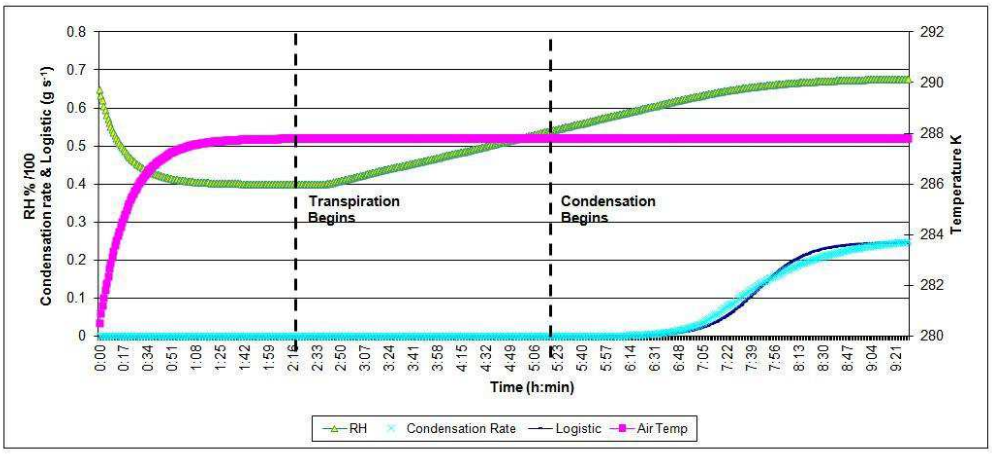

Fig. 2.8. Evolution of RH, condensation rate and temperature following a step-change in transpiration.

With the onset of transpiration, the RH began to increase, while the condensation rate began to increase once the water vapour in the air was sufficient to produce condensation on the roof (*time* ≈ 6:15). The reduction in the slope of the relative humidity curve also coincided with the onset of condensation, which indicated that the simulation is approaching to the steady state.

The final RH, 67.8%, was the same as the RH for the CFD simulation with plant transpiration enabled from the beginning. This confirms that RH depends on SHF under the set of outside air conditions considered in this study.

The inside temperature reached a constant value after a few simulations and did not change when the vapour source (transpiration) was enabled. The final inside air temperature, 287.8 K, was the same as for the CFD simulation with plant transpiration enabled from the beginning of the simulation.

With regard to condensation, Fig. 2.8 shows the time course of the simulated condensation rate and the logistic function presented in Fig. 2.6. As mentioned previously, the logistic function was obtained for the water vapour source enabled from the start of the simulation. Both curves show a similar pattern, and their relative root mean square error was 10.39 %. As demonstrated by Baptista (2007) the performance of most available greenhouse climate models is around 10%.

Interestingly, condensation occurred for a relatively low greenhouse air RH (67.8%); condensation formed because the average roof temperature was 281.4 K, which was 6.4 K less than the average greenhouse air temperature. Under these conditions the average greenhouse air dew point temperature was slightly higher than the roof temperature. Moreover the greenhouse air near the roof was cooler than the average greenhouse air, so air conditions near the roof were more favourable to condensation formation.

2.6 Discussion

The CFD model predicted that the roof was the coolest surface of the greenhouse (approximately 1 K lower than the greenhouse air temperature for unheated greenhouses) since most of the energy losses were due to infrared radiation. This produced thermal inversion, which is a well known phenomenon in unheated Mediterranean greenhouses. The fact that the model is able to predict situations that occur in practice is a demonstration of its reliability. The model was also able to detect minor differences in temperature and humidity even for soil heat fluxes as low as 10 W m^{-2}, as shown in Figs 2.2 and 2.3.

Since the roof was the coolest surface, its inner side was the sink of the water vapour produced by the crop, and the roof temperature controlled the humidity ratio in the greenhouse air. This strong link between roof temperature and water vapour content in the air was observed for heated and unheated greenhouses. This means that it may be possible to control greenhouse humidity and condensation by controlling roof temperature, although this in itself is quite difficult to achieve.

Changing the optical properties of the cover, its reflectivity, transmissivity and absorptivity, to far IR can change the roof temperature. NIR filters have been tested for greenhouse cooling (Hemming, Kempkes, Van der Braak, Dueck, & Marissen, 2006) but there has been little recent research on the far IR properties of greenhouse covering materials. Nijskens, Deltour, Coutisse, and Nisen (1984) made a comprehensive study on heat transfer through greenhouse covering materials. They found differences of up to 5 °C in cover temperature, with a low emissivity

glass with IR reflective properties on the inner side being the warmest material. The study was conducted for an outside temperature of -10 °C in a heated greenhouse, so heat transfer by convection played a relevant role. In unheated greenhouses, where radiation losses are more important than convective losses, the far IR properties of the covering materials may have a major effect on condensation formation on the greenhouse roof and consequently on greenhouse absolute humidity. In contrast, RH is more dependent on SHF as mentioned before, and so it is less affected by the optical properties of the cover.

The aforementioned research was based on unventilated (closed) greenhouses. In CFD modelling it is difficult to consider infiltration loses, since this would require the definition of the location and geometry of the openings through which the greenhouse air could exit, information which is not usually available. In this research it was not possible to measure the infiltration rate, although infiltration would be expected to play a secondary role since most modern greenhouses can be considered as airtight. Nonetheless if an infiltration rate of 0.5 exchanges per hour is assumed, for the conditions shown in Figs. 2.2 & 2.3 (see section 2.3.2), the inside air humidity ratio W_{int} was 0.0039 kg kg^{-1} and the outside air humidity ratio W_{out} was 0.00316 kg kg^{-1}; the estimated rate of water vapour lost by infiltration was 0,0376 kg s^{-1}, which is approximately 15% of the night time transpiration rate. This lost would have probably reduced the quantity of condensed water by about the same amount. Future model developments should try to improve accuracy by including a sink of water vapour due to infiltration.

The condensation model used a constant vapour source, i.e. constant transpiration from the crop. This is not a shortcoming of the model itself, since the transient model allows the inclusion of new boundary conditions for each time step. The model also reacted well to a step change in the water vapour source, a relevant variable, so changing boundary conditions can be included. The simulations were limited to a constant vapour source as there is a lack of knowledge on night-time crop transpiration and the link of transpiration rate with VPD and temperature at night. Probably the most reliable information on night transpiration in greenhouses comes from the work by Seginer, et al (1990). Values of transpiration presented in that work could be used in future simulations to analyse the greenhouse performance for different crops at different stages of development.

This study was concerned with a greenhouse of a particular geometry, the 45º slope flat roof greenhouse, designed to collect roof condensation, due to the roof inclination (Stanghellini & Montero, 2010). The goal is the development of semi-closed greenhouses for Mediterranean

climates, for energy saving and to increase in crop production by CO_2 enrichment, provided that excessive humidity can be controlled (Stanghellini, Incrocci, Gázquez, & Dimauro, 2007).

The CFD condensation model is currently being used to study the effect of a number of techniques such as the use of double walls, the night-time ventilation regime and selection of cover properties. In terms of night-time ventilation the model can answer questions such as: how much ventilation is needed for the control of humidity and temperature in heated and unheated greenhouses, what will happen if ventilators are open before the onset of condensation, or when is best to open the ventilators?

In terms of cover properties preliminary simulations have shown that, under clear sky conditions, a film with low emissivity, high reflectivity on the outer side and high emissivity, low reflectivity on the inner side can increase roof temperature by 1.9 K and greenhouse temperature by approximately 1.5 K. Such a temperature increase is relevant for unheated greenhouses and can be important in terms of energy saving for heated greenhouses.

The combination of these techniques under investigation is expected to provide relevant information for the development of strategies for humidity reduction.

2.7 Conclusions

A comprehensive analysis of the condensation process during night-time conditions was carried out. The ability of the CFD model to correctly predict the main greenhouse climate variables was validated against experimental data.

The simulations showed that there was a strong correlation between roof temperature and greenhouse humidity ratio for the twelve combinations of sky temperature and SHF considered in this study. In addition, it was found that the RH depended on the SHF more than on the roof temperature.

For a wide range of boundary conditions, greenhouse condensation followed the same characteristic pattern, so that the condensation rate could be modelled by a single logistic function that well represented all the conditions studied.

The ability of the model to correctly predict the greenhouse climate was tested through a step-change in the water vapour source value; the model reacted to this step-change and reached a final solution very similar to that achieved for a steady vapour source.

2.8 Appendix

The condensation model applied in this study was developed by Bell (2003). This model was implemented as UDF into the general CFD simulation code. In Bell's model the condensation rate is governed by the rate of diffusion of water vapour towards the cold surface.

According to Bird, Stewart and Lightfoot (1960), the species mass flux for water vapour at the liquid vapour interface ($\dot{m}''_{H_2O}$) can be written as

$$\dot{m}''_{H_2O} = \rho W_{H_2O} v_i - \rho D \frac{\partial W_{H_2O}}{\partial n_i} \qquad [\text{kg m}^{-2}\ \text{s}^{-1}] \qquad \text{(A 2.1)}$$

Where v_i is the interface normal velocity, D is the mass diffusivity and n_i is the interface normal direction.

The mixture mass flux at the liquid vapour interface ($\dot{m}''$) is:

$$\dot{m}'' = \dot{m}''_{air} + \dot{m}''_{H_2O} = \rho v_i \qquad [\text{kg m}^{-2}\ \text{s}^{-1}] \qquad \text{(A 2.2)}$$

Since the liquid phase consist of only water

$$\dot{m}''_{air} = 0 \qquad \text{(A 2.3)}$$

Substituting Eq. (A 2.1) into Eq. (A 2.2):

$$\rho v = \frac{1}{(W_{H_2O} - 1)} \rho D \frac{\partial W_{H_2O}}{\partial n_i} \qquad [\text{kg m}^{-2}\ \text{s}^{-1}] \qquad \text{(A 2.4)}$$

The CFD code treats the liquid-vapour interface as a wall with velocity *v*= 0. Therefore Eq. (A3) cannot be used directly for the calculation of condensation rate. However it is possible to include a mass sink/source term in the volume of the near wall cell to account for the condensation rate (where $A_{cell\ wall}$ is the cell area and V_{cell} is the volume cell).

$$\dot{m}''' = \rho v \frac{A_{cell\ wall}}{V_{cell}} \qquad [\text{kg m}^{-3}\ \text{s}^{-1}] \qquad \text{(A 2.5)}$$

Substituting Eq. (A 2.3) into Eq. (A 2.4) .

$$\dot{m}''' = \frac{1}{(W_{H_2O} - 1)} \rho D \frac{\partial W_{H_2O}}{\partial n_i} \frac{A_{cell\ wall}}{V_{cell}} \qquad [\text{kg m}^{-3}\ \text{s}^{-1}] \qquad \text{(A 2.6)}$$

Also the species equation for the cell volume states that

$$\dot{m}'''_{H_2O} = W_{H_2O}\dot{m}''' \qquad [\text{kg m}^{-3}\ \text{s}^{-1}] \qquad \text{(A 2.7)}$$

By writing Eqs. (A 2.5) and (A 2.6) into the source code of the UDF, the CFD code can calculate the volumetric mass source for the air mixture and the water vapour

Acknowledgments

The work presented here has been carried out within the project EUPHOROS. European Commission, Directorate General for Research, 7th Framework Programme of RTD, Theme 2 – Biotechnology, Agriculture & Food, contract 211457. This research has also been supported by INIA (project RTA2008-00109-C03) with contribution of FEDER founds. Thanks are also given to INIA fellowship FPI-INIA.

2.9 References

Ansys, F. (2009). User Guide 12.0. *Lebanon, NH, USA*.

ASHRAE Handbook (2001). Fundamentals. American Society of Heating, Refrigerating and Air Conditioning Engineers, Atlanta, GA, USA.

Baptista, F., Abreu, P., Meneses, J., & Bailey, B. (2001). Comparison of the climatic conditions and tomato crop productivity in Mediterranean greenhouses under two different natural ventilation management systems. *Proc Int Symp AgriBuilding*, 3-7.

Baptista, F. J. F. (2007). Modelling the climate in unheated tomato greenhouses and predicting Botrytis cinerea infection. Ph.D Thesis, Univerisade de Évora, Portugal.

Baxevanou, C., Bartzanas, T., Fidaros, D., & Kittas, C. (2008). Solar radiation distribution in a tunnel greenhouse. *Acta Hort, 801*, 855-862.

Bell, B. (2003). UDF for condensation of steam from moist air (available from Ansys Fluent UDF repository) . *Ansys Fluent Inc*.

Berdahl, P., Martin, M., & Sakkal, F. (1983). Thermal performance of radiative cooling panels. *International Journal of Heat and Mass Transfer, 26*(6), 871-880.

Bird, R. B., & Stewart, W. E. (1960). Lightfoot Transport Phenomena. John & Sons, New York, NY, USA.

Boulard, T., Fatnassi, H., Roy, J., Lagier, J., Fargues, J., Smits, N., et al. (2004). Effect of greenhouse ventilation on humidity of inside air and in leaf boundary-layer. *Agricultural and Forest Meteorology, 125*(3-4), 225-239.

Boulard, T., & Wang, S. (2000). Greenhouse crop transpiration simulation from external climate conditions. *Agricultural and Forest Meteorology, 100*(1), 25-34.

Bournet, P., Ould Khaoua, S., & Boulard, T. (2007). Numerical prediction of the effect of vent arrangements on the ventilation and energy transfer in a multi-span glasshouse using a bi-band radiation model. *Biosystems Engineering, 98*(2), 224-234.

Caird, M. A., Richards, J. H., & Donovan, L. A. (2007). Nighttime stomatal conductance and transpiration in C3 and C4 plants. *Plant Physiology, 143*(1), 4.

Campen, J., & Bot, G. (2001). SE--Structures and Environment:: Design of a Low-Energy Dehumidifying System for Greenhouses. *Journal of Agricultural Engineering Research, 78*(1), 65-73.

Campen, J., & Bot, G. (2002). SE--Structures and Environment:: Dehumidification in Greenhouses by Condensation on Finned Pipes. *Biosystems Engineering, 82*(2), 177-185.

Campen, J., Bot, G., & De Zwart, H. (2003). Dehumidification of greenhouses at northern latitudes. *Biosystems Engineering, 86*(4), 487-493.

Campen, J., Kempkes, F., & Bot, G. (2009). Mechanically controlled moisture removal from greenhouses. *Biosystems Engineering, 102*(4), 424-432.

De Halleux, D., Deltour, J., Nijskens, J., Nisen, A., & Coutisse, S. (1984). Dynamic simulation of heat fluxes and temperatures in horticultural and low emissivity glass-covered greenhouses. *Greenhouse Construction and Covering Materials 170*, 91-96.

Filiben, J. (2010). NIST/SEMATECH e-Handbook of Statistical Methods, http://itl.nist.gov/div898/handbook/.

Garzoli, K., & Blackwell, J. (1981). An analysis of the nocturnal heat loss from a single skin plastic greenhouse. *Journal of Agricultural Engineering Research, 26*(3), 203-214.

Hemming, S., Kempkes, F., Van der Braak, N., Dueck, T., & Marissen, N. (2006). Greenhouse cooling by NIR-reflection. *International Symposium on Greenhouse Cooling 719*, 97-106.

Liakatas, A., Clark, J., & Monteith, J. (1986). Measurements of the heat balance under plastic mulches. Part I. Radiation balance and soil heat flux. *Agricultural and Forest Meteorology, 36*(3), 227-239.

López Hernández, J. (2003). Sistemas de calefacción en invernaderos cultivados de judía en el litoral mediterráneo. Ph.D Thesis, Universidad de Almería, Spain.

Montero, J., Anton, A., Muñoz, P., & Lorenzo, P. (2001). Transpiration from geranium grown under high temperatures and low humidities in greenhouses. Agricultural and Forest Meteorology , 107(4), 323-332.

Montero, J., Muñoz, P., Antón, A., & Iglesias, N. (2004). Computational Fluid Dynamic Modelling of Night-time Energy Fluxes in Unheated Greenhouses. *International Conference on Sustainable Greenhouse Systems-Greensys* 12-16 September 2004*,* Louvain, Belgium 691, 403-410.

Nijskens, J., Deltour, J., Coutisse, S., & Nisen, A. (1984). Heat transfer through covering materials of greenhouses. *Agricultural and Forest Meteorology, 33*(2-3), 193-214.

Pieters, J., & Deltour, J. (1997). Performances of Greenhouses with the Presence of Condensation on Cladding Materials 1. *Journal of Agricultural Engineering Research, 68*(2), 125-137.

Seginer, I., Kantz, D., Levav, N., & Peiper, U. (1990). Night-time transpiration in greenhouses. *Scientia Horticulturae, 41*(3), 265-276.

Stanghellini, C. (1987). Transpiration of greenhouse crops; an aid to climate management. Ph.D Thesis, University of Wageningen, Netherland.

Stanghellini, C., Incrocci, L., Gázquez, J., & Dimauro, B. (2007). Carbon dioxide concentration in Mediterranean greenhouses: how much lost production? *International Symposium on High Technology for Greenhouse System Management: Greensys* 4-6 October ,Naples, Italy 801, 1541-1550.

Stanghellini, C., & Montero, J. (2010). Resource use efficiency in protected cultivation: towards the greenhouse with zero emissions. *IHC* 22-27 August 2010, Lisbon,Portugal.

Versteeg, H., & Malalasekera, W. (1995). Computational fluid dynamics: Longman Group.

3 A night time climate analysis of a screened greenhouse based on CFD simulations

The contents of this chapter have been submitted to Biosystem Engineering as a paper entitled : A night time climate analysis of a screened greenhouse based on CFD simulations
Davide Piscia, J. I. Montero, P. Muñoz, E. Baeza, B. J. Bailey

3.1 Abstract

A computational fluid dynamics (CFD) model was developed and validated for studying the influence of a thermal screen on the night-time greenhouse climate. The model took into account temperature and humidity, transpiration and condensation; transpiration was considered to be a constant source of water vapour and condensation was modelled with a user defined function (UDF). The greenhouse studied was a four-span plastic screened (SC) greenhouse. The CFD model was verified by comparing CFD predictions with experimental measurements. Root mean square values for the differences between the CFD and experimental values of the internal air, screen and cover temperatures and humidity values showed a good level of agreement. A parametric study was carried out with a combination of soil heat flux (SHF) (10, 25, 50 and 100 W m^{-2}) and the equivalent sky temperature (256, 263, 273 and 276 K). The influences of external conditions, equivalent sky temperature and SHF were then assessed. Linear relationships between screen temperature and greenhouse air temperature and humidity were found and presented. A comparison with a single layer (SL) greenhouse was carried out and showed that heat transfer losses associated with radiation were reduced. The CFD results showed that using a screen greatly reduced the probability of thermal inversion which only occurred under extreme conditions (equivalent sky temperature lower than -9 ^{o}C and SHF less than 10 W m^{-2}). The response of the CFD model to a double step-change in equivalent sky temperature and SHF was also studied.

3.2 Nomenclature

a	constant
b	slope coefficient
c_p	heat capacity at constant pressure (J kg^{-1} $^oC^{-1}$)
$C_r(t)$	condensation rate (g s^{-1})
DOM	discrete ordinate model
k	turbulence kinetic energy (m s^{-2})
n	number of measurements
p	pressure (Pa)
RMSE	root mean square error
RH	relative humidity (%)
$s^2_{y\cdot x}$	residual mean square
S_ρ	mass source
S_U	momentum source
S_T	heat source
SC	screened
SHF	soil heat flux (W m^{-2})
SL	single-layer
t	temperature (^{o}C)
t	time (s)
t_{sky}	equivalent sky temperature (^{o}C)
T	absolute temperature (K)
u	velocity component of the x coordinates (m s^{-1})
$\vec{U}$	velocity vector (m s^{-1})
UDF	user defined function
W	humidity ratio (kg kg^{-1})
y^+	non-dimensional distance indicator
$y_{Data,i}$	experimental value at time i
$y_{Mod,i}$	simulated value at time i
α	location parameter of logistic function
β	scale parameter of logistic function

χ limiting value (or asymptotic value)

ε turbulence kinetic energy dissipation rate ($m^2\ s^{-3}$)

λ thermal conductivity ($W\ m^{-1}\ ^oC^{-1}$)

μ turbulent viscosity ($kg\ m^{-1}\ s^{-1}$)

ρ density ($kg\ m^{-3}$)

Subscript

CFD modelled

Exp experimental

3.3 Introduction

Since the beginning of intensive horticulture, particular attention has been paid to increases in night-time temperature for frost protection or optimal crop development in both heated and unheated greenhouses. In terms of greenhouse heating, energy saving became a particularly key issue after the oil crisis of the 1970s. As a consequence, the greenhouse industry developed a number of techniques, including: more efficient heating systems; the use of renewable energy; double walls for reducing heat transfer; and fixed and/or movable screens made from different materials, etc.

Since the 1970s, screens of different types have been used to conserve energy in heated greenhouses. The scientific literature particularly addressed the study of thermal screens during the period 1978 to 1988, focusing not only on their energy saving effects, but also on greenhouse climate relating to temperature, humidity and solar radiation and to crop responses in screened greenhouses.

Bailey (1981) reported that thermal screens in glasshouses can reduce heat loss by between 35 and 60%; in this paper, he used an electrical analogue model to study the influence of the emissivity and transmissivity of the screen on radiation exchange and screen temperature.

Heat losses in greenhouses with and without screens were comprehensively analysed by Nijskens, Deltour, Coutisse and Nisen (1984). One of the main conclusions reached was that air was the most important insulating element and that thermal screens created a very large air zone that acted as an insulating system.

In the case of screen control, Bailey (1988) studied five different strategies to enhance the performance of thermal screens in greenhouses. In this study, the thermal screen in question

was movable and the study was based on a macro-balance energy model. It was concluded that the most effective method of climate control was the combination of reduced day-time and increased night-time temperatures with optimized control during the day.

Less is known about the effects of screens in unheated greenhouses, in spite of the fact that most of the world's greenhouses are unheated. In terms of heat transfer, one major difference is that while convective heat exchange is the most relevant heat transfer process in heated greenhouses, in unheated ones radiative exchanges prevail. Teitel, Peiper and Zvieli (1996) analysed the connection between low temperatures and frost and also the damage to crops produced by frost. They suggested that three parameters affect net thermal radiation; the shading percentage of the screen, it's radiometric properties, and the relationship between screen area and ground area. According to this study, the aluminized screen was the best choice for reducing frost damage.

Baille, Aries, Baille and Laury (1985) studied the thermal optical properties of screens for unheated greenhouses through a software simulation based on macro energy balances. They concluded that when a one-sided aluminised face was used, the greatest loss reduction was obtained when the aluminised side faced directly upwards; in a pulsed air-heating mode the aluminised screen performed much better than a PE screen.

Silva, Miguel and Rosa (1991) developed a model which computed net thermal radiation for a greenhouse equipped with a thermal screen. Based on the results generated by the model, the authors concluded that the radiometric properties of the screen would have different influences upon the net thermal radiation flux inside the greenhouse. When the temperature was the same everywhere and the cladding material was not totally opaque, the higher the emissivity of the bottom side of the screen, the smaller the cooling rate would be; however, when the temperature decreased from the internal ground up to the roof, the higher the screen emissivity of the bottom side of the screen, the larger the cooling rate would be.

Teitel and Segal (1995) presented a model for computing net radiation under woven shading screens and then compared model results to experimental data. One major conclusion was that the screen performed better when it had low emissivity and low transmittance. They also recommended that the screen should have a high degree of solidity, because this reduced the exchange of thermal radiation between the ground and the sky. This study also demonstrated that heat losses exhibited a positive linear relationship with the ratio between the screen area and floor area.

Excessive humidity is also a key issue at night. In winter, growers may face several factors, including high relative humidity and condensation dripping, which may lead to the

development of plant diseases, low temperatures and thermal inversion. This situation is mainly associated with thermal radiation losses, particularly under clear sky conditions. Baptista (2007) reported that high relative humidity together with the presence of free water on leaves created favourable conditions for the development of fungal diseases.

Korner and Holst (2004) presented a mathematical model simulating crop climate and calculated the durations of leaf wetness and leaf dryness. Their aim was to provide a tool for climate control and to prevent high relative humidity which could contribute to the development of *Botrytis cinerea*.

The effect of a thermal screen on humidity and condensation received little attention and, to the best of our knowledge, only one work (Bailey 1981) explicitly discussed this aspect. One of the conclusions was that for practical considerations the lower surface of the screen should have a high level of emissivity in order to increase screen temperature and thereby reduce condensation.

All of these studies were based on the solution of macro energy balance equations. Since early in 1990, the CFD technique has tended to replace the macro energy balance model in the study of greenhouse climate; the main reason for this has been that CFD models provide much greater accuracy and detailed information for each study zone (micro model).

Montero, Muñoz, Anton and Iglesias (2004) presented a CFD model for the study of thermal screens in unheated multi-tunnel greenhouses. They concluded that the thermal screen temperature was 2.8 ^{o}C higher than the cover of a single-layer greenhouse under clear-sky conditions and that for overcast nights, the greenhouse air was 1.8 ^{o}C warmer.

Iglesias (2005) developed a CFD model to study the use of thermal screens. She compared CFD results obtained from simulated results without a screen. The conclusion was that a polyethylene thermal screen could improve temperatures by 1.9 to 2.8 ^{o}C depending on sky conditions. She also simulated the use of an aluminized thermal screen and reported gains with respect to a PE screen ranging from 2.7 ^{o}C (under overcast conditions) to 3.5 ^{o}C (under a clear sky).

Thermal radiation exchange plays a key role in climate studies. Bournet, Ould Khaoua and Boulard (2007) were among the first authors to introduce a CFD model which took into account short and long wave radiation applied to greenhouse climate studies.

All the CFD night-time studies have focussed on the thermal features of greenhouses but have not provided in-depth information relating to the role of humidity, night time crop transpiration, condensation on cold surfaces such as covering roofs, and water vapour exchanges due to ventilation or infiltration, etc. Piscia, Montero, Baeza and Bailey (2011) have

recently undertaken studies of single layer greenhouses and developed a comprehensive model that includes condensation. A parametric study with different boundary conditions was conducted and strong relationships between climate variables and external conditions were reported. To the best of our knowledge, no analysis has been conducted for screened greenhouses comparable to that conducted by Piscia et al. (2011) for SL greenhouses.

The main objective of the present study was to analyse the transient and steady-state night-time climate of a screened greenhouse by investigating the effect of boundary conditions on temperature and humidity. This analysis was based on the development, validation and application of a CFD model for a wide range of the boundary conditions of equivalent sky temperature and soil heat flux.

A second objective was to assess the potential advantages of screened over SL greenhouses, particularly in the case of unheated greenhouses, by comparing the SC and SL air and cover temperatures, absolute and relative humidities, and condensation rates. This work forms part of a wider study which addresses the issue of controlling humidity and condensation in screened and un-screened greenhouses through the optimization of greenhouse design, covering materials and air exchanges to save energy and reduce the risk of fungal diseases.

3.4 Materials and methods

As previously mentioned, this paper on screened greenhouses is related to a previous one on the night-time climate in single layer greenhouses (Piscia et al., 2011) and most of the materials and methods used in this work were the same as those explained in that publication. Consequently, we have briefly summarised the common aspects and have only described the novel aspects in detail.

The greenhouse SC configuration was analysed by two methods, one based on a CFD model study and the other based on an analysis of experimental data.

3.4.1 Computational fluid dynamics simulation

3.4.1.1 2.1.1 Numerical method

The CFD model solves the governing equations of momentum, energy and continuity applied to the greenhouse. The momentum equation, also known as the Navier-Stokes equation is obtained by the application of Newton's law of motion to a fluid element:

$$\frac{\partial \rho u}{\partial t} + \nabla(\rho \vec{U} u) = \nabla(\mu \nabla u) - \frac{\partial p}{\partial x} + S_U \tag{3.1}$$

in which ρ is the density, t the time, $\vec{U}$ the velocity vector, u the velocity component in x-direction, ∇ the divergence operator, μ the turbulent viscosity, p the pressure, and S_U the momentum source.

In this situation, the assumption of incompressibility applies and the mass conservation or continuity equation has to be solved:

$$\nabla \cdot (\rho \vec{U}) = S_\rho \tag{3.2}$$

where S_ρ is the mass source.

The study also involved energy, so the CFD model also included the energy equation:

$$\frac{\partial \rho c_p T}{\partial t} + \nabla(\rho \vec{U} T) = \nabla(\lambda \nabla T) + S_T \tag{3.3}$$

where T is the temperature, λ the thermal conductivity, S_T the heat source, and c_p the heat capacity at constant pressure.

Turbulence was modelled using the standard $k-\varepsilon$ model. This is based on two equations, one for k, which accounts for kinetic energy, and the other for ε which accounts for the rate of dissipation of energy in unit volume and time. This is probably the most widely used and validated turbulence model and in the greenhouse CFD literature it has been used in many research studies (Boulard & Wang, 2000).

Condensation was also included in the CFD model by applying a user defined function (UDF); the condensation rate was included in eq. 3.2 and 3.3 as part of the source term. Details of the condensation model can be found in Piscia et al. (2011).

The crop was a lettuce crop; it was considered as homogeneous and having a constant vapour source with a production rate of 1.74 x 10^{-6} kg m^{-2} s^{-1}. The aerodynamic resistance between the greenhouse air and the lettuce crop was not included; firstly, because no specific aerodynamic resistance coefficients for lettuce were available in the scientific literature and, secondly, because the crop height was only 0.3 m, which is relatively short compared to the height of the greenhouse; as a result, no significant effect on internal air movement would have been expected. In real conditions the difference in temperature between the lettuce leaves and surrounding air at night is rather small, particularly in unheated greenhouses. Therefore heat transfer from the leaves was not included .

Ventilation was not considered because the vents were closed at night and air leakage could not be measured.

During the validation process, wind speeds did not exceed 2.1 m s^{-1}; as a result, no relevant air infiltration was expected. Similarly, no infiltration through the thermal screen was considered because of the low air velocities both above and below the screen. Temperature differences can lead to some air flows, but as discussed later in CFD modelling it is rather difficult to consider infiltration losses.

The main settings of the CFD model are summarised in Table 3.1

Table 3.1. Numerical method models

Setting	Model	Reference
Turbulence model	k-epsilon	Boulard and Wang (2000)
Radiation	DOM	Versteeg and Malalasekera (1995)
Condensation	UDF	Piscia et al. (2011)
Transpiration	Constant source	Piscia et al. (2011)
Density	Incompressible perfect law gas	Fluent User guide (Ansys, 2009)

The convective terms in the CFD equations were modelled using a second order up-wind scheme. The viscous term was modelled by a second order central scheme and the transient term was modelled using an implicit scheme. The pressure-velocity coupling was resolved by

the algorithm SIMPLEC method, which uses a relationship between velocity and pressure corrections to enforce mass conservation and to obtain the pressure field (Ansys, 2009).

3.4.1.2 Mesh and boundary conditions

The addition of a thermal screen introduced a change in the greenhouse geometry which had to be regenerated; a thin horizontal screen (0.2 mm) was added and this was simulated as semi-transparent solid.

The presence of a thermal screen gave the sidewalls relevance in the condensation process. They were therefore modelled not as a thin surface, but as a solid, in order to enhance temperature accuracy (Ansys, 2009).

The dimensions of the domain were 160 m in the x-direction, 50 m in the y-direction and 12 m in the z-direction (the x axis was oriented from left to right, the y axis from bottom to top and the z axis represented the depth of the domain).

The number of mesh cells was 914.000. The usual mesh indicators (y^+ and skewness ratio) were applied to test mesh quality. The wall y^+ parameter was a non-dimensional parameter that indicated whether the mesh refinement close to the boundary condition was appropriate or not. The upper limit of y^+ was kept under 300 and the average value was 143. The average value of skewness was 0.097 and the maximum value was 0.81 for 24 cells.

The geometry and boundary assignment are presented in Table 3.2.

Table 3.2. Boundary and initial conditions

Boundary conditions	Type
Top domain surface	Sky temperature 256, 263, 273, 276 K
Bottom domain surface	Greenhouse soil heat flux 10, 25, 50, 100 W m^{-2}
Left domain surface	Inlet temperature 276 K and velocity 2 m s^{-1} at a height of 2 m (logarithm profile) (Richards & Hoxey, 1993)
Right domain surface	Outlet boundary conditions
Parallel domain surface (parallel to wind direction)	Symmetry

Initial conditions	
Temperature	280 K
Relative humidity	68%

Two sets of simulations were conducted. The first was used to validate the CFD model and the second to study the greenhouse humidity and temperature regimes for a range of boundary conditions that included the equivalent sky temperatures and SHF.

The CFD model was validated through a comparison between experimental values and simulated ones. Experimental data obtained from a datalogger were recorded every five minutes and stored in MySql database. A python utility was developed to retrieve data from the database and convert them to a Fluent compliant format before transferring them, as a plain text file, to the CFD program. Transient simulations were run with a time step of 60 s; each time step consisted of 300 iterations.

For the second set of simulations (i.e. use of the model), steady-state conditions were used for the range of boundary conditions shown in Table 3.2.

3.4.2 Greenhouse measurements

The greenhouse type and its location were the same as in Piscia et al. (2011) and all the sensors described were again used in this work. The only difference was the presence of a PE thermal screen, whose optical properties are described in section 2.2.1. This was fixed to the ridges and the temperature was measured using two thermocouple sensors (diameter µm 200, type T, RS components Ltd., Corby, UK). In the installation process, special attention was given to making the screen as airtight as possible.

The air temperature and humidity inside the greenhouse were measured using two air humidity and temperature sensors (Campbell hmp45c, Logan, UT, USA) which were located at a height of 2 m in the central spans; two thermocouples (diameter 200 mm, type T, RS Components Ltd., Corby, UK) were used to measure the roof temperature in combination with the previously mentioned thermocouples applied to the screen. The sensors used were: a net radiometer (Hukseflux NR01, Delft, The Netherlands), a temperature probe (Campbell, Pt100) for measuring soil surface temperature, and a heat flux sensor (Hukseflux hfp01sc, Delft, The Netherlands), located in the middle of the greenhouse. A pyrgeometer (Hukseflux IR02, Delft,

The Netherlands) and a hmp45c RH probe were placed outside but close to the greenhouse. A datalogger (Campbell CR10X, Logan, UT, USA) took measurements every 5 s and recorded 5 min averages.

Lettuce transpiration was measured using a weighing lysimeter (Mettler, KCC-150, capacity 150 kg, accuracy 1 g, Columbus, OH, USA). Attempts were made to establish a relationship between measured transpiration, VPD and greenhouse air temperature. However (as in the case of SL), no significant regressions were found among any of the variables considered: it was therefore decided to take the average transpiration value used in the SL work, which was 0.247 g s^{-1}, in order to make comparisons between the two CFD models. Outside data were taken from a meteorological station located approximately 50 m from the experimental greenhouse; the equipment used was: a net radiometer (Kipp & Zonen NR-Lite, Delft, The Netherlands), a temperature and humidity probe (Campbell hmp45c, Logan, UT, USA) and a wind anemometer (Campbell 05305-L, Logan, UT, USA) positioned at a height of 2 m above the ground. The meteorological station provided hourly averaged values.

The plastic used to make the thermal screen was different from that used as the cover material. The optical properties were measured using an emissometer (RD1, Devices and Services Company, Dallas, Texas, USA). The polyethylene plastic used as a screen had an emissivity value of 0.17, a transmissivity value of 0.51 and a reflectivity value of 0.32. The PE plastic used as the roof material had an emissivity value of 0.69, a transmissivity value of 0.19 and a reflectivity value of 0.12, as reported in Piscia et al. (2011).

3.5 Results

3.5.1 CFD Model Validation

3.5.1.1 Validation under transient conditions

The CFD model results were validated against experimental data relating to the night between 13th and 14th February 2011, when the equivalent sky temperature ranged from a minimum of -3.5 ^{o}C to a maximum of 10 ^{o}C (Fig. 3.1a). It can be observed that the outside air temperature was stable throughout the night while the sky temperature underwent a number of sudden changes, particularly after about 2:15 am. This night was chosen for the validation process as it

was considered to be the best for studying the transient behaviour of the CFD model. The validation process was based on comparisons of measured and CFD simulated values of four climate variables: cover, screen and inside air temperatures and the humidity ratio of the whole greenhouse volume. In the SC greenhouse the volume under the screen was used for validation.

The time trend of the previously mentioned variables is shown in Fig. 3.1, where the black lines represent CFD simulations and the red ones represent experimental data. Figures 3.1b and 3.1c show the cover and screen temperatures respectively, while Fig. 3.1d shows the greenhouse air temperature. The cover and screen temperatures followed similar time trends to the greenhouse air temperature, but the agreement between measured and simulated values was better (with a maximum differences of less than 1 ^{o}C for the cover and screen temperatures and up to 1.5 ^{o}C for the greenhouse air temperature).

The fact that the agreement was slightly poorer for the greenhouse air temperature can be explained by the influence of the front walls on the greenhouse climate: the CFD model considered that the front walls presented “symmetric boundary conditions”, implying that neither heat nor mass transferred through them. By doing so, the CFD model was intended to represent an infinitely long greenhouse along the z-axis. The experimental greenhouse was, in fact, 12 m long and the front-wall temperature may therefore have had an effect on the air temperature, which was not considered in the CFD simulations. Even so, and as discussed at the end of this section, the accuracy of the model can be considered sufficient for the goals of this study.

Figure 3.1 also shows the different responses of the greenhouse components to sky temperature. It can be observed that in the second part of the night, after a sudden change in sky temperature, the influence of sky temperature was strongest on the cover temperature, while its influence on the screen was smaller and its influence on the air even smaller as these were more strongly coupled to the SHF. The cover also reacted fastest to changes in sky temperature.

The agreement was particularly good during the first part of the night, but major differences were observed when the equivalent sky temperature was unstable. It seems the model was more accurate for clear sky conditions (low sky temperatures) than for overcast conditions (higher sky temperatures) and that maximum divergence occurred at 6:00 am when the sky temperature approached the outside air temperature.

Figure 3.1e shows the time trend of the measured and calculated humidity ratio. The difference increased during the first hour of the simulation. This difference is explained by the

fact that condensation in the CFD simulation started after about 20 minutes and then took more than half an hour to reach an equilibrium state. The difference was then maintained throughout the night, but did not increase. A possible explication for this difference could be related to the front-walls: in this experimental screened greenhouse, condensation was observed on the front walls (because the front walls can be cooler than the screen surface), while in the CFD model, the front walls were considered to be symmetrical, which would not have permitted the formation of condensation. This difference could also have been caused by the assumption of a constant rate vapour source; in the experimental greenhouse some variations in the vapour source rate may have occurred, but given the difficulties involved in measuring minor weight loses with the lysimeter, the vapour source was assumed to be constant throughout the night for the CFD calculations. However, the differences between the measured and calculated humidity ratios were only 0.001 kg/kg, which is about 15% of the values measured experimentally.

Assessment of the accuracy of the model

The model was assessed from a quantitative point of view using the root mean square error (RMSE).

This can be expressed as:

$$\sqrt{\frac{1}{n}\sum_{i=1}^{n}(y_{Mod,i} - y_{Data,i})^2} \qquad (3.4)$$

where *n* is the number of measurements (120), $y_{Mod,i}$ the simulated value at period i and $y_{Data,i}$ the measured value. For the CFD model, the RMSE values were:

inside temperature RMSE = 0.53 ^{o}C

screen temperature RMSE = 0.58 ^{o}C

cover temperature RMSE = 0.53 ^{o}C

humidity ratio RMSE = 0.00082 (kg/kg)

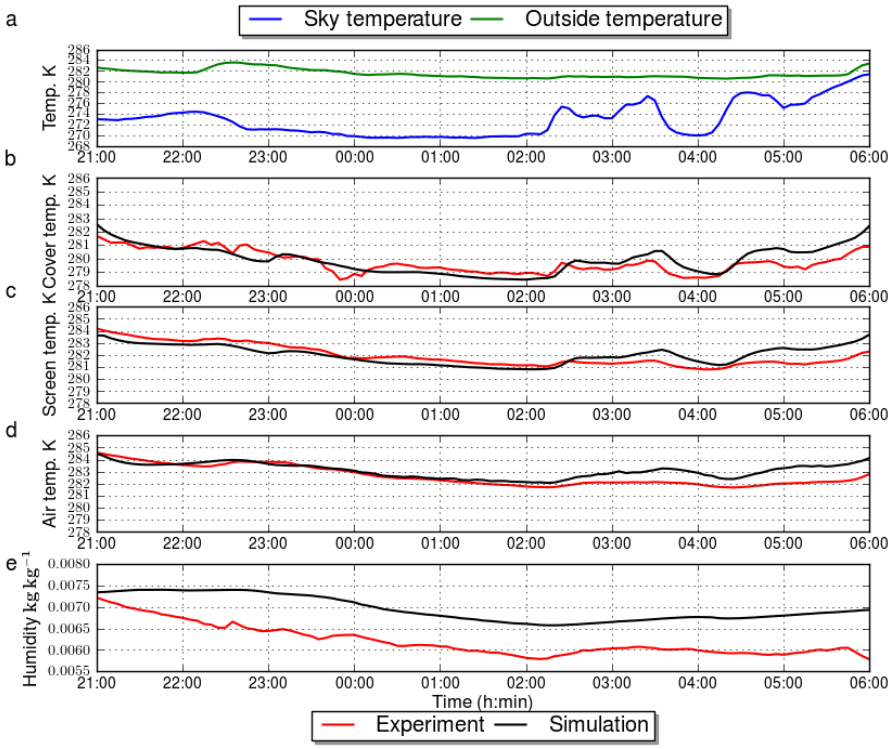

Fig. 3.1. (a) Equivalent sky temperature and outside temperature: experimental and simulated values of (b) cover temperature, (c) screen temperature, (d) air temperature, and (e) humidity ratio for the night of 13th-14th February 2011.

These values agree with the RMSE values reported by Baptista (2007), who developed a model for studying night-time humidity in single-layered greenhouses. As discussed by Baptista (2007), most greenhouse climate models have an RMSE of around 10%, which is within the limits of most of the variables considered for model validation in the present study.

3.5.1.2 Model validation under steady-state conditions

The response of the CFD model under steady-state conditions was validated against experimental values by comparing a number of relevant variables such as inside and screen temperatures. The data set from the experiments was larger than that used in the simulations; each experimental point corresponded to a 5-minute average of measurements and a total of 120 experimental points were used for comparisons. Since it was impractical to run 120 different computer simulations, it was decided to select a range of boundary conditions that could cover a similar range of simulated temperatures to that observed experimentally.

Inside and screen temperatures

Figure 3.2 shows a strong relationship between screen temperature and inside air temperature for the experimental and simulated values.

The regression analysis for the experimental results yielded:

$$t_{EXP,SC,inside} = 1.64 + 0.91 * t_{screen} \quad [^oC] \tag{3.5}$$

The R^2 value was 0.99 and the standard error 0.21^oC.

A similar regression for the simulated values was:

$$t_{CFD,SC,inside} = -0.118 + 1.24 * t_{screen} \quad [^oC] \tag{3.6}$$

The R^2 value was 0.96 and the standard error 0.33 ^oC.

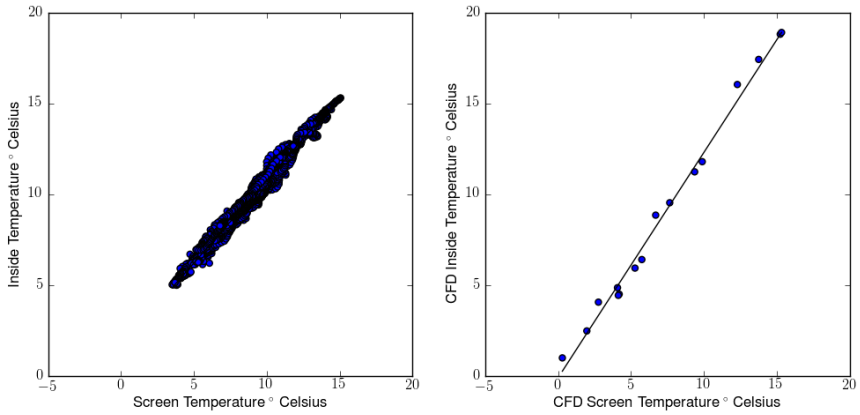

Fig. 3.2. Scatter plot for experimental SC values (left) and simulated values (right) of screen temperature (x axis) and inside temperature (y axis).

Humidity ratio and screen temperature

A previous study involving single layer greenhouses demonstrated that the humidity ratio depended mainly on the cover temperature (Piscia et al., 2011); therefore, the same pattern was also examined for the SC configuration. Whereas in SL greenhouses condensation mostly occurred on the greenhouse cover, in the SC greenhouse the screen is the surface that is most directly in contact with the greenhouse air; the water vapour produced by the crop therefore mainly condenses on the screen surface. As previously seen in SL, the humidity ratio primarily depended on the cover temperature, while for SC greenhouses, the humidity ratio mainly depended on the screen temperature. As shown in Fig. 3.3, the relationship between screen

temperature and humidity ratio was linear for both the experimental and the simulated data sets.

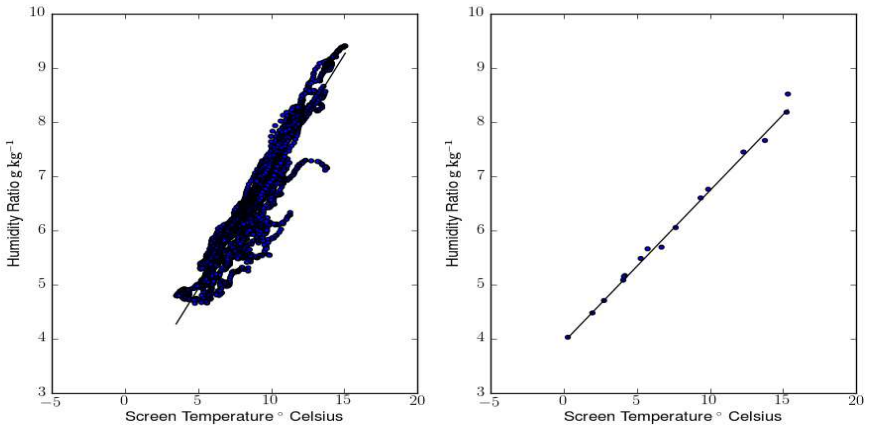

Fig. 3.3. Scatter plot for experimental SC values (left) and simulated values (right) for screen temperature (x axis) and humidity ratio (y axis).

For the experimental values, the regression line was:

$W_{EXP,SC}$= 2.75+ t_{screen}* 0.43 [kg kg^{-1}] (3.7)

The R^2 value was 0.93 and the standard error 0.26 kg kg^{-1}.

For the simulated values the regression line was:

$W_{CFD,SC}$ = 3.93 + t_{screen} * 0.28 [kg kg^{-1}] (3.8)

The R^2 value was 0.99 and the standard error 0.67 kg kg^{-1}.

Tests of Parallelism

In the previous sections, the linear equations between the humidity ratio and screen temperature were found for both CFD and experimental data. In this section, the aim was to statistically test whether the slope coefficients of the two linear equations were the same for the two populations (the CFD and the experimental population).

The procedure for testing the hypothesis that $b_{CFD;SC} = b_{EXP,SC}$ is described below:

I. Compute the estimated regression lines

$$\hat{Y}_{CFD,SC} = a_{CFD,SC} + b_{CFD,SC}X$$

$$\hat{Y}_{EXP,SC} = a_{EXP,SC} + b_{EXP,SC}X$$

II. Compute the residual mean square $s^2_{y\cdot x}$ (CFD,SC) and $s^2_{y\cdot x}$ (EXP,SC)

$$s^2_{y\cdot x} = \frac{\sum y^2 - \frac{(\sum xy)^2}{\sum x^2}}{n-2} \tag{3.9}$$

where $\sum x^2 = \sum_{i=1}^{n}(X_i - \bar{X})^2$, $\sum y^2 = \sum_{i=1}^{n}(Y_i - Y)^2$, $\sum xy = \sum_{i=1}^{n}(X_i - \bar{X})(Y_i - \bar{Y})$

III. Calculate the residual mean square:

$$s^2 = \frac{(n_1 - 2)s^2_{y\cdot x}(CFD) + (n_2 - 2)s^2_{y\cdot x}(EXP)}{n_1 + n_2 - 4} \tag{3.10}$$

IV. Calculate t-value

$$t = \frac{b_{CFD,SC} - b_{EXP,SC}}{\sqrt{s_p^2\left(\frac{1}{\sum x^2_{CFD,SC}} + \frac{1}{\sum x^2_{EXP,SC}}\right)}} \tag{3.11}$$

The t-value for the regression between the humidity ratio and screen temperature was 7.35 (but only 1.83 in the unheated case) and for the regression analysis between the inside temperature and the screen temperature it was 22.21 (only 0.95 in the unheated cases). The level of significance for both t-values was 0.001. As a result, the test hypothesis that both slopes are statistically similar can be accepted.

After comparing the simulated and experimental values for the screened greenhouse under transient and steady-state conditions, the CFD model can be considered capable of providing sufficiently reliable predictions of the main greenhouse climate variables. Consequently, this model is used for the following analysis of greenhouse climate and comparison of screened and single layer greenhouses**.**

3.5.2 Climate analysis of the screened greenhouse

3.5.2.1 Climate description under steady-state conditions

The greenhouse climate of the SC greenhouse was examined using the validated CFD model. Figure 3.4 and Fig. 3.5 respectively show a map of the temperature of a greenhouse cross section and a map of relative humidity. The conditions were: soil heat flux 21 Wm^{-2}, outside air temperature 281.2 K, equivalent sky temperature 270 K and wind speed 1.2 ms^{-1}. These conditions corresponded to data recorded at around 3 am on the night chosen for the validation process. This case represented the behaviour of SC unheated greenhouses under a partially-clear sky when the equivalent sky temperature was about 11°C lower than the outside air temperature.

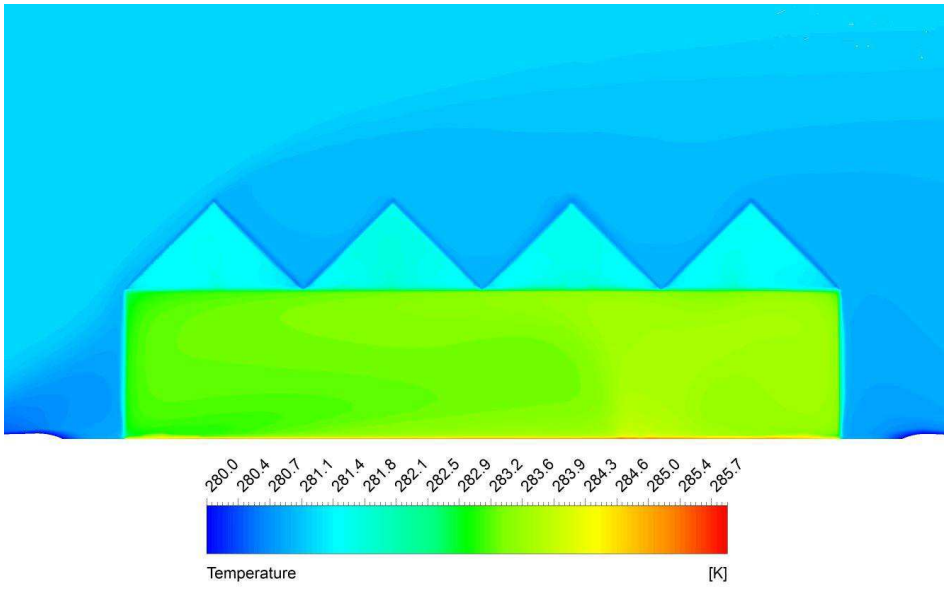

Fig. 3.4. Map of temperature in a screened greenhouse cross section

Figure 3.4 shows that the roof was the coolest surface of the greenhouse. In this case, the average roof temperature was approximately 280 K, which was about 1.2 °C lower than the outside air temperature. The fact that the roof was cooler than the outside air had been previously reported (Montero et al., 2004) and was mainly due to emission of thermal radiation from the cover.

The inside air temperature was more than 2 ^{o}C higher than the outside temperature, while the air temperature above the screen was almost identical to the outside temperature. An air chamber was created above the screen, which helped to insulate the greenhouse air from the colder roof. This temperature gain demonstrated the advantage of using an internal screen with respect to the single-layer greenhouse configuration. The temperatures of the sidewalls, which partially faced the sky and were directly in contact with outside temperatures, were about one degree colder than the inside air temperatures.

It can be observed that the temperature distribution inside the greenhouse was not homogenous. Differences in air temperature of up to 2 ^{o}C can be seen in Fig. 3.4, with the right-hand side being warmer than the left-hand side. This difference was caused by the wind blowing against the left side of the greenhouse and cooling the left wall by convection. A small area with a higher temperature was observed between the third and fourth spans. This was the result of the formation of two air circulation cells: an anticlockwise cell occupying the first three spans and a clockwise one in the fourth span. At the right end of the greenhouse, the outside temperature also appeared to be low because the outside air was slightly cooled after passing over the cool greenhouse roof. The difference between the end wall temperatures and the heat losses to the outside probably helped to create the two rotating cells inside the greenhouse.

In Fig. 3.4 it is also possible to observe that the soil surface was the warmest surface in the greenhouse. As previously reported (Montero et al., 2004), in unheated greenhouses the soil acts as the main energy source while the roof is the main energy sink.

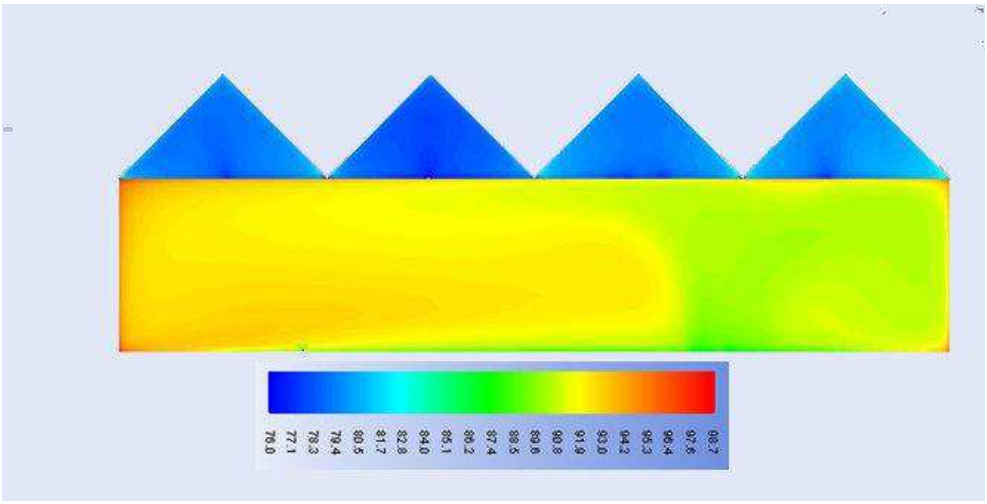

Fig. 3.5. Map of relative humidity in a cross section view of a screened greenhouse

The distribution of relative humidity (Fig. 3.5) showed a heterogeneity which was linked to that of the inside air temperature. Thus, the higher relative humidity on the left side corresponded to a colder inside area (due to the previously mentioned wind effect). The lack of a water vapour source and the assumption of total tightness in the areas above the screen would explain the lower relative humidity in these regions.

3.5.2.2 Relationships between relevant climate variables

From the range of CFD simulations, it was possible to obtain a number of expressions relating the greenhouse air, cover and screen temperatures and the relative humidity to the equivalent sky temperatures and soil heat fluxes. The equivalent sky temperature could be derived from data registered at neighbouring meteorological stations, while the soil heat flux could be directly measured or determined from the soil surface temperature. The regressions shown below can help in understanding the SC greenhouse climate and, in some cases, to predict the internal climate for control purposes.

Inside temperature

The equivalent sky temperature and SHF represented the relevant boundary conditions for the CFD simulations. Multi-variable linear regression analysis was therefore applied to main CFD steady-state climate variables and the results were applied the following equation:

$$t_{CFD,SC,\ inside} = 2.406 + t_{sky}*0.16 + SHF * 0.14 \quad [^{o}C] \qquad (3.12)$$

The R^2 value was 0.99 and the standard error 0.19 ^{o}C.

The inside temperature therefore had a positive linear relationship with SHF and sky temperature; as a consequence, an increase in either of these two factors is reflected in a linear increase in inside temperature.

Screen and cover temperatures

Screen and cover temperatures, as in the case of inside temperature, depend on the boundary condition values. Their values can also be used to estimate the humidity ratio (Piscia et al., 2011) and the inside temperature.

For these reasons, surface layer temperatures were analysed using a multi-variable linear regression with the relevant boundary conditions as estimators. The results are shown below:

$t_{CFD,SC,cover} = 2.22 + t_{sky}*0.21 + SHF * 0.04$ [^{o}C] (3.13)

The R^2 value was 0.99 and the standard error 0.21 ^{o}C.

$t_{CFD,SC,screen} = 2.46 + t_{sky}*0.16 + SHF * 0.12$ [^{o}C] (3.14)

The R^2 value was 0.76 and the standard error 0.42 ^{o}C.

From the above equations, it can be deduced that the cover temperature is more dependent on the equivalent sky temperature than on the screen temperature. However, it is less dependent on SHF than on screen temperature. This supports the observation mentioned in section 3.1.1 and shows that the heat flux path runs from the greenhouse soil to the internal air and then to the screen, roof cover and finally to the external air and sky.

Relative humidity

In the SL greenhouse, for any given night-time transpiration rate, relative humidity only depends on SHF (Piscia et al., 2011). Based on this conclusion, the same analysis was applied to the SC greenhouse. The regression analysis between SHF and RH obtained from the CFD simulations yielded:

$RH_{SC,CFD} = 101 – 0.4 * SHF$ [%] (3.15)

The R^2 value was 0.98 and the standard error 1.8 %.

The high R^2 value also demonstrated that the same rule applies in the SC configuration. In other words, as in the SL greenhouse, RH is strongly dependent on SHF and so an increase in SHF corresponds to a decrease in RH. This can be taken into account if the aim is to limit excessive RH.

3.5.3 SC Transient climate analysis

3.5.3.1 Condensation curve

The same pattern that was found for the SL model condensation curves (Piscia et al., 2011) was also applicable to the SC condensation curves. Indeed the condensation rate curve can be split into three parts: the initial phase, where condensation starts; the condensation rate growth phase, which under equilibrium conditions can be modelled by a logistic curve; and the steady-state phase, where the condensation rate is the same as the transpiration rate.

The general equation of a logistic function is given by:

$$f(x) = \frac{\chi}{(1 + e^{((-t+\alpha)/\beta))}} \tag{3.16}$$

where α is the location parameter which translates the logistic function with time , β is the scale parameter which has the effect of stretching out the graph and χ is the limiting value (asymptotic value).

Once condensation starts, for the whole set of boundary conditions under consideration, the condensation rate was described by a single logistic curve that represented all cases studied and whose β mean slope was 28.22 and whose α average parameter was 143.58.

Hence the general logistic curve can be modelled by the following logistic curve:

$$C_r(t) = \frac{0.247}{(1 + e^{((-t+143.58)/28.22)})} \tag{3.17}$$

This condensation rate curve can be compared to the corresponding curve for SL (Piscia et al., 2011), which was:

$$C_r(t) = \frac{0.247}{(1 + e^{((-t+65.89)/19.06)})} \tag{3.18}$$

From equations 3.17, 3.18 and Fig. 3.6, it can be seen that SL produced a steeper slope than SC. Once condensation started, it therefore developed more slowly in SC greenhouses. Even though SC and SL had the same vapour source rate per unit of floor area, the air volume was lower for SC because of the screen. The higher slope of SL could be explained by the fact that condensation in SL was produced on the inner roof surface, whilst in SC condensation occurred

on the side walls and the underside of the internal screen. Both of these surfaces are generally warmer than the roof surface since they are not so dependent on sky temperature.

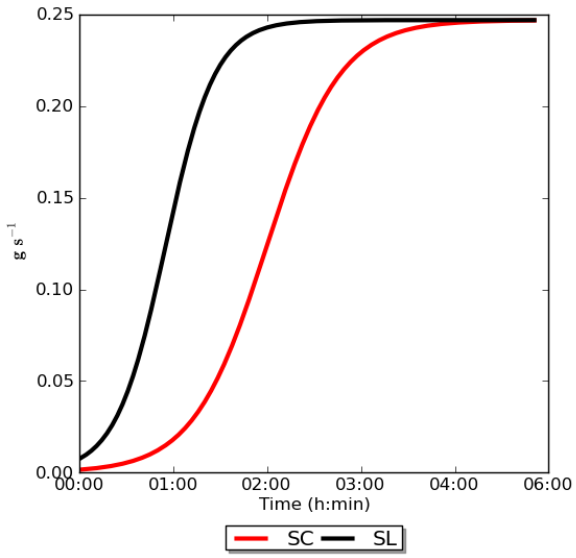

Fig. 3.6. General logistic condensation rate curve for SC and SL greenhouses

3.5.3.2 Model response to a step-change in a boundary condition

In order to assess the response of the SC model to sudden changes in some of the relevant boundary conditions, a two step-change simulation was run (both step changes are plotted in Fig. 3.7). The initial conditions were: 263 K as the equivalent sky temperature and 50 W m^{-2} as the SHF. After 144 time-steps of five minutes (a time period of 12 hours), a change from 263 to 276 K in the equivalent sky temperature was applied to the CFD runs. This change was intended to represent a sudden variation in sky cloudiness. It should be remembered that solar radiation was not considered in these analyses as the study was concerned only with the night-time climate. After an additional 144 time steps, a second change was made to the SHF, switching it from 50 to 100 W m^{-2}. This change represented a sudden increase in heating power, which is a situation likely to happen if additional heating is turned on.

Figure 3.7 shows the transient response of the SC greenhouse to the two boundary condition step changes. For all the variables under consideration, a steady state value was reached after some initial fluctuations; after each step-change, the main variables presented a sudden change which moved the variables to new steady-state values. These last responses were due to the fact that none of the greenhouse components (roof, screen and air) had considerable thermal inertia.

For the first step-change (sky temperature), the roof showed a greater change than either the screen or the air temperature. In contrast, for the second step change (soil heat flux), the greenhouse air and screen temperatures reacted more than the roof temperature (Fig. 3.7b). Such responses show that the model produced results which were compatible with the physics of the situation. As expected, the greenhouse component that was closest (in terms of heat and mass transfer processes) to the boundary condition which changed (for instance, the roof for the first step-change) reacted most directly to the new boundary condition and modulated the response of the other components (the screen and greenhouse air).

The relative humidity response was very similar to the greenhouse air response (Fig. 3.7c). An increase in greenhouse air temperature produced a decrease in RH. For the second step change, the RH dropped quickly and then recovered a little before reaching a new equilibrium. Figure 3.7c shows the time trend for the condensation rate. As with the RH, the condensation rate reacted quickly to a change in air temperature. For both time-step changes, the final condensation rate was very close to the water vapour rate: under steady-state conditions, the same amount of vapour produced by the crop was condensed on the greenhouse screen and walls while the humidity ratio of the greenhouse air (not shown for brevity) remained unchanged.

The time lag for the RH and condensation curves relative to the temperature responses to the SHF change can be explained by the increase in screen temperature produced by the increase in SHF. The screen temperature controls the absolute humidity in the greenhouse and the condensation rate. It is possible that after the step change in SHF, the screen temperature can be very close to, or even above, the dew point temperature; as a result, the condensation rate was slow or zero. The CFD model assumed a constant water vapour source rate and so condensation did not progress until enough water vapour was given to the greenhouse air, and this required some time. Under real conditions the crop would probably transpire more when the air temperature increases and the VPD would also increase, so the time response of humidity and condensation to a step change would be reduced. However, such a variable vapour source was not considered in this CFD model.

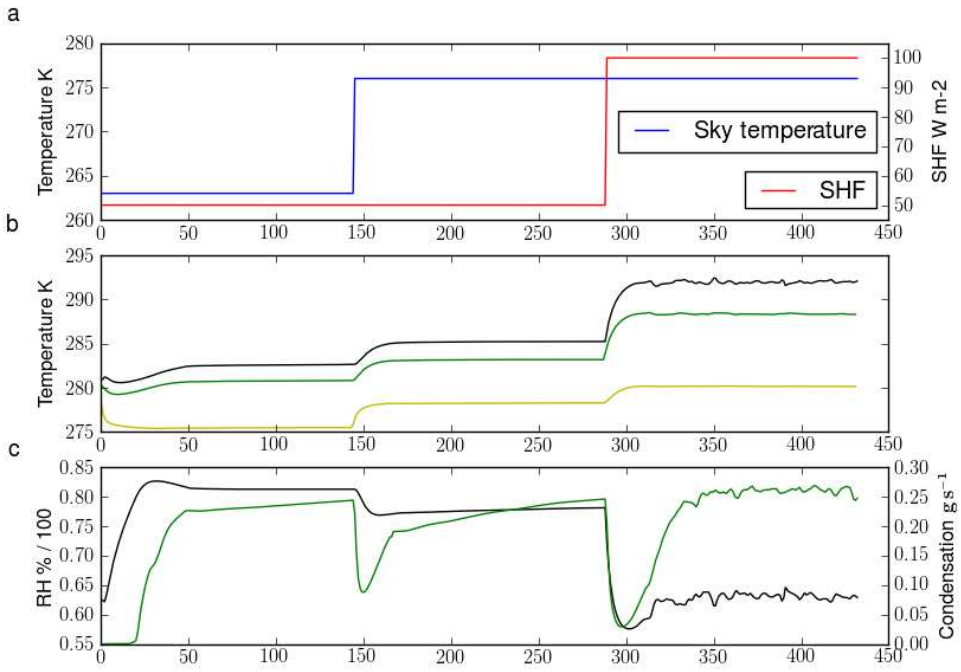

Fig. 3.7. Model response to a step change in a boundary condition. (a) Step change of equivalent sky temperature and SHF, (b) time trend of inside temperature (black line), screen temperature (green line) and roof temperature (light-brown line), (c) relative humidity (black line), and condensation rate (green line).

3.5.4 Comparison of screened and single layer greenhouses

The rationale for using a thermal screen is to increase the inside temperature with respect to the SL case by passive means in unheated greenhouses and to save energy in heated greenhouses. To compare SC and SL, data for SL were taken from the study by Piscia et al. (2011) which was conducted during February-March 2010 in the same experimental greenhouse, but without the internal screen.

3.5.4.1 Greenhouse air temperature

In both SC and SL greenhouses, the link between T_{int} and T_{out} (not shown for brevity) was strong. For the range of experimental conditions, T_{SC} was always higher than T_{SL} for any given T_{out}. For unheated greenhouses, the maximum difference occurred with the lowest T_{out}, for which SC was about 1.5 ^{o} C higher than SL.

Equation 3.14 for the SC greenhouse can be compared to the corresponding regression equation for the SL house:

$$t_{CFD,SL,\ inside} = 3.13 + t_{sky}*0.26 + SHF * 0.10 \quad [^{o}C] \quad (3.19)$$

The R^2 value was 0.99 and the standard error 0.1 ^{o}C.

If the estimator coefficients of the single layer and screened equations are compared, the following conclusions can be drawn:

1. The t_{sky} estimator coefficient is higher in the SL than the SC greenhouse. This confirms that the use of internal screens weakens the relationship between the inside and sky temperatures because the screen isolates the greenhouse air from the sky conditions.
2. The SHF estimator coefficient is lower in the SL house than the SC. This means that the inside temperature is more sensitive to the SHF value in the SC greenhouse.

Thermal inversion (when the greenhouse temperature is lower than the outside air temperature) has been previously reported in SL greenhouses (Piscia et al., 2011). Figure 3.8 presents the combination of boundary conditions (namely t_{sky} and SHF) associated with thermal inversion in the SL and SC greenhouses. The blue area shows the conditions for which thermal inversion takes place in SC greenhouses. It can be seen that for a SHF of more than 17 W m^{-2}, thermal inversion does not occur, even on clear nights (with sky temperatures equivalent to -17 ^{o}C). In contrast, thermal inversions are more likely to occur (green area) in SL. For instance, under clear night conditions (t_{sky}= -17 ^{o}C), a minimum SHF of 40 W m^{-2} is required to prevent thermal inversion. To the best of our knowledge, no such SHF values have been reported in any unheated greenhouses. From Fig. 3.8 it is possible to deduce the advantages of SC over SL in terms of greenhouse air temperature.

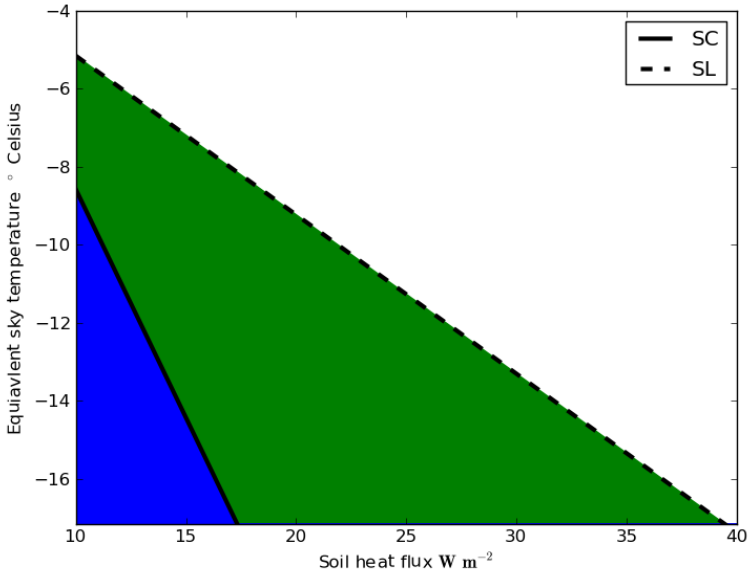

Fig. 3.8. Combination of boundary conditions for which thermal inversion occurs in SC (blue area) and SL (green area) greenhouses.

3.5.4.2 Relative humidity

In the SL greenhouse relative humidity steady-state values were independent of equivalent sky temperature and dependent on SHF. The relationship which quantifies this relationship is:

$RH_{SL,CFD} = 102 - 0.34 * SHF$ [%] (3.20)

The R^2 value was 0.99 and the standard error 1 %.

The constant was almost identical to the SC relationship (eq. 3.15), while the SHF coefficient was lower than that of the SC greenhouse. For the same SHF, the SC greenhouse had a lower RH. One possible interpretation of this is that with the same heating power in a SC greenhouse, it is possible to obtain a lower RH since the air temperature is higher.

3.6 Discussion

Energy saving in greenhouses was a key issue during the energy crisis of the late 1970s and mid 1980s. At that time effort was devoted to studying the performance of thermal screens in heated greenhouses. The CFD model presented in this article was developed with the intention

of producing a more detailed study of the SC greenhouse climate, since previously reported analyses had mostly been based on macroscopic energy balances or full scale experimentation. The CFD model offered the possibility of simulating physical situations which occur under real conditions. It therefore becomes possible to make short-term studies of different climatic situations and operational parameters. One significant contribution of CFD models is that by running a set of simulations, it is possible to derive statistical regressions between relevant variables of greenhouse climate from the CFD results; we, for example, obtained a closed regression between screen temperature and greenhouse humidity. We observed that the screen was the major sink for energy and humidity (since it was the major condensation surface) of the greenhouse air. Such relationships between variables should help us to improve our understanding of SC greenhouse climate. They should also help to improve the predictive control of SC greenhouse climate if such relationships can be built into a suitable control system.

CFD modelling has also permitted the study of internal climate uniformity. Different areas with different temperatures and humidities were identified inside the SC greenhouse. We observed that the screen created a cold air chamber in the area delimited by the roof and the screen. In some cases, this area was colder than the outside air, particularly when infrared radiation losses prevailed over convective losses. The chamber acted as a buffer and weakened the dependence between inside climate and sky temperature since it isolated the crop area from the exterior conditions. This could, however, be detrimental if for some reason the cold air were to enter the crop area. Some ventilation would probably be needed to increase the temperature in the cold chamber. An external screen of the type used in some greenhouses for shading (Lorenzo et al., 2004) could also help to eliminate the cold chamber. However, neither of these alternatives has been investigated in this study.

This article has focused on comparisons between SC and SL greenhouses, particularly for passive unheated greenhouses. One problem which affects unheated SL greenhouses at night in winter is thermal inversion; this study has shown that internal screens greatly reduce the situations in which thermal inversion can take place.

Furthermore, radiation exchanges between the cover and the plants are reduced by the presence of the screen; this results in higher plant temperature for any given air temperature. Preventing thermal inversion will increase air temperature which will lead to an additional increase in plant temperature, above that obtained as a result of the reduction of radiative losses. Temperature gains in unheated greenhouses ranged from 2 ^{o}C for a clear sky to almost zero for an overcast sky. Indeed in a very clear sky scenario, with a sky temperature about 17

^{o}C lower than the outside temperature, a SC greenhouse can prevent a thermal inversion with a SHF of about 17 W m^{-2}, while for the same scenario, in an SL greenhouse a SHF of about 40 W m^{-2} will be required.

In terms of humidity, the comparison between SC and SL greenhouses showed that thermal screens slightly reduced relative humidity despite the humidity ratio being higher for the SC greenhouse. This would be explained by the higher temperature of the screen and the greenhouse air under the same boundary conditions. This result could seem controversial since it is generally believed that screens tend to increase RH. A possible explanation for this apparent discrepancy is that screened greenhouses tend to be more air tight that single layer greenhouses and would therefore tend to be more humid. This would be particularly true in the case of heated greenhouses in cold areas, where the internal absolute humidity would be high and the value outside would be low. In a real life situation, there is likely to be some air exchange through the screen and the greenhouse cover, but in CFD modelling it is rather difficult to consider infiltration losses. In the previous study conducted for SL greenhouses (Piscia et al., 2011), it was estimated that infiltration would account for nearly 15% of night-time transpiration. It is thought that modelling infiltration losses requires further research but could potentially increase the accuracy of the model presented in this paper.

It is important to mention that crop transpiration was simulated as a constant water vapour source. Night-time transpiration would not be the same for screened and single layer greenhouses and this could also justify attributing a lower level of RH in screened greenhouses. Night-time transpiration modelling is, however, a difficult task; transpiration rates tend to be low at nights it is therefore difficult to measure transpiration with a lysimeter. Attempts were made to establish experimental regressions between measured transpiration rates, greenhouse temperatures and humidity levels and also net radiation values, but none of these attempts were successful; we therefore decided to use a constant value reported in a previous study. The accuracy and applicability of the model could be enhanced by replacing the constant source with a night-time crop transpiration model; there are plans to do this in future research activities.

As in the SL model (Piscia et al., 2011), the SC model produced condensation rate curves which could be accurately modelled by a single logistic function representing a wide range of boundary conditions. The condensation curves showed that condensation progressed more slowly in the SC greenhouse; this is another potential advantage of this type of greenhouse.

One drawback of using a fixed thermal screen is the reduction in PAR transmission, which could have a negative influence on crop growth; this problem could be avoided by using a

moveable shading system, though this would have the drawback of requiring a greater initial investment in the installation.

The present CFD model paves the way for a possible optimization of night-time greenhouse climate involving only a small energy input; it is possible to optimize the optical cover properties as new covering materials, such as ultrathermic films (Kempkes and Hemming, 2010), now available, which are particularly opaque to far IR and potentially interesting for use in both heated and unheated greenhouses. It is also possible to optimize soil mulching by increasing the soil heat flux, because at night the soil is the major energy source in unheated greenhouses. Greenhouse geometry (roof slope, greenhouse width and height) may also play a role in night-time climate; a parametric study of greenhouse geometry with a view to optimizing energy use is therefore another area of research that the methodology presented in this paper could investigate.

3.7 Conclusions

A comprehensive analysis was made of screen greenhouses at night, with CFD model results being validated against experimental data. This analysis also took into account humidity by including transpiration and condensation.

Simulated and experimental results showed linear correlations between cover temperature, air temperature and air humidity and external conditions.

A thorough comparison between CFD results obtained from a single-layer and a screened greenhouse was presented; advantages in terms of temperature gains were apparent, both in terms of steady-state and transient results.

The global condensation rate curve was modelled and compared to a single layer curve.

The response of the model to a sudden step-change in equivalent sky temperature and SHF was also tested.

Acknowledgements

The work presented here was carried out within the project EUPHOROS: the European Commission, Directorate General for Research, 7th Framework Programme of RTD, Theme 2 e Biotechnology, Agriculture & Food, contract 211457. This research was also supported by INIA

(project RTA2008-00109-C03) with contributions from the FEDER funds. Thanks are also given to INIA fellowship FPI-INIA.

3.8 References

Ansys (2009). User guide 12.0. Lebanon, NH, USA.

Bailey, B. J. (1981). The reduction of thermal radiation in glasshouses by thermal screens. Journal of Agricultural Engineering Research, 26(3), 215-224.

Bailey, B. J. (1988). Control strategies to enhance the performance of greenhouse thermal screens. Journal of Agricultural Engineering Research, 40(3), 187-198.

Baille, A.,Aries, F., Baille, M., & Laury, JC. (1985). Influence of thermal screen optical properties on heat losses and microclimate of greenhouses. International symposium greenhouse climate and its Control, Acta horticulturae, 174, 111-118.

Baptista, F. J. F. (2007). Modelling the climate in unheated tomato greenhouses and predicting Botrytis cinerea infection. Ph.D. thesis, Univerisade de Evora, Portugal.

Boulard, T., & Wang, S. (2000). Greenhouse crop transpiration simulation from external climate conditions. Agricultural and Forest Meteorology, 100(1), 25-34.

Bournet, P., Ould Khaoua, S., & Boulard, T. (2007). Numerical prediction of the effect of vent arrangements on the ventilation and energy transfer in a multi-span glasshouse using a bi-band radiation model. Biosystems Engineering, 98(2), 224-234.

Iglesias, N. (2005). Estudio de condiciones térmicas y lumìnicas y determinación de alternativas tecnológicas para el ahorro de energía en invernaderos de la Patagonia norte – Argentina . Ph.D Thesis, Univerisade de LLeida, Spain.

Kempkes, F. L. K., & Hemming, S. (2010). Calculation of NIR effect on greenhouse climate in various conditions. *IHC* 22-27 August 2010, Lisbon, Portugal., 927,543-550.

Körner, O., & Holst, N. (2006). Model based humidity control of Botrytis in greenhouse cultivation. International Conference on Sustainable Greenhouse Systems-Greensys, 691,141-148.

Lorenzo, P., Garcia, M.L., Sanchez-Guerro, M.C., Medrano, E., Caparros, I., & Giménez, M.(2006). Influence of mobile shading on yield, crop transpiration and water use efficiency. International Symposium on Greenhouse Cooling, 719,471-478.

Montero, J. ,Munoz, Anton, A., & Iglesias (2004), N. Computational fluid dynamic modelling of night-time energy fluxes in unheated greenhouses. International Conference on Sustainable Greenhouse Systems-Greensys 12-16 September 2004, Louvain, Belgium 691, 403-410.

Nijskens, J., Deltour, J., Coutisse, S., & Nisen, A. (1984). Heat transfer through covering materials of greenhouses. Agricultural and Forest Meteorology, 33(2-3), 193-214.

Piscia, D., Montero, J.I., Baeza, E., & Bailey, B.J.(2011). A CFD greenhouse night-time condensation model. Biosystems Engineering, 111(2),141-154.

Richards, P. J., & Hoxey, R. P. (1993). Appropriate boundary conditions for computational wind engineering models using the k-ϵ turbulence model. Journal of Wind Engineering and Industrial Aerodynamics, 46, 145-153.

Silva, A.M. ,Miguel, A., & Rosa, R.(1991). Thermal radiation inside a single span greenhouse with a thermal screen. Journal of agricultural engineering research, 49, 285-298.

Teitel, M., & Segal, I.(1995). Net thermal radiation under shading screens. Journal of agricultural engineering research,61(1),19-26.

Teitel, M. ,Peiper, UM., & Zvieli, Y. (1996). Shading screens for frost protection. Agricultural and forest meteorology, 81(3-4),273-286.

Versteeg, H., & Malalasekera, W. (1995).An introduction to Computational fluid dynamics: the finite volume method, Longman Group.

4 A new optimization methodology used to study the effect of cover properties on night-time greenhouse climate.

The contents of this chapter have been submitted to Biosystem Engineering as a paper entitled: A new optimization methodology used to study the effect of cover properties on night-time greenhouse climate.

Davide Piscia, J. I. Montero, , B. J. Bailey, P. Muñoz, A. Oliva.

4.1 Abstract

This study presents an optimization method for improving greenhouse design. The approach was based on the surrogate-based method and combines the use of energy balance simulation (ES) and CFD. The optimization was applied to study the effects of cover properties on the night-time greenhouse climate. The ES model was verified by comparing its predictions with experimental data. The RMSE values for internal temperature and humidity showed there was good agreement between the ES and experimental values. The optimization process highlighted the importance of using a low emissivity and low transmissivity cover material. Under a clear sky the predicted temperature gain by using a high reflectance material compared to a regular one on an unheated greenhouse was approximately 4 ^{o}C. The relative humidity in the same scenario was reduced by almost 10%. Two ES parametric studies were carried out, the first showed the effects of different combinations of thermal radiation properties in term of temperature and humidity; the second showed the effects of the high reflectance material in different external conditions (equivalent sky temperature and soil heat flux (SHF)). This paper suggests that ES and CFD can be used together to provide a complete approach to greenhouse modeling.

4.2 Nomenclature

A area (m^2)

c_p heat capacity at constant pressure (J kg^{-1} $^oC^{-1}$)

DOM discrete ordinate model

ES energy balance simulation

$F_{i->j}$ view factor between surfaces j and i

g incident radiation flux (W m^{-2})

GPS general pattern search

h enthalpy condensation (J kg^{-1})

j outgoing radiation flux (W m^{-2})

k turbulence kinetic energy (m s^{-2})

M absolute humidity content (kg)

n number of measurements

p pressure (Pa)

PAR photosynthetically active radiation

PE polyethylene

PSO particle swarm optimization

q heat flux (W m^{-2})

Q absolute heat flux (W)

RMSE root mean square error

RH relative humidity (%)

S_ρ mass source

S_U momentum source

S_T heat source

SHF soil heat flux (W m^{-2})

t time (s)

T absolute temperature (K)

u velocity component of the x coordinates (m s^{-1})

$\vec{U}$ velocity vector (m s^{-1})

UDF user defined function

w humidity ratio (kg kg^{-1})

y^+ non-dimensional distance indicator

$y_{Data,i}$ experimental value at time i

$y_{Mod,i}$ simulated value at time i

α convective heat transfer coefficient (W m^{-2} $^oC^{-1}$)

ε emissivity

ε_{tur} turbulence kinetic energy dissipation rate (m^2 s^{-3})

λ thermal conductivity (W m^{-1} $^oC^{-1}$)

μ turbulent viscosity (kg m^{-1} s^{-1})

ρ density (kg m^{-3})

τ transmissivity

ξ reflectivity

σ Boltzmann constant 1.3806503 × 10^{-23} (m^2 kg s^{-2} $^oC^{-1}$)

Ω condensation rate (kg s^{-1})

Γ_{crop} transpiration rate (kg s^{-1})

ψ constant transpiration rate (kg m^{-3} s^{-1})

Subscript

a dry air

air greenhouse air

air_out outside air

conv convective

cov_in inner cover

cov_out outer cover

Exp experimental

face_in inner face

face_out outer face

rad radiation

sid_in inner sidewall

sid_out outer sidewall

soil_in greenhouse soil

w H_2O

4.3 Introduction

Most greenhouses and crop protection structures used in the Mediterranean area as well as in many other greenhouse areas are unheated; during cold periods the night-time temperature can be too low and far from optimal for most crops. Low temperature is often associated with high humidity and crops exposed to high humidity levels present a higher risk of developing fungal diseases (Bakker, 1991).

In terms of heat transfer, one major consequence of not heating is that while convective heat exchange is the most relevant heat transfer process in heated greenhouses, in unheated ones radiative exchanges prevail. This effect is particularly evident during clear nights where the greenhouse air temperature can be lower than the outside air. This is caused by the fact that the greenhouse cover emits more infrared radiation than it receives from the sky. During a clear winter night, the equivalent sky temperature can be 20 ^{o}C lower than air temperature and as a consequence the cover can be up to 3 ^{o}C cooler than the outside air (Piscia, Montero, Baeza & Bailey, 2011).

Therefore, any means of weakening the relationship between the inside and sky is of great importance, particularly if this is achieved by passive means without external heating.

One of the most frequently used solutions is the placement of a thermal screen.

Thermal screens were extensively studied during the period 1978 to 1988. One of the most relevant studies was published by Bailey (1981) showing that it is desirable to install a screen with low transmissivity to far infrared radiation (τ) and low emissivity (ε).

A paper on this subject was published by Montero, Muñoz, Anton and Iglesias (2004), the climate was studied by means of CFD modelling. A major conclusion was that using a screen can induce increases in air temperature of around 2.8 ^{o}C on clear nights in unheated greenhouses.

The main drawback of using a thermal screen is the loss of PAR transmission (Vanthoor, 2011) in the case of a fixed screen.

In addition to thermal screens, another possible solution is selecting the cover material in order to reduce the heat loss due to radiative exchange. Nijskens, Deltour, Coutisse and Nisen (1984) analyzed the effects of radiometric properties on heat losses, and concluded that the primary interest for thin materials (where thermal conductivity can be neglected) was to reduce transmittance and increase the reflectance on both sides of single-layer plastic. These results are based on heat and mass balance equations applied to a flat plane (cover) facing another plane (representing the sky). Several values of global heat transfer coefficient were plotted as function of different pairs of transmittance and reflectance. The paper provided a quantitative assessment of thermal radiation properties of several commercial covering

materials. However the paper did not aim to study the effect of different optical properties for a given greenhouse within a specific climate framework.

The selection of the most suitable covering material can be done by applying an optimization process or parametric study to a greenhouse model. Most optimization papers applied to greenhouse design used energy balance simulations (ES) (Engel, 1984; Vanthoor, 2011) also referred as perfectly stirred tank approach (Roy, Boulard, Kittas & Wang, 2002). ES models are based on the homogeneity assumption, which considers uniform distribution of the greenhouse climate variables, and rely on semi-empirical formulae to compute convective heat transfer coefficients and ventilation rate (Roy et al., 2002).

A different approach to optimizing greenhouse design is to use CFD modelling. For instance Kacira, Sase and Okushima (2004) used CFD to optimize wind-induced ventilation by selecting different greenhouse vent configurations. CFD models can simulate the heterogeneity of climate, air movement, etc., but are complex to configure and have very high computational cost making it extremely difficult to couple directly them to an optimization algorithm; Therefore, CFD has been used mainly to carry out detailed studies of given space under a number of specific boundary conditions (parametric study) .

A hybrid approach is the surrogate-based method of optimization which provides a way to achieve high-fidelity design optimization at reduced computational cost by using a high-fidelity model in combination with lower-fidelity models that are less expensive to evaluate (Robinson Eldred, Willcox & Haimes, 2008). Surrogate (low-fidelity) models are inexpensive approximate models that are intended to capture the relevant features of an expensive high-fidelity model. The low-fidelity or surrogate model can be derived directly from data (polynomial regression, Taylor series expansion, multivariate adaptative regression splines, etc.), be multifidelity (a model that is still physics-based but is of lower fidelity), or a reduced-order model surrogate.

This study presents a multifidelity surrogate-based method optimization applied to greenhouse design, where the ES model was used as the low-fidelity model and the CFD model as the high-fidelity model. The ES model was considered as the surrogate model for two reasons, the assumption of homogeneity, and the reliance on semi-experimental convective heat transfer coefficients which are difficult to choose from the literature without a previous experimental study.

The purpose of this work is twofold. Firstly it develops an optimization method applicable to greenhouse design by using CFD and ES models. Secondly it applies the methodology to study the effects of optimal thermal properties on the night-time climate, specifically in terms of temperature, humidity and condensation.

4.4.1 Simulations

In this study a combination of ES and CFD (Fluent 13.0, Ansys, 2009) simulations was used. The design optimization was carried out in two stages; in the first stage the optimization programme (Wetter, 2009) was coupled to an ES model to find the optical properties which minimized RH . In the second stage, the CFD model was used to simulate the proposed solution and provide detailed information on the optimal case.

4.4.1.1 Optimization

The idea was to optimize a low-fidelity model (ES) and then apply the optimization result to a high-fidelity model (CFD) (Robinson et al., 2008).

The low-fidelity model, ES, is a well-behaved response function (which is smooth, unimodal, and only mildly nonlinear) and as a consequence there was no need to implement correction methods to ensure convergence.

The optimization process used a combination of two algorithms, this selection was based on an article by (Peeters, Wetter & Ferguson, 2010). This showed that when the cost function to be optimized is the output of an energy simulation program, an efficient, reliable and robust strategy is to use a combination of two algorithms.

The first is the Particle Swarm Optimization (PSO) algorithm and the second is the Generalized Pattern Search (GPS). A full description of these algorithms can be found in Wetter (2009). Here only the most important characteristics are explained.

The PSO algorithm randomly generates a score of initial points to be used, each point is called a particle and all points form the population. The first population is randomly generated to distribute the particles uniformly in parametric space. The algorithm moves towards the optimal point by using an update equation, which is derived from the social behaviour of members of bird flocks. PSO algorithms are global optimization algorithms and are gradient-free methods. The advantage of these algorithms is that they can explore a large space and reach a point close to the global minimum; the drawback is that they need a lot of time to refine the solution, this behaviour is caused by the fact that they are inherently stochastic.

GPS algorithms perform well in small region; they determine the parameter values for the next iteration based on the local descent. GPS algorithms split the domain space into a mesh and search on this mesh for a decrease in the objective function. If no further decrease can be obtained, the mesh is refined and another search is made, starting from the currently best known iterate. This process provides convergence to a local minimum under appropriate smoothness conditions.

The initial starting point of the GPS algorithm was the optimal point found by the PSO search.

The advantage of combining the GPS and PSO algorithms is that the GPS algorithm refines the local space much faster than the PSO one.

The ES model provided outputs for four greenhouse variables: inside air temperature, cover temperature, condensation rate and internal air humidity content. In order to configure the optimization process ideally only one variable has to be selected, or alternatively a weighted sum of two or more output variables; the latter approach presents the difficulty of choosing correct and relevant weighting factors.

In order to take into account more than one variable and to avoid the choice of weighting factors, it was decided to take relative humidity as the output variable to be minimised; indeed relative humidity is a function of temperature and humidity content, and moreover is a key element in climate management.

The properties to be optimized were the transmissivity and emissivity of the cover material.

Table 4.1 shows the conditions used in the optimization process.

Table 4.1 Optimization process conditions

Optimization settings	**Value**
Low-fidelity system	ES model
High-fidelity system	CFD model
Reference scenario	256 K, equivalent sky temperature and 25 W m^{-2} SHF
Variables	τ optical transmissivity and ε absorptivity of cover material
Variables bounds	2.5% <= τ <70% 2.5% <= ε <70%
Variables constraint	$\tau + \varepsilon <= 95\%$
Cost function to minimize	Min RH=f(τ , ε)

4.4.1.2 Energy balance system (ES)

This program was based on the resolution of energy and mass conservation in a large volume.
The ES models in the greenhouse literature are also referred to as the perfectly stirred tank approach. This requires the assumption of uniform temperature, humidity and CO_2 content inside the greenhouse and uses a 'big leaf' model to treat the plant canopy and describe the exchanges of latent and sensible heat with the inside air (Roy et al., 2002).
ES models have the advantage of being faster than CFD models and easier to configure and handle, but they also present some drawbacks, among which is their reliance on empirical (or semi-empirical) formulae for the determination of convective transfer coefficients and ventilation rate computation. A complete comparison between the ES and CFD approaches was made by Zhai and Chen (2005).
One conclusion was that CFD convective coefficient predictions can be used to make the ES model more robust and accurate, and to be less experiment dependent.
The main programming language used was C++, but many added features were implemented in Python. The aim was to implement computationally heavy operations in a compiled language as C++, and implement the others functions in a more intuitive and integrated language such as Python.

Convective heat transfer coefficients

Convection heat transfer is one of the most important mechanisms of heat exchange in greenhouses. Convective exchanges occur between the cover, the soil and the interior air and between the cover and the exterior air. The process of heat transfer is governed by a combination of forced convection (due to the wind pressure) and free convection, due to buoyancy forces caused by temperature differences between the solid surfaces of the walls, the soil, the plants and the inside air. These two convection modes are dependent on greenhouse type, outside climate and ventilation conditions. In well ventilated greenhouses, forced convection is dominant, due to strong air movement. In tightly closed greenhouses, natural convection is the dominant process, and induces very low interior air velocities.
In this paper the greenhouse studied was tightly closed, hence natural convection coefficients were used. As previously mentioned, the choice of correct convective heat transfer coefficients (together with ventilation rate formulae) makes ES more prone-error or more experiment dependent.

In order to overcome this problem, CFD simulations of the same greenhouse under the same boundary conditions were made. The convective heat transfer coefficients for the inner cover surface, outer cover surface and greenhouse soil surface were extracted from the CFD results and used as a benchmark for comparison with published coefficients. Details of this comparison can be found in Piscia (2010). From this comparison the following equations were used in the macro model.

$$\alpha_{\mathrm{cov}\_in\rightarrow air} = 2.21\,(T_{\mathrm{cov}\_in} - T_{air})^{0.33} \qquad [\mathrm{Wm^{-2}\,{}^{o}C^{-1}}] \qquad (4.1)$$

Papadakis, Frangoudakis and Kyritsis (1992)

$$\alpha_{soil\_in\rightarrow air} = 1.86\,(T_{soil\_in} - T_{air})^{0.33} \qquad [\mathrm{Wm^{-2}\,{}^{o}C^{-1}}] \qquad (4.2)$$

De Halleux (1989)

$$\alpha_{\mathrm{cov}\_out\rightarrow air\_out} = 0.95 + 6.76\,v^{0.49} \qquad [\mathrm{Wm^{-2}\,{}^{o}C^{-1}}] \qquad (4.3)$$

Papadakis et al. (1992)

Details of the equations used in the ES implementation are given in the Appendix.

4.4.1.3 CFD

Numerical method

The CFD model solves the governing equations of momentum, energy and continuity applied to the greenhouse. The momentum equation, also known as the Navier-Stokes equation is obtained by the application of Newton's law of motion to a fluid element:

$$\frac{\partial \rho u}{\partial t} + \nabla \cdot (\rho \vec{U} u) = \nabla \cdot (\mu \nabla u) - \frac{\partial p}{\partial x} + S_U \qquad (4.4)$$

in which ρ is the density, t the time, $\vec{U}$ the velocity vector, u the velocity component in the x-direction, ∇ the divergence operator, μ the turbulent viscosity, p the pressure, and S_U the momentum source.

In this situation, the assumption of incompressibility applies and the mass conservation or continuity equation has to be solved:

$$\nabla \cdot (\vec{U}) = S_\rho \qquad (4.5)$$

where S_ρ is the mass source.

The study also involved energy, so the CFD model also included the energy equation:

$$\frac{\partial \rho c_p T}{\partial t} + \nabla \cdot (\rho \vec{U} T) = \nabla \cdot (\lambda \nabla T) + S_T \quad (4.6)$$

where T is the temperature, λ the thermal conductivity, S_T the heat source, and c_p the heat capacity at constant pressure.

Turbulence was modelled using the standard $k - \varepsilon_{tur}$ model (Launder & Spalding ,1972). This is based on two equations, one for k, which accounts for kinetic energy, and the other for ε_{tur} which accounts for the rate of dissipation of energy in unit volume and time. This is probably the most widely used and validated turbulence model and in the greenhouse CFD literature it has been used in many research studies (Boulard & Wang, 2000).

Condensation was also included in the CFD model by applying a user defined function (UDF); the condensation rate was included in eq. 4.2 and 4.3 as part of the source term. Details of the condensation model can be found in Piscia et al. (2011).

The crop was a lettuce crop; it was considered as homogeneous and having a constant vapour source with a production rate of 1.74 x 10^{-6} kg m^{-2} s^{-1} (Piscia et al., 2011).

The convective terms in the CFD equations were modelled using a second order up-wind scheme. The viscous term was modelled by a second order central scheme and the transient term was modelled using an implicit scheme. The pressure-velocity coupling was resolved by the algorithm SIMPLEC method (Van Doormaal ,& Raithby ,1984), which uses a relationship between velocity and pressure corrections to enforce mass conservation and to obtain the pressure field.

Mesh and boundary conditions

The domain was divided in 383,226 cells. The dimensions of the domain were 160 m in the x-direction, 50 m in the y-direction and 12 m in the z-direction, chosen following the recommendations of Bournet, Ould Khaoua, and Boulard(2007). The quality of the grid was checked through the skewness and the y^+ parameters. The mesh used gave a maximum skewness parameter of 0.669 (which falls into the “fair” range, according to the software standard) and an average value, based on all the mesh cells, of 0.19 (“very good” range). The mesh parameter y^+ was kept under the 300 value (the upper limit suggested by the software company) and the average y^+ of all boundary conditions defined as “wall” was 26.

In the 3D model, the top domain surface was defined as a non-slip wall (corresponding to the sky) and the bottom domain as a non-slip wall that corresponds to the ground. The air flows in from the left surface (yz plane) and flows out of the domain through the right surface. The domain surfaces (xy plane) parallel to the wind direction were modelled as symmetrical.
The mesh was generated by using the Ansy mesh software.

Table 4.2 - Boundary and initial conditions used for the steady state CFD simulations

Boundary conditions	Values
Top domain surface	Sky temperature: 256 K
Bottom domain surface	Greenhouse soil heat flux 25 W m^{-2}
Left domain surface (normal to wind direction)	Inlet temperature was set to 276 K, and velocity to 2 m s^{-1} (average values measured during the night used for model validation)
Right domain surface (normal to wind direction)	Outlet boundary condition
Parallel domain surface (parallel to wind direction)	Symmetry
Initial conditions	
Temperature	280 K
Relative humidity	68%

4.4.2 Experimental greenhouse

The experimental details are the same as described by Piscia et al. (2011). As a consequence only a brief summary of the experiment is given here. The 4-span greenhouse was 19.6 m wide, 12 m long, the height was 3.5 m at the gutter and 4.5 m at the ridge. The roof slope was 45^{o} and it was covered was 200 micron polyethylene film. The air temperature and humidity inside the greenhouse were measured using two air humidity and temperature sensors (Campbell hmp45c, Logan, UT, USA) which were located at a height of 2 m in the central spans; two thermocouples (diameter 0.2 mm, type T, RS Components Ltd., Corby, UK) were used to measure the roof temperature in combination with the previously mentioned thermocouples applied to the screen. The sensors used were: a net radiometer (Hukseflux NR01, Delft, The Netherlands), a temperature probe (Campbell, Pt100) for measuring soil surface temperature,

and a heat flux sensor (Hukseflux hfp01sc, Delft, The Netherlands), located in the middle of the greenhouse. A pyrgeometer (Hukseflux IR02, Delft, The Netherlands) and a hmp45c RH probe were placed outside but close to the greenhouse. A datalogger (Campbell CR10X, Logan, UT, USA) took measurements every 5 s and recorded 5 min. averages.

Lettuce transpiration was measured using a weighing lysimeter (Mettler, KCC-150, capacity 150 kg, accuracy 1 g, Columbus, OH, USA). Outside data were taken from a meteorological station located approximately 50 m from the experimental greenhouse; the equipment used was: a net radiometer (Kipp & Zonen NR-Lite, Delft, The Netherlands), a temperature and humidity probe (Campbell hmp45c, Logan, UT, USA) and a wind anemometer (Campbell 05305-L, Logan, UT, USA) positioned at a height of 2 m above the ground. The meteorological station provided hourly averaged values.

The polyethylene (PE) plastic used as the roof material had an emissivity value of 0.69, a transmissivity value of 0.19 and a reflectivity value of 0.12.

4.5 Results

4.5.1 Validation of ES

The Macro-balance energy model was validated against experimental results for the night of 13 and 14 February 2010. This night was chosen because it had a change in outside boundary conditions (more specifically the sky temperature underwent a number of sudden changes, particularly after about 2:15 am) which allowed a study of the transient response of the model to changing boundary conditions. Also, CFD simulations were available for the same night, so results from the macro model could be compared with the CFD predictions.

Validation was based on three main climate variables, inside air and cover temperatures and humidity ratio. Both the experimental and simulated data are 5 minute averages.

In figure 4.1a, the inside temperature, shows good agreement, the trending patterns of the two lines are the same. Figure 4.1b, the cover temperature, presents very good agreement, the model and experimental data indeed are almost identical during the first and central parts of validation process.

Figure 4.1c, contains the humidity ratio comparison, the good agreement of cover temperature is reflected in the good agreement of the humidity ratio, whilst the biggest

difference which occurs at the end of the period, coincides with biggest difference in cover temperatures.

By looking at Figs 4.1b and 4.1c, it is possible to recognize the strong dependency of humidity ratio on cover temperature, this is described in more detail by Piscia et al. (2011).

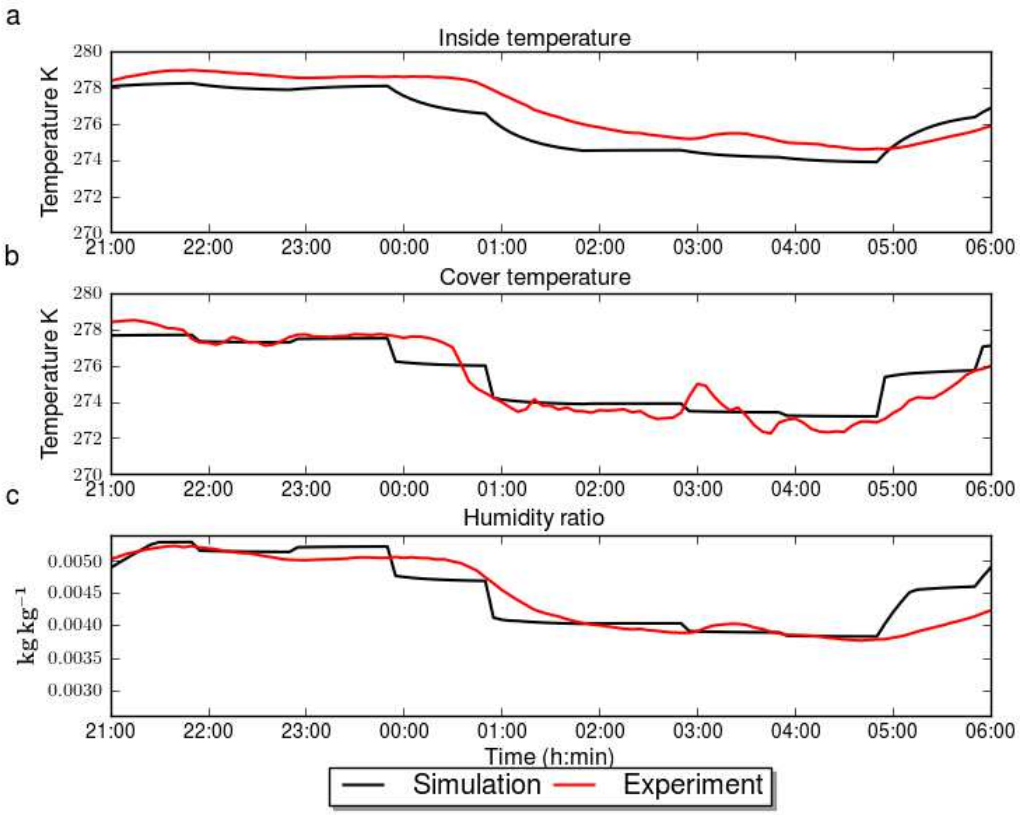

Fig. 4.1. Experimental and ES simulated values of the greenhouse air temperature. Night 14 -15 February 2010: a) greenhouse air temperature, b) greenhouse cover temperature and c) greenhouse humidity ratio.

The RMSE values were computed for the inside, cover temperatures and humidity ratio, the RMSE approach is the same used in Piscia et al. (2011)

RMSE of the three comparisons were:

- inside temperature = 0.98 ^{o}C
- cover temperature = 0.82 ^{o}C
- humidity ratio = 0.00029 kg kg^{-1}

RMSE values were acceptable according to the study in unheated greenhouses by (Batista 2007). For the same night the RMSE for the CFD model were 0.37 ^{o}C, 0.89 ^{o}C and 0.00029 kg kg^{-1} respectively (Piscia et al., 2011). The comparison of the ES and CFD models shows close

RMSE values: it can be seen that inside temperature was computed with a higher accuracy by the CFD model, whilst similar accuracies were obtained in the computation of the cover temperature and humidity ratio.

4.5.2 ES simulation

4.5.2.1 ES optimization

As described in Section 2.1.1, an optimization process was carried out to find which thermal radiation properties minimized the greenhouse cost function (RH). The optimization process can be seen as a two step process, the first was the application of optimization software to the macro-balance model, which leads to an optimization point. Based on the optimization process result, a set of CFD simulations were made in order to add more information to overall optimization process.

Optimization process setting

The optimization process was defined by a cost-function output, which in this case was relative humidity, and two independent variables, which were the transmissivity and absorptivity of the cover material. The two independent variables were bounded, with a lower limit of 2.5% and upper limit of 70%. There was also a constraint, which was that the sum of transmissivity and absorptivity could not exceed 95%, this was implemented through a penalty function.

The rationale behind a penalty function is to add (or subtract) a large quantity to the cost function output when the constraint is exceeded. Though in this case, the constraint was not exceeded, because the optimal of the variables values coincided with their lower limits.

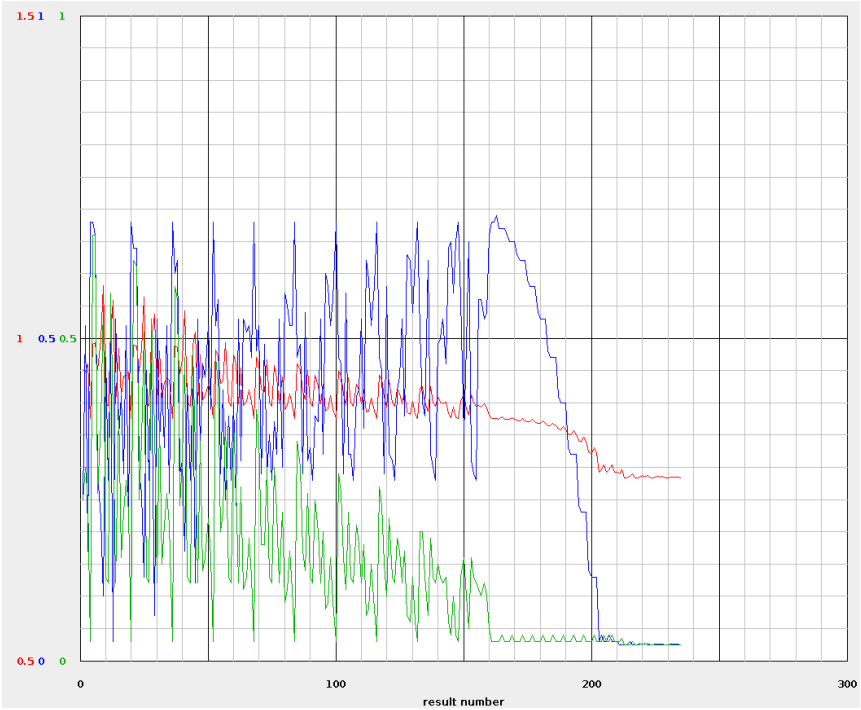

Fig. 4.2. Optimization process, the red line ___ is RH [%/100], the variable which is optimised, the blue line ___ represents the emissivity value [%/100] and the green line ___ represents the transmissivity of the cover material [%/100].

The lowest RH value, 78.1% was achieved for values of both transmissivity and absorptivity of 2.5%.

The optimal point was reached after 162 iterations for algorithm 1 (PSO algorithm which lead to the point ε = 0.47 and τ = 0.03) and 70 for algorithm 2 (GPS algorithm which lead to the optimal point). In table 4.3 the ES simulation results of reference and optimal cases are summarised.

Table 4.3 Results of ES simulations obtained by using the regular cover material and the optimal material for case of 256 K equivalent sky temperature and 25 W m^{-2} SHF

	Reference	Optimal
Inside temperature (K)	274.1	280.6
Inside humidity ratio (kg $kg^{-1)}$	0.0037	0.0050
Inside RH (%)	91.7%	78.1%
Cover temperature (K)	272.9	277
Outer cover total heat flux (W m^{-2})	19.3	16.4

Outer radiation heat flux (W m^{-2})	51.7	5.6
Outer convective heat flux (W m^{-2})	-32.4	10.8
Inner cover total heat flux (W m^{-2})	-19.3	-16.3
Inner radiation heat flux (W m^{-2})	-16.5	-4.4
Inner convective heat flux (W m^{-2})	-2.8	-11.9

4.5.2.2 ES parametric study

The ES model was used to carry out two parametric analyses, the first used different values of transmissivity and emissivity and the second took into account different combinations of external boundary conditions, equivalent sky temperature and SHF.

Parameter study of thermal radiation properties

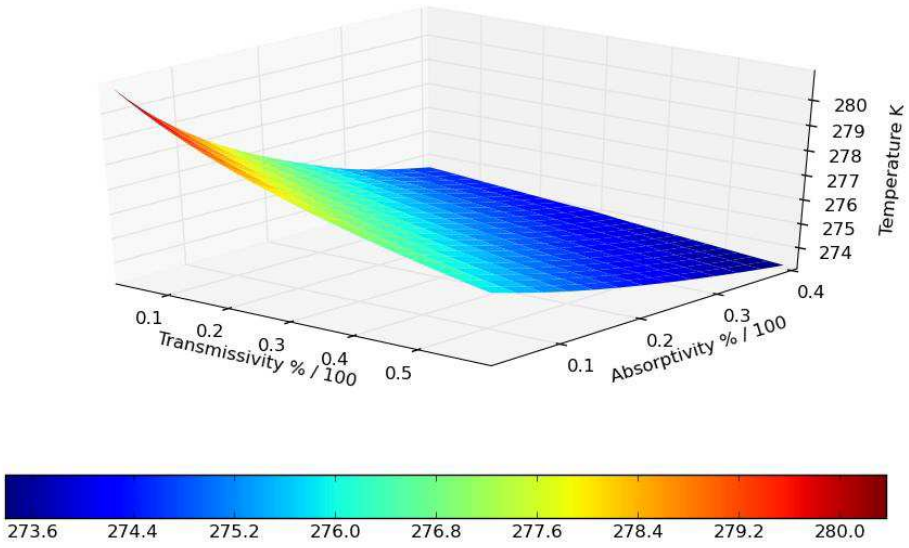

Fig. 4.3. Inside temperature for different combinations of thermal absorptivity ε and transmissivity τ for the case of 256 K equivalent sky temperature and 25 W m^{-2} SHF.

Figure 4.3 shows the inside temperature for different combinations of the thermal radiation properties; it shows that the highest temperature, more than 280 K, was achieved with ε = 2.5% and τ = 2.5%. The lowest temperature was achieved with the highest values of τ and ε. The difference between highest temperature and the one obtained using the reference material, which is the current standard polyethylene cover material (absorptivity 0.69 and transmissivity 0.19), was approximately 6 ^{o}C.

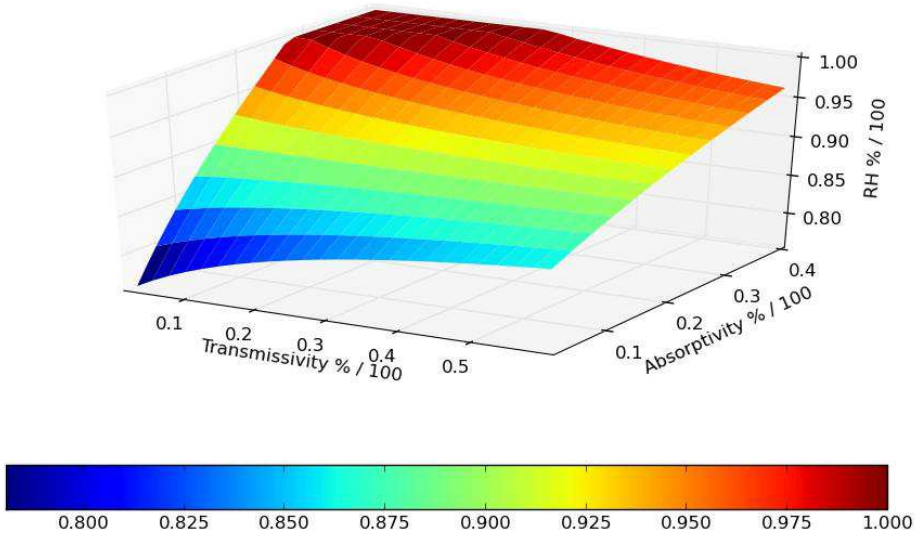

Fig. 4.4. Inside RH for different combinations of thermal absorptivity ε and transmissivity τ for the case of 256 K equivalent sky temperature and 25 W m^{-2} SHF.

Figure 4.4 shows that the lowest RH, about 78% was achieved with ε = 2.5% and τ = 2.5%, whilst the highest humidity was achieved with the highest values of τ and ε. The difference between the values obtained with the higher temperature and the reference material was approximately 14%.

The optimized case corresponded to the least favourable situation which was 256 K for the equivalent sky temperature, and 25 W m^{-2} as the SHF. Gains from the optimal pair of thermal radiation properties were lower when the boundary conditions depended on both the equivalent sky temperature and the SHF.

In all cases optimal thermal radiation properties improved climate conditions, this pattern can be seen in Fig. 4.5, which shows the increase in temperature obtained with the high emissivity material above that obtained with the reference material.

Parameter study of boundary conditions

A second parameter analysis was made, in which the exploration space was the combination of different equivalent sky temperatures and SHFs. The aim was to assess the importance of the thermal radiation properties in different conditions. Figure 4.5 shows the gains obtained by using a cover material with optimal thermal radiation properties compared to the reference material.

The temperature gains increase linearly when the sky temperature diminishes and decrease when SHF diminishes. A covering material with optimized properties brings advantages not only in unheated, but also in heating scenarios for which the effect is stronger for clear skies.

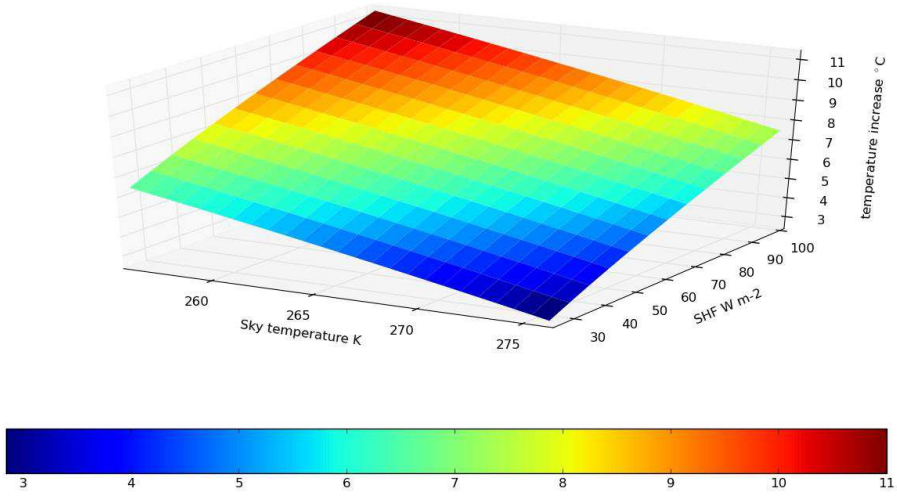

Fig. 4.5. 3D surface of the inside temperature gain, between optimal and reference thermal radiation properties for different boundary conditions.

Figure 4.6 shows the gains of using the optimized material in terms of RH decrease. The RH reductions are greater for the heated case, and are positively dependent on equivalent sky

temperature as it decreases.

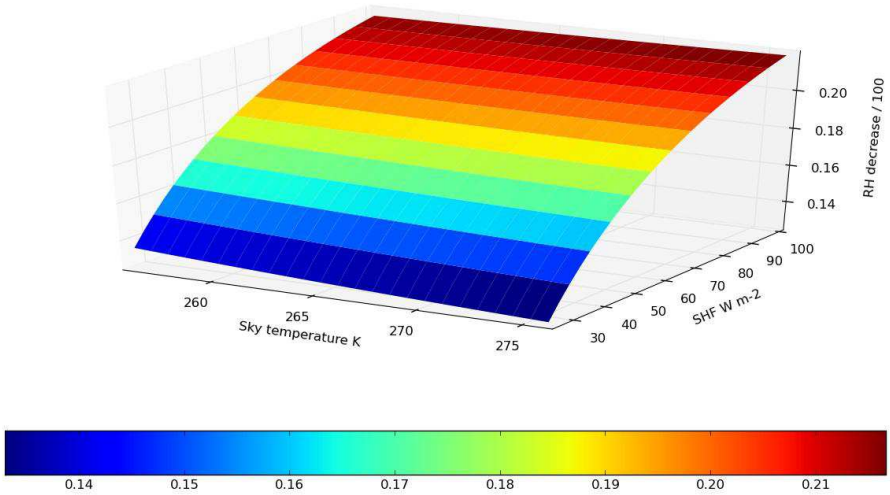

Fig. 4.6. 3D surface of the inside relative humidity gains, between optimal and reference thermal radiation properties for different boundary conditions.

The consequence of the optimization process is clear, the cover material has to reflect as much thermal radiation as possible, in this way it will increase the cover temperature and as a consequence the inside temperature will be increased and the relative humidity will be reduced. This agrees with the previous study by Bailey (1981) and Nijskens et al. (1984).

4.5.3 CFD simulations

Two CFD simulations were made, one with a cover material having low emissivity/high reflectivity surfaces, as suggested by the optimization method. The results were compared with the case run using the reference material.

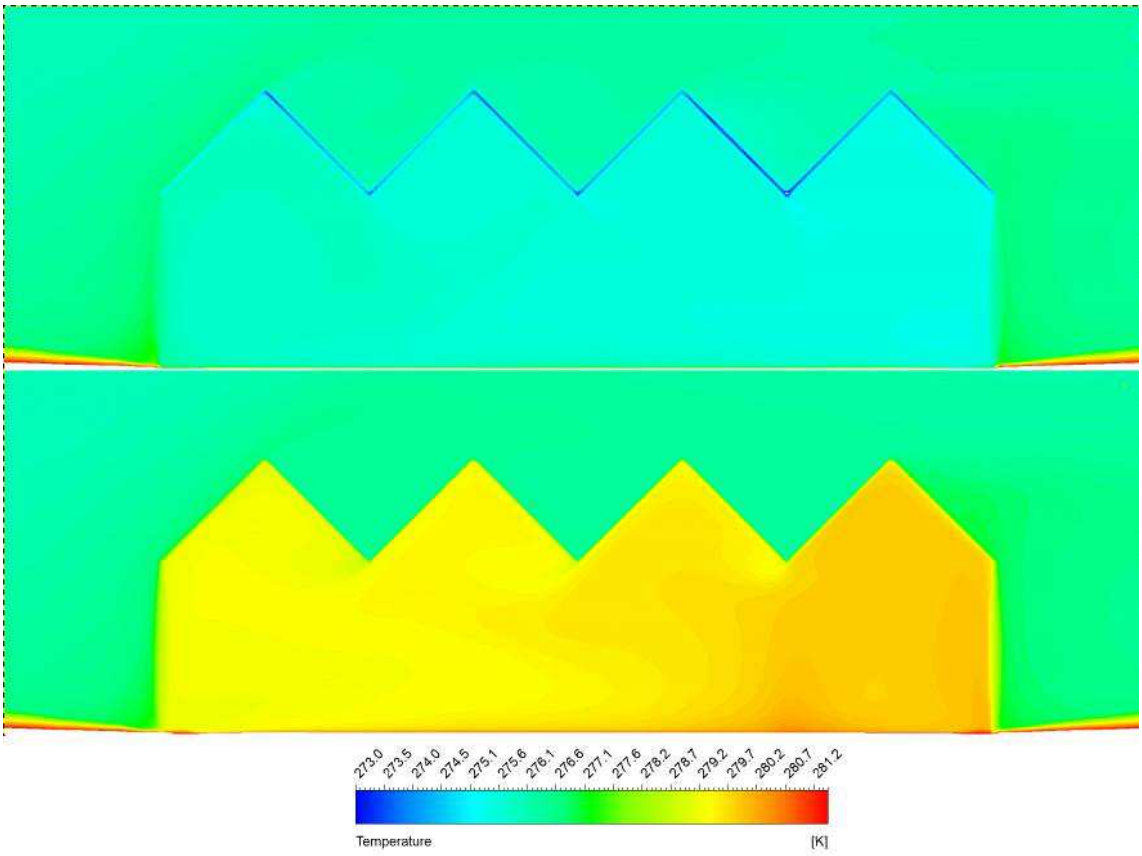

Fig. 4.7. Cross-section map of temperature for equivalent sky temperature of 256 K and SHF of 25 W m-2, the lower figure corresponds to the cover with optimal thermal radiation properties and the upper figure to the cover with the reference properties.

From Fig. 4.7 it can be seen that temperature was approximately 4 ^{o}C higher compared to the reference case. This is mainly due to the cover temperature, for the low-emissivity, the temperature is 3 ^{o}C higher than for the reference cover. In the reference case, the left side temperature is higher than that in the central and right-side zones; this is due to the wind effect which blows directly onto the left side, causing the convective heat transfer to be higher than on the right side.

The same effect can be seen in the cover temperature distribution, indeed the cover temperature is lower than the outside temperature (reference case) hence the higher heat transfer coefficient results in a higher temperature. In the low-emissivity case, the wind effect on temperature is the opposite, while in this case there is no thermal inversion, the left side is colder than the central and right-side areas. In this case, the wind cools the greenhouse.

As a consequence the cover temperature is lower on the left side, where the convective heat transfer is higher, than on the right side.

The inside temperature for the reference case was 275.7 K, while for the optimal case it was 279.6 K, theoretical gain of about 4 ^{o}C.

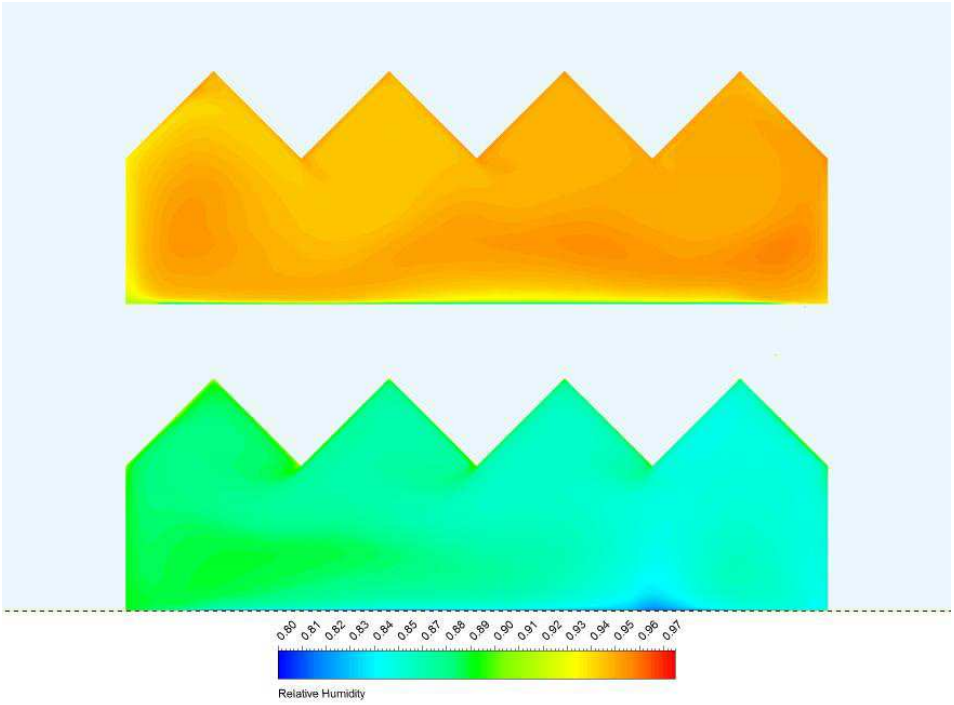

Fig. 4.8. Cross-section map of relative humidity (RH) for equivalent sky temperature of 256 K and SHF of 25 W m^{-2}. The lower figure corresponds to the optimal properties cover material and the upper figure to the cover with the reference properties.

The increase of inside temperature was also accompanied by a rise in cover temperature; the reference case cover temperature was 273.9 K versus 276.7 K for the optimal case.

The humidity content was higher in the optimal case (Fig. 4.8), due to the fact that the cover temperature was also higher, but the relative humidity was lower in the optimal case, 86.5% versus 94.7% for the reference case.

In the optimal case, the convective heat transfer from the cover to the outside air was negative (loss of energy) and the total heat transfer was 12.1 W m^{-2}, whilst in the reference case the total heat transfer was 17.4 W m^{-2} (radiation exchange loss of 35 W m^{-2}). In table 4.4 the CFD simulation results of reference and optimal cases are shown.

Table 4.4. Results of CFD simulations obtained using the reference and optimal covers for the case of 256 K equivalent sky temperature and 25 W m^{-2} SHF

	Reference	Optimal
Inside temperature (K)	275.7	279.6
Inside humidity ratio (kg kg^{-1})	0.0042	0.0051
Inside RH (%)	94.7%	86.5%
Cover temperature (K)	273.9	276.7
Outer cover total heat flux ($W\ m^{-2}$)	17.4	12.1
Outer radiation heat flux ($W\ m^{-2}$)	35.0	11
Outer convective heat flux ($W\ m^{-2}$)	-17.6	1.1
Inner cover total heat flux ($W\ m^{-2}$)	-17.4	-12.1
Inner radiation heat flux ($W\ m^{-2}$)	-14.1	-6.6
Inner convective heat flux ($W\ m^{-2}$)	-3.3	-5.5

Condensation

According to CFD predictions, condensation in the optimal case started approximately 120 minutes later compared to the reference case. This was due to the fact that the optimal material achieved a steady-state temperature almost 3 ^{o}C degree higher, and as a consequence the absolute humidity needed to achieve the equilibrium state close to the cover surface is higher than the one needed with a temperature of 273.9 K (the reference case). The transpiration rate was kept constant, hence condensation starting time was delayed by a relevant value.

4.6 Discussion

The optimization method suggested using a very reflective covering material, as the replacement for the regular plastic material. The gains in terms of temperature rise and RH decrease are significant. The insight provided is clear, under a clear cold sky, the objective of the cover is to reduce heat losses by radiation, if such a highly reflective material were used, thermal inversions would be avoided in all meteorological situations.

At the moment no such material is available on the market with this characteristic, nevertheless this work gives guidance for future developments in plastic thermal radiation properties and gives a reference for growers.

In this paper an optimization approach to greenhouse climate study has been presented. The independent inputs of the process were two (transmissivity and emissivity), so the space to be explored was a 2 dimensional grid. The same approach can be used for optimization of n variables (where $n \geq 2$), where the space to be explored is n-dimensional.

This multi-variable optimization approach could be useful when the aim is to optimize variables which are strongly correlated or where the optimization process is used as part of a greenhouse real-time control algorithm. In the latter case, the multiple inputs have to be taken into account.

The cost function in this paper was one variable, but there are cases where the optimization cost function can be a set of outputs, in such a situation, weighted relationships between the selected outputs can reduce the outputs to one. The drawback of this approach is in the selection of the correct weights.

The surrogate methods optimization supports the use of a correction factor to improve the local accuracy of the surrogate models. The correction factors force the low-fidelity models to match the high-fidelity model. Details of the different correction approaches can be found in Eldred, Giunta and Collis (2004). The application of this correction feedback makes the process more robust because the ES model explores part of the parameter space and then requires the CFD model to check that the two models are not diverging. This implementation increases the computational cost of the overall process as it requires more CFD simulations. In a more complex optimization (where the cost function is not well-behaved) case, the implementation of correction feedback has to be taken into account.

The ES and CFD models are complementary models, where the weakness of one can be strengthened by the other. A strong coupling between the two models can result in a coupled model (conflated model, Negrao, 1995) which can study a long time period with high accuracy and less dependence on empirical data.

There have been several studies on the relationship between CFD and ES models when applied to the climate inside buildings (Negrao, 1995; Beausoleil-Morrison, 2000; Zhai et al., 2005; Wang , 2007), but the method has not been used in studies on the greenhouse climate. In this paper, a first coupling approach is proposed; indeed the convective coefficients for ES models were selected after a comparison with the CFD coefficient predictions. ES-CFD coupling in greenhouse modelling can reach a higher degree of integration; and further studies are required to assess the capabilities of a greenhouse conflated model.

The comparison of results in terms of inside temperature and humidity between CFD and ES simulations highlights that although ES was partially coupled by CFD convective coefficients, a

stronger coupling can be achieved to obtain ES results closer to CFD ones. A further degree of integration can be obtained by using the CFD coefficients directly in the ES model.

4.7 Conclusions

A new optimization methodology for greenhouse design was proposed and tested. The method consists of three modules, the first represents the optimization algorithms, the second the ES model and the third the CFD model. It was shown that this methodology combines the advantages of ES models with those of CFD, to build a coupled approach to optimize the greenhouse design.

The optimal greenhouse covering material has to be as highly reflective to thermal radiation as possible, potential improvements in terms of temperature gains, and humidity decreases are significant. Condensation formation on the cover can be delayed by approximately 2 hours.

Two parametric analyses were carried out, the first showed the effects of different thermal radiation properties of the covering material on the inside climate, and the second highlighted the effect of boundary conditions on the performance of a high reflective material.

4.8 Appendix

Radiation

Outgoing radiation from a surface with non zero transmissivity cover and sidewalls

$$j_{i,face\_in} = \varepsilon_i \sigma T_i^4 + \zeta_i g_{face\_in} + \tau_i g_{face\_out} \qquad [Wm^{-2}] \qquad \text{(A 4.1)}$$

Teitel (95)

where ε_i is the emissivity, σ Boltzmann constant ξ_i the reflectivity and τ_i the transmissivity.

Outgoing radiation from opaque surface, soil, external soil, sky

$$j_i = \varepsilon_i \sigma T_i^4 + \xi_i g_i \quad [Wm^{-2}]$$

Incident radiation on a surface is:

$$g_i = \sum_{j=surfaces} F_{i\to j}\, J_j \qquad [Wm^{-2}] \qquad \text{(A 4.2)}$$

where $F_{i->j}$ is the view factor between surfaces j and i

Net radiation balance can be computed as:

$$q_{rad,i} = j_i - g_i \qquad [Wm^{-2}] \qquad \text{(A 4.3)}$$

$$Q_{rad,i} = A_i(j_i - g_i) \qquad [W] \qquad \text{(A 4.4)}$$

Convection

Convective exchange depends on convective heat transfer coefficients, in this simulation they were taken from the following proposed formulae, which were selected based on the convective heat transfer comparison between ES formulae and CFD results described in Master thesis (Piscia, 2010):

Convective heat transfer coefficients

$$\alpha_{sid\_in\to air} = 1.24\,(T_{sid\_in} - T_{air})^{0.33} \qquad [Wm^{-2o}C^{-1}] \qquad \text{(A 4.5)}$$

Tantau (1975)

$$\alpha_{\mathrm{cov}\_in\to air} = 2.21\,(T_{\mathrm{cov}\_in} - T_{air})^{0.33} \qquad [Wm^{-2}\,{}^{o}C^{-1}] \qquad \text{(A 4.6)}$$

Papadakis et al (1992)

$$\alpha_{soil\_in\to air} = 1.86\,(T_{soil\_in} - T_{air})^{0.33} \qquad [Wm^{-2}\,{}^{o}C^{-1}] \qquad \text{(A 4.7)}$$

De Halleux (1989)

$$\alpha_{\mathrm{cov}\_out\to air\_out} = 0.95 + 6.76\,v^{0.49} \qquad [Wm^{-2}\,{}^{o}C^{-1}] \qquad \text{(A 4.8)}$$

Papadakis et al (1992)

$$\alpha_{sid\_out\to air\_out} = 0.95 + 6.76\,v^{0.49} \qquad [Wm^{-2}\,{}^{o}C^{-1}] \qquad \text{(A 4.9)}$$

Papadakis et al (1992)

Once the convective heat transfer are obtained, the convective fluxes are given by:

$$q_{conv,i} = \alpha_i(T_i - T_{air}) \qquad [Wm^{-2}] \qquad \text{(A 4.10)}$$

$$Q_{conv,i} = \alpha_i(T_i - T_{air})A_i \qquad [W] \qquad \text{(A 4.11)}$$

Condensation

The condensation rate is computed by calculating the humidity content of the greenhouse air ($M_{w,air}$) and the saturated humidity content of air at the cover temperature (M_{w,cov_in}), if the latter is lower than the former then condensation is the difference between the former quantity and the latter.

$$\Omega_{cov\_in} = \frac{\max(0, M_{w,air} - M_{w,cov\_in})}{\partial t} \qquad [kg\ s^{-1}] \qquad (A\ 4.12)$$

Transpiration

Transpiration was considered as constant source, because of the lack of a crop model adapted for night-time conditions.

$$\Gamma_{crop} = \psi Vol_{crop} \qquad [kg\ s^{-1}] \qquad (A\ 4.13)$$

where ψ is the constant transpiration rate kg m^{-3} s^{-1}

Ventilation

This was not taken into account, because the simulation conditions assumed a closed greenhouse.

Cover energy balance

$$Q_{conv,cov\_in} + Q_{rad,cov\_in} + Q_{cond,cov\_in} = Q_{conv,cov\_out} + Q_{rad,cov\_out} \qquad [W] \qquad (A\ 4.14)$$

Sidewalls energy balance

$$Q_{conv,sid\_in} + Q_{rad,sid\_in} = Q_{conv,sid\_out} + Q_{rad,sid\_out} \qquad [W] \qquad (A\ 4.15)$$

Soil energy balance

$$Q_{cond,soil} = Q_{conv,soil} + Q_{rad,soil} \qquad [W] \qquad (A\ 4.16)$$

Energy and mass balance

Energy balance of greenhouse air

$$\frac{V\rho_{air}(c_{p,a}\partial T_{air} + w(c_{p,w}\partial T_{air} + h_e))}{\partial t} = A_{soil}\cdot q_{conv,soil} + A_{sid\_in}q_{conv,sid\_in} + A_{\mathrm{cov}\_in}q_{conv,\mathrm{cov}\_in}$$

[*W*] (A 4.17)

Mass coupling of greenhouse air

$$\frac{M_{w,air}}{\partial t} = \Gamma_{crop} - \Omega_{\mathrm{cov}} \qquad [\mathrm{kg\ s^{-1}}] \qquad \text{(A 4.18)}$$

where $\rho_{air} = \frac{(M_w + M_a)}{Vol}$, $w = \frac{M_w}{M_a}$

Acknowledgments

The work presented here has been carried out within the project EUPHOROS. European Commission, Directorate General for Research, 7th Framework Programme of RTD, Theme 2 – Biotechnology, Agriculture & Food, contract 211457. This research work has also been supported by INIA (project RTA2008-00109-C03) with contribution of FEDER founds. Thanks are given to INIA fellowship FPI-INIA.

4.9 References

Ansys (2009). User guide 12.0. Lebanon, NH, USA.

Bailey, B. J. (1981). The reduction of thermal radiation in glasshouses by thermal screens. Journal of Agricultural Engineering Research, 26(3), 215-224.

Bakker, J. C. (1991). Analysis of humidity effects on growth and production of glasshouse fruit vegetables, Ph.D. thesis, Agricultural University of Wageningen.

Baptista, F. J. F. (2007). Modelling the climate in unheated tomato greenhouses and predicting Botrytis cinerea infection. Ph.D. thesis, Univerisade de Evora, Portugal.

Beausoleil-Morrison, I. (2000). The adaptive coupling of heat and air flow modelling within dynamic wholse-building simulation. Ph.D. thesis, University of Strathclyde.

Boulard, T., & Wang, S. (2000). Greenhouse crop transpiration simulation from external climate conditions. Agricultural and Forest Meteorology, 100(1), 25-34.

Bournet, P., Ould Khaoua, S., & Boulard, T. (2007). Numerical prediction of the effect of vent arrangements on the ventilation and energy transfer in a multi-span glasshouse using a bi-band radiation model. Biosystems Engineering, 98(2), 224-234.

De Halleux, D. (1989). Dynamic model of heat and mass transfer in greenhouses: theoretical and experimental study. PhD Thesis, Gembloux, Belgium.

Eldred, M. S., Giunta,A. A., & Collis, S. S.(2004). Second-order corrections for surrogate-based optimization with model hierarchies. In Proceedings of the 10th AIAA/ISSMO Multidisciplinary Analysis and Optimization Conference, Albany, NY,, Aug. 30–Sept. 1, 2004. AIAA Paper 2004-4457.

Engel, R. D. (1984). Using simulation to optimize solar greenhouse design. Annual simulation symposium , IEEE Tampa, USA, 119-139.

Kacira M., Sase , S., & Okushima, L. (2004). Optimization of vent configuration by evaluating greenhouse and plant canopy ventilation rates under wind-induced ventilation. Transactions of the American society of agricultural engineers, 47(6), 2059-2067.

Launder, B. E., & Spalding, D. B. (1972). Lectures in Mathematical Models of Turbulence. Academic Press, London.

Montero, J. ,Munoz, Anton, A., & Iglesias, N. (2004). Computational fluid dynamic modelling of night-time energy fluxes in unheated greenhouses. International Conference on Sustainable Greenhouse Systems-Greensys 12-16 September 2004, Louvain, Belgium 691, 403-410.

Negrao, C.O.R. (1995). Conflation of computational fluid dynamics and building thermal simulation. . Ph.D. thesis, University of Strathclyde.

Nijskens, J., Deltour, J., Coutisse, S., & Nisen, A. (1984). Heat transfer through covering materials of greenhouses. Agricultural and Forest Meteorology, 33(2-3), 193-214.

Papadakis G; Frangoudakis A; & Kyritsis, S. (1992). Mixed, forced and free convection heat transfer at the greenhouse cover. Journal of Agricultural Engineering Research, 51, 191–205.

Peeters, L., Wetter, M., & Ferguson, A. (2010). The Coupling of ESP-R and GenOpt: A Simple Case Study. New York SimBuild 2010. Fourth National Conference of IBPSA-USA. 102-109

Piscia, D. (2010). A greenhouse climate model for night-time conditions. Master Thesis, Universidad politecnica de Catalonia.

Piscia, D., Montero, J.I., Baeza, E., & Bailey, B.J. (2011). A CFD greenhouse night-time condensation model. Biosystems Engineering, 111(2),141-154.

Richards, P. J., & Hoxey, R. P. (1993). Appropriate boundary conditions for computational wind engineering models using the k-ϵ turbulence model. Journal of Wind Engineering and Industrial Aerodynamics, 46, 145-153.

Robinson, T.D., Eldred, M.S., Willcox, K.E., & Haimes, R.(2008). Surrogate-Based Optimization using Multifidelity Models with Variable Parameterization and Corrected Space Mapping, AIAA Journal, 46(11), 2814-2822.

Roy, J.C., Boulard, T., Kittas ,C., & Wang , S. (2002). PA—Precision Agriculture: Convective and Ventilation Transfers in Greenhouses, Part 1: the Greenhouse considered as a Perfectly Stirred Tank. Biosystems Engineering, 83(1), 1-20.

Tantau, H. J. (1975). Der einfluss von einfach und doppelbedachungen auf dasKlima und den warmehaushalt von gewachshausern. [Effects of single and double covering on climate and heat management in greenhouses.] PhD Thesis, Fak.Gartenbau und Landeskultur Tech.Univ. Hannover, Germany.

Teitel, M. , & Segal, I. (1995). Net thermal radiation under shading screens. Journal of agricultural engineering research, 61(1), 19-26.

Van Doormaal, J.P. ,& Raithby, G.D. (1984). Enhancements of the SIMPLE method for predicting incompressible fluid flows. Numerical heat transfer, 7(2), 147-163.

Vanthoor, B. (2011). A model-based greenhouse design method. Ph.D. thesis, Agricultural University of Wageningen.

Wang, L. (2007). Coupling of multizone and CFD programs for building airflow and contaminant transport simulation. Ph.D. thesis, Purdue university.

Wetter, M. (2009). Generic Optimization program (genopt). User Manual Version 2.0.

Zhai, Z.J., & Chen, Q.Y.(2005). Performance of coupled building energy and CFD simulations. Energy and buildings, 37(4), 333-344.

5 A method of coupling CFD and Energy Balance models and their use to study humidity control in unheated greenhouses

5.1 Abstract

A coupling method used for the study of greenhouse night-time climate is presented. The approach was based on two simulation models, the Energy balance Simulation (ES) and Computational Fluid Dynamics CFD. The coupled approach took advantage of each model and reduced their weakness. Two CFD parametric studies were carried out; the first analysed the effects of different wind speed and ventilator openings on ventilation rate; the second assessed the effects of different sky temperature and ventilator openings on the convective heat transfer coefficients. The CFD model was coupled to the ES model by the exchange of two variables: firstly the CFD model provided the ventilation rate to the ES model and secondly CFD model gave the convective heat transfer coefficients to the ES model. This coupling approach was applied to the study of night-time ventilation in a polyethylene covered, unheated greenhouse. Two scenarios were studied, the first one represented clear sky conditions and the second one a cloud covered sky. Results from the two studies indicated that ventilation during winter nights improved greenhouse climate. In the clear sky case RH was reduced and temperature was raised, whilst in the overcast sky situation ventilation reduced the RH content but also reduced the temperature. As expected, the changes in temperature and humidity depended also on the external conditions and on ventilation rate which was determined by the opening angle of roof ventilators. Minor opening angles produced the largest changes in greenhouse air temperature and relative humidity.

5.2 Nomenclature

A	area (m^2)
a	constant associated to the inner cover heat transfer coefficient
c_p	specific heat capacity at constant pressure (J kg^{-1} K^{-1})

DOM	discrete ordinate model
ES	energy balance simulation
h	condensation enthalpy (J kg^{-1})
k	turbulence kinetic energy (m s^{-2})
M	absolute humidity content (kg)
Num_var	variable number
p	pressure (Pa)
PE	polyethylene
q	heat flux (W m^{-2})
RMSE	root mean square error
RH	relative humidity (%)
S_ρ	mass source
S_U	momentum source
S_T	heat source
SHF	soil heat flux (W m^{-2})
t	time (s)
T	absolute temperature (K)
u	velocity component of the x coordinates (m s^{-1})
$\vec{U}$	velocity vector (m s^{-1})
UDF	user defined function
V	volume (m^3)
w	humidity ratio (kg kg^{-1})
y^+	non-dimensional distance indicator
α	convective heat transfer coefficient (W m^{-2} K^{-1})
ε	turbulence kinetic energy dissipation rate (m^2 s^{-3})
λ	thermal conductivity (W m^{-1} K^{-1})
μ	turbulent viscosity (kg m^{-1} s^{-1})
ρ	density (kg m^{-3})
Ω	condensation rate (kg s^{-1})
Γ	transpiration rate (kg s^{-1})
Φ	ventilation rate (kg s^{-1} m^{-1})
Λ	ventilator opening angle (rad)

Subscript

a	dry air
air	greenhouse air
air_out	outside air
conv	convective
cov	cover
sid	inner sidewall
soil	greenhouse soil
w	H_2O

5.3 Introduction

Greenhouse climate is a complex ecosystem, where several physical phenomena take place, i.e. transpiration, condensation, ventilation, leakage, etc. Greenhouses can be equipped with several devices, such as heating, dehumidification and cooling systems. Its performances have to be calculated for all seasons' conditions for continuously varying external conditions. The enormous variety of boundary conditions and design elements makes greenhouse design a complex task (Vanthoor, 2011).

Greenhouse climate has been mainly simulated by means of energy macro simulation (ES) and CFD.

Zhai and Chen (2004) summarised the advantages and drawbacks of the two techniques.

ES, also called perfectly stirred tank in greenhouse literature (Roy, Boulard, Kittas, & Wang, 2002), is based on the assumption of uniformity/homogeneity of greenhouse variables (such as temperature, humidity). This assumption makes ES computationally fast and straightforward to implement, but there are some limitations, ES needs some previous and empirical knowledge (Zhan, Lam, Yao, & Zhang, 2012) of different coefficients, such as the convective coefficients, wind pressure coefficients, and moreover ES can hardly describe the effects of air movement caused by thermal difference or wind.

CFD gives detailed air flow patterns and can compute accurate heat transfer fluxes, but it has high computational cost which makes CDF unfeasible to make simulations over long-time periods. Moreover the conjugate coupling between wall and air make the equations' system stiff (this is due to the inertia difference between a solid wall and the surrounding air) and

requires additional computational cost. Therefore, CFD has been used to carry out detailed studies of a given space under a number of specific boundary conditions.

The aforementioned greenhouse climate characteristics make complete greenhouse modelling hard to carry out, indeed some aspects, such as the long time frame can only be modelled by energy macro system (ES) whilst other such air movement can be properly modelled by CFD.

In this perspective coupling CFD with ES can be attractive and advantageous, ES can take advantage of air movement patterns and convective coefficients provided by CFD, whilst ES can provide the initial value such as inside temperature or cover temperature to CFD.

In the building simulation literature several studies treated the coupling between ES and CFD models.

Zhang et al. (2012) reported that three different coupling techniques exist, these coupling approaches between the ES model and CFD model can be grouped into three types. The first is the full internal coupling, where the set of equations for the ES and CFD models are solved together iteratively. Research (Negrao, 1998) showed that such internal coupling generates a set of equations referring to different models (such as ES zones and CFD equations and plant systems), which is large and sparse. The second approach is the iterative external coupling, where the set of equations for ES model and set of equations for CFD model are solved in a segregated way, the variables are exchanged using an iterative procedure until a converged state is obtained. The last approach is the progressive-replacement external coupling, where the set of variables are exchanged after each model has reached a converged state at each time step.

Zhai et al. (2002) wrote that there are three types of discontinuities between ES and CFD programmes. The first is a time-scale discontinuity, ES has a characteristic time-scale of hours for heat transfer in a building enclosure, but CFD has a time steps of seconds for room air. The second is a modelling discontinuity, the values predicted for each variable in ES are spatially averaged, while CFD presents field distributions of the variables. The third is a speed discontinuity which is related to the computational time needed for solving the model; ES usually needs a few seconds per zone for an annual energy analysis and requires little computer memory, whereas a CFD calculation for a zone may take several hours or more (according to the computational capability available) and require a large amount of memory. Depending on the type of coupling used, some or all of these discontinuities have to be solved.

Another different type of coupling exists, indoor coupling and outdoor coupling, the former refers to the coupling between inside air and inner walls, and the latter refers to the coupling between outside air and outer walls.

Indoor coupling was extensively studied by Negrao (1995), he implemented a full iterative coupling approach of ES and CFD model. Beausoleil-Morrison (2000) continued in the same direction and proposed a conflation controller to configure the CFD model at each time step based on the results obtained from the ES model. The controller estimated the nature of the air flow and based on this estimation selected the proper turbulence model to be used in the CFD simulation. The results of these researches were included in the open-source Esp-r program (Hand, & Arch, 2010). Wang (2007) also took into account the outdoor coupling, and its findings were made available in the open-source program Contam (Walton, & Dols, 2005). Zhang et al. (2012) presented a coupling between Energyplus (ES) and Fluent (CFD), the communication passed through a BCVTB (Building Controls Virtual Test Bed) programme, which provided a platform for the coupling of different tools.

All the aforementioned studies on ES-CFD coupling focused on building energy climate.

Most building climate simulation aspects can be found also in greenhouse climate analysis, indeed the governing equations are the same. Despite the strong similarity between building and greenhouse climate, some aspects make them different. Among the most relevant differences is that the inertial loads are different, the typical building envelop has a much higher inertia than a greenhouse cover. Another difference, which causes a major impact on the coupling strategy, is that the greenhouse indoor climate is strongly coupled to the outdoor climate, this is due to the fact that covering material is semi-transparent (being a plastic or glass), therefore the radiation exchange between indoor and outdoor is higher in greenhouses. For these reasons, most of the approaches suggested for buildings (separation between indoor and outdoor climate study) are not completely valid for greenhouse.

In Chapter 4 a first coupling approach was proposed, indeed the convective coefficients for ES models were selected after a comparison with the CFD coefficient predictions. Nevertheless this was a link used in a surrogated-method optimization context, where the aim of ES model was to orientate the CFD model toward the optimum point.

As a consequence of the strong relationship between indoor and outdoor climates, the ES-CFD coupling used in this study was conjugate (that is, CFD resolves the heat transfer process for both solids and fluids); the CFD simulates both indoor and outdoor climate and passes information to the ES for a correct computation of ventilation rate and convective heat transfer.

Greenhouse ES models have a lack of knowledge on a number of aspects, one is the computation of ventilation rate and another one is the estimation of convective heat transfer coefficients. As reported by Roy et al. (2002) ventilation rate for greenhouse ES model can be

computed by using the Bernoulli equation and values of the semi-empirical formulas. Parameters of these semi-empirical equations were either derived from direct determination of the discharge coefficients or by in situ determination (by regressing an overall coefficient of wind velocity on ventilation to measure air exchange rate). In this work the greenhouse studied was an innovative structure, and neither ventilation experiments nor specific empirical formula were available. To overcome this problem, a parametric study relating ventilation rate with air speed and ventilator opening angle was carried out using CFD simulation.

The convective heat transfer is governed by a combination of forced convection (due to the wind pressure) and free convection, due to buoyancy forces caused by temperature differences between the solid surfaces of the walls, soil, plants and the air. As a consequence the convective coefficients are dependent on greenhouse type, outside climate and ventilation conditions. This strong dependence on several factors makes the choice of convective coefficients difficult. As in the case of ventilation parameters, a parametric study of the greenhouse was done by means of CFD simulations, and then the CFD convective predictions were used in the ES model.

The purpose of this work is twofold. Firstly it presents and uses a method of coupling CFD-ES models for greenhouse climate simulation. Secondly it applied the methodology to study the effect of ventilation on night-time greenhouse climate in terms of humidity, temperature and condensation for a range of situations. The latter purpose aims to address a well-known issue, which is the high humidity during winter nights in unheated greenhouses. Several ES parametric analyses were carried out to assess the effects on inside temperature and relative humidity of different ventilator opening angles for different outside humidity ratios.

5.4 Material and methods

There were two ways in which the CFD and ES models for a ventilated greenhouse were coupled: the CFD model provided information to the ES model on ventilation rate and on convective heat transfer coefficients. The ES model was then used to define strategies for humidity control based on the management of night-time ventilation.

The process followed can be summarised in these steps:

1- A CFD parametric study of ventilation rate in which only the momentum equation was considered, the heat and mass equations were not solved.. The study consisted of the 24 combinations of ventilator opening angles (5 ^{o}, 10 ^{o}, 15 ^{o}, 30 ^{o}, 60 ^{o}, 90 ^{o}) and wind speeds (1, 2, 3, 4 m s^{-1}).

2- A CFD parametric study of convective heat transfer in which the heat and mass equations were solved. This consisted of six CFD simulations, for combinations of vent opening angles of 0^{o}, 5^{o}, 90^{o} and sky temperature of 256, 273 K.
3- Introduction of the CFD parametric results into ES model.

Use the ES model to carry out a parametric study of two scenarios, which were the unheated greenhouse under clear and overcast skies

5.4.1 CFD model

The CFD model solved the governing equations of momentum, energy and continuity applied to the greenhouse. The momentum equation, also known as the Navier-Stokes equation was derived by the application of Newton's law of motion to a fluid element:

$$\frac{\partial \rho u}{\partial t} + \nabla(\rho \vec{U} u) = \nabla(\mu \nabla u) - \frac{\partial p}{\partial x} + S_U \qquad (5.1)$$

in which ρ is the density, t the time, $\vec{U}$ the velocity vector, u the velocity component in x-direction, ∇ the divergence operator, μ the turbulent viscosity, p the pressure, and S_U the momentum source.

In this situation, the assumption of incompressibility applies and the mass conservation or continuity equation has to be solved:

$$\nabla \cdot (\vec{U}) = S_\rho \qquad (5.2)$$

where S_ρ is the mass source, which in the greenhouse case is the crop transpiration.

Turbulence was modelled using the standard $k-\varepsilon$ model (Launder & Spalding, 1972). This is based on two equations, one for k, which accounts for kinetic energy, and the other for ε which accounts for the rate of dissipation of energy in unit volume and time.

The convective terms in the CFD equations were modelled using a second order up-wind scheme. The viscous term was modelled by a second order central scheme and the transient term was modelled using an implicit scheme. The pressure-velocity coupling was resolved by the algorithm SIMPLEC method (Van Doormaal ,& Raithby ,1984), which uses a relationship between velocity and pressure corrections to enforce mass conservation and to obtain the pressure field. The CFD software used was the Ansys Fluent 13.0 (Ansys, 2012).

5.4.1.1 Mesh and geometry

The CFD model used was the same described in article (Piscia, Montero, Baeza & Bailey, 2011), but it presented a change in the geometry, because the geometry model and the associated mesh changed automatically with the angle of greenhouse ventilator (parametric mesh).
The mesh was unstructured, the total number of cells was 443000 and the average skewness was 0.11 (deviation of 0.11) . The dimensions of the domain were 160 m in the x-direction, 50 m in the y-direction and 12 m in the z-direction.

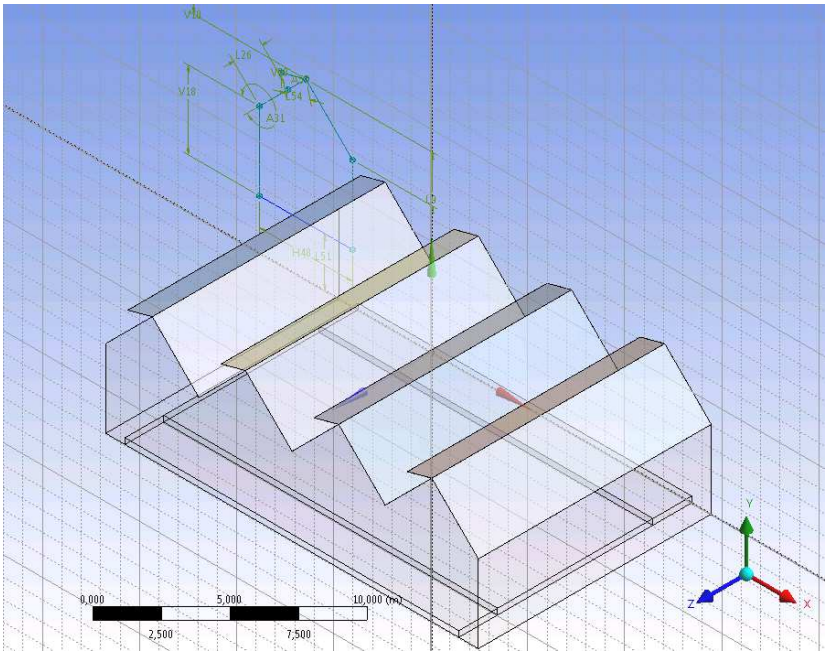

Fig. 5.1 3D view of parametric greenhouse geometry with 30^{o} roof ventilator opening

The mesh was generated by using the Ansys mesh software.

5.4.1.2 CFD model used for ventilation rate parametric study

The CFD ventilation rate parametric study simulated 24 different situations, the simulations were made in steady-state, because the objective of parametric study was to compute the equilibrium ventilation rate. The ventilation studied was windward (only windward vents were open).

Table 5.1 Boundary conditions for ventilation rate parametric study

Boundary conditions	Type
Top domain surface	No-slip wall
Bottom domain surface	No-slip wall
Left domain surface	Inlet velocity 1, 2, 3, 4 m s^{-1} at a height of 2 m (logarithm profile) (Richards & Hoxey, 1993)
Right domain surface	Outlet boundary conditions
Parallel domain surface (parallel to wind direction)	Symmetry
Ventilator opening angles	5 °, 10 °, 15 °, 30 °, 60 °, 90 °

5.4.1.3 CFD model used for convective heat transfer parametric study

The study also involved energy, so the CFD model also included the energy equation:

$$\frac{\partial \rho c_p T}{\partial t} + \nabla(\rho \vec{U} T) = \nabla(\lambda \nabla T) + S_T \qquad (5.3)$$

where T is the temperature, λ the thermal conductivity, S_T the heat source, and c_p the heat capacity at constant pressure.

This set of CFD simulations also took into account water vapour, therfore species equation was also included. Condensation was considered in the CFD model by using a user defined function (UDF); Details of the condensation model can be found in Piscia et al. (2011).

The crop was a lettuce crop; it was considered as homogeneous and having a constant vapour source with a production rate of 1.74 x 10^{-6} kg m^{-2} s^{-1} (Piscia et al., 2011).

This parametric study was based on 6 CFD simulations; the CFD model simulated two extreme ventilator opening degrees, 5 and 90° degrees. The aim was to obtain the convective coefficients for these two cases and use a linear interpolation to extract the coefficients between these two points. For each situation two different sky temperatures were simulated, the objective was to test the effect of different sky values on convective heat coefficients

values. Lastly the same approach was applied to closed greenhouse, in which case the coefficients are expected to be completely buoyancy driven based.

Only one wind speed was considered, (because of computational cost limitation) and the convective coefficients were used in ES model only under this condition.

Table 5.2 Boundary conditions for ventilation rate parametric study

Boundary conditions	Type
Top domain surface	Sky temperature 256, 273 K
Bottom domain surface	Greenhouse soil heat flux 25 W m^{-2}
Left domain surface	Inlet temperature 276 K and velocity 2 m s^{-1} at a height of 2 m (logarithm profile) (Richards & Hoxey, 1993)
Right domain surface	Outlet boundary conditions
Parallel domain surface (parallel to wind direction)	Symmetry
Ventilator opening degrees	0^{o}, 5^{o}, 90^{o}
Initial conditions	
Temperature	280 K
Relative humidity	68%

5.4.2 ES model

The energy balance model is based on the resolution of energy and mass conservation in a large volume. The ES models in the greenhouse literature are also referred to as the perfectly stirred tank approach. This requires the assumption of uniform temperature, humidity and CO2 content inside the greenhouse and uses a 'big leaf' model to treat the plant canopy and describe the exchanges of latent and sensible heat with the inside air (Roy et al., 2002).

The ES model used in this study was described in Chapter 4, however the equations proposed didn't take into account ventilation, and hence the corresponding equations A 4.17 and A 4.18 appendix of Chapter 4 had to be modified.

In the energy and mass balance of greenhouse air the two aforementioned equations were modified by adding the ventilation term:

$$\frac{\rho V c_p \Delta T}{\Delta t} = \sum_i q_i A_i + \Phi(c_p T_{out} - c_p T_{in}) \qquad [W] \tag{5.4}$$

$$\frac{M_w}{\partial t} = \Gamma_{crop} - \Omega_{cov} + \Phi(w_{air} - w_{air\_ou}) \quad [\text{kg s}^{-1}] \tag{5.5}$$

Where Φ is the ventilation rate (Kg s^{-1}), $\sum_i q_i A_i$ (W) is the sum of convective contribution, Γ_{crop} (Kg s^{-1}) is the transpiration rate, w_{air} (kg kg^{-1}) is inside humidity ratio, $w_{air\_outside}$ (kg kg^{-1}) is the outside humidity ratio and M_w is the water vapour mass. More details about equation 5.4 are given in the appendix section.

5.5 Results

5.5.1 CFD ventilation rate parametric study

Ventilation

The CFD greenhouse model (described in section 5.2.1.2) studied six different vent opening degree configurations and 4 different wind speeds.

Results are drawn in Fig. 5.2:

Table 5.3 Ventilation rate Kg $sec^{-1}m^{-1}$ for different combination of wind speed and open window degree

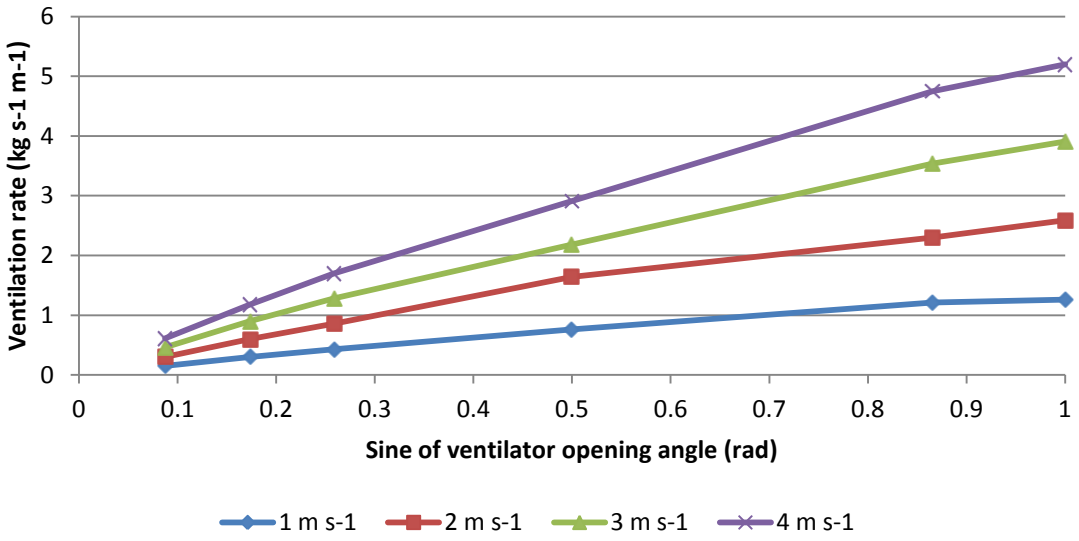

Fig. 5.2. Ventilation rate (kg $s^{-1}m^{-1}$) for different combinations of wind speed and sine of vent opening angle

From Fig. 5.2 a strong linearity can be seen between sin of opening angle and ventilation rate, as reported also by Jong (1990).

The result of a complete linear multivariate regression on all the samples gives the following results:

$$\Phi = 0.3 * u_{wind} + 2.36 * \sin(\Lambda) \qquad [\text{Kg sec}^{-1}\text{m}^{-1}] \qquad (5.6)$$

The R^2 value was 0.89 and the standard error 0.7 kg $sec^{-1}m^{-1}$.

The standard error of the regression was high, especially when compared with the low ventilation rates, and for this reason it was decided to compute a spline to achieve higher accuracy in the interpolation. A quadratic spline was used to capture the behaviour of ventilation rate as a function of wind speed and sine of the vent opening angle, this reduced the standard error to 0.35 and so improved the accuracy of Eqn 5.6). Details of the spline are given in the appendix. The spline equation was used by the ES model to compute the ventilation rate. The latter action represented the coupling between the CFD and ES models, which according to the definition of type of couplings (Zhang et al. ,2012) was an external, static coupling.

5.5.2 CFD convective coefficients rate parametric study

The CFD greenhouse model (described in section 5.2.1.3) was used to study the six combinations of two different equivalent sky temperatures and three different ventilator opening angles.

The values from Table 5.3 were included in the ES model, the differences between the values are a function of ventilation opening angle, so a linear interpolation as a function of vent opening was implemented, between 5^{o} and 90^{o} degrees. When the ventilators were closed, the coefficients were taken as the CFD values obtained for the 0^{o} degree case. This action was the second coupling link between the CFD and ES models, and as in the case of ventilation rate, it was an external and static coupling.

Table 5.3 Ventilation rate Kg $sec^{-1}m^{-2}$ for different combination of wind speed and open window degree

T_{sky}, angle / Alpha (W m^{-2} C^{-1})	273K 90 ^{o}	256K 90 ^{o}	273K 5 ^{o}	256K 5 ^{o}	273K 0 ^{o}	256K 0 ^{o}
Cov_in	5.2	5.2	3.4	3.5	2.2	2.3
Cov_out	3.9	3.9	3.8	3.7	9.4	9.3
Sid_in	8.9	8.7	5.1	5.1	1. 6	1.8
Sid_out	4.0	4.1	6.8	6.7	6.0	5.9
Soil_in	12.4	12.2	7.4	7.0	3.1	3.1

Looking at Table 5.3 the following conclusions can be made:

<u>Convective coefficient for the external surface of the roof</u>

The coefficient value was highest for the fully open ventilator (90^{o}), when it was than for a 5^{o} opening. The convective coefficient for the closed greenhouse was the lowest. For each ventilator opening angle, two sky temperatures were used, but the results showed that the inner convective coefficients had a low correlation with this parameter.

In this way the formula can be compared directly to the ones presented in greenhouse climate literature. The alpha taken into account was the ones referring to the closed greenhouse, this choice was made because in literature formulas were given for natural ventilation.

The CFD inner cover convective coefficients can be compared with existing values from previous publications, but this can be done only for the closed greenhouse since there are no such convective coefficients for greenhouses with open ventilator in literature. For comparison purposes the CFD inner cover coefficients can be expressed as $\alpha = a\Delta T^{0.33}$ (where a is a constant and ΔT is the difference between cover and inside temperature). From CFD simulations ΔT was taken as 1.8 and so the CFD convective formula was $\alpha = 1.9\Delta T^{0.33}$, which is between the formula $\alpha = 1.86\Delta T^{0.33}$ given by De Halleux(1989) and $\alpha = 2.21\Delta T^{0.33}$ given by Papadakis, Frangoudakis and Kyritsis (1992).

Convective coefficient for the external surface of the roof

The convective coefficient was greater in the closed greenhouse case, indeed it was more than twice the value in the ventilated situations. Once the ventilator was opened, the difference between 5 and 90 ^{o} opening angles was very low. The difference between closed and ventilated greenhouse was due to the fact that by opening the roof ventilators the greenhouse geometry was changed and consequently the outside air pattern also changed so the overall air speed was lower than for the closed greenhouse.

This behaviour was difficult to take into account by using the semi-empirical formulas found in the greenhouse research literature. As with the inner cover coefficients, the effect of sky temperature on the convective coefficients was insignificant.

The CFD outer cover convective coefficients can be compared to the values reported by other papers.

For the closed greenhouse, the CFD convective coefficient was approximately 9.4 W m^{-2} $^{o}C^{-1}$ for a wind speed of 2 m s^{-1}. This value is between 8.33 W m^{-2} $^{o}C^{-1}$ which is the value given by De Halleux (1989) and 10.4 W m^{-2} $^{o}C^{-1}$ which was provided by Papadakis et al. (1992).

Convective coefficient for the internal surface of the sidewall

The lowest coefficient was found for the closed greenhouse case; this was due to the low air movement occurring inside the greenhouse compared to the ventilated case. When ventilator was open, the coefficients was higher in 90º case, this can again be explained by the higher ventilation rate obtained by higher ventilator opening degrees. As in previous coefficients, the sky temperature had low effect on the convective coefficients.

Convective coefficient for the external surface of the sidewall

The lowest coefficient was found for the closed greenhouse case; this was due to the low air movement occurring inside the greenhouse compared to the ventilated case. When the ventilator was open, the coefficients was highest for the 90º case, this can again be explained by the higher ventilation rate obtained by higher ventilator opening. As with the previous coefficients, sky temperature had only a small effect on the convective coefficient.

Convective coefficient at the soil surface

This coefficient followed the same pattern as the sidewall internal convective coefficients, indeed it was positively correlated to the quantity of air entering into the greenhouse. The coefficient was close greenhouse was almost four times lower than the fully ventilated case and two times lower than the 5^{o} opening degrees case. As in previous coefficients, the sky temperature had small effect on the convective coefficients.

The CFD soil coefficients can be expressed as $\alpha = a\Delta T^{0.33}$ (where ΔT is the difference between soil and inside temperature). From CFD simulations ΔT was taken as 2.9 and so the CFD convective formula was $\alpha = 3.1\Delta T^{0.33}$, which is between the formula $\alpha = 1.86\Delta T^{0.33}$ given by De Halleux(1989) and $\alpha = 3.4\Delta T^{0.33}$ given by Stoffers (1985).

5.5.3 ES parametric study

Ventilation strategies were based on the analysis of two ES parametric analysis applied to scenarios. The ES model used the ventilation rate and convective coefficients found by the CFD models and presented in sections 5.5.1 and 5.5.2.

Two scenarios were studied:

- Cold case, where inside temperature was colder than outside (unheated case and clear sky)
- Intermediate case where inside temperature was warmer than outside, but RH was high (unheated case and overcast sky)

The first scenario was chosen, because a previous study (Piscia et al., 2011) showed that thermal inversion occurred in an unheated greenhouse for which the soil heat flux to the air was SHF 25 W m^{-2} under clear sky (256 K) conditions . This is caused by the fact that the greenhouse cover emits more infrared radiation than it receives from the sky. During a clear

winter night, the equivalent sky temperature can be 20 ^{o}C lower than air temperature and as a consequence the cover can be up to 3 ^{o}C cooler than the outside air.

The second scenario was chosen because the study also showed that under these conditions thermal inversion was avoided but the humidity could be greater than the maximum acceptable value of 85% (Campen , 2009).

5.5.3.1 Cold case: 256 K equivalent sky temperature and 25 W m^{-2}soil heat flux

As explained before, this scenario can occur during cold and clear sky night in unheated greenhouses, in this situation the inside temperature is lower than outside and also relative humidity is higher than the maximum value recommended. The effect on the inside climate of different ventilator openings are a function of outside climate conditions, for this reason the parametric study simulated a combination of different ventilator opening angles and different external humidity ratios.

A set of 225 ES simulations with different external conditions and vent opening angles were made, with the aim of assessing the effects of ventilation for different external humidity ratios.

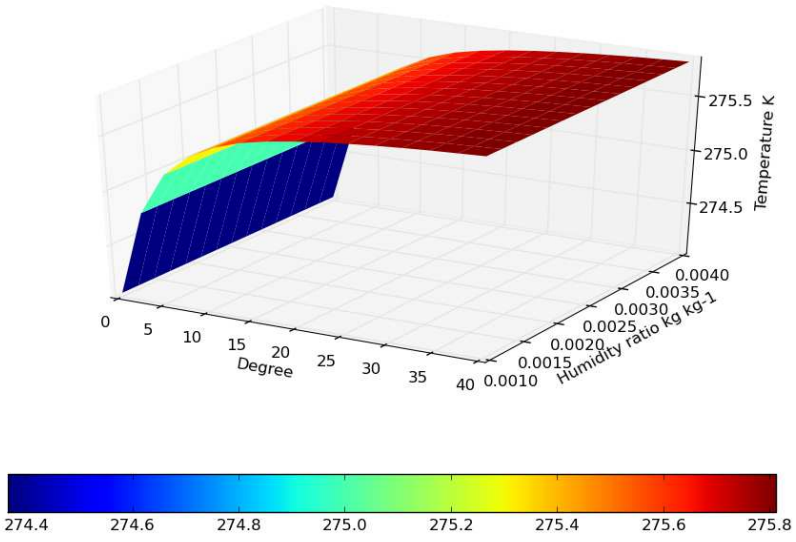

Fig. 5.3. Inside temperature for different combinations of ventilator opening angle and external humidity ratio for the case of 256 K equivalent sky temperature and 25 W m-2 SHF.

Figure 5.3 shows that thermal inversion is avoided by opening the ventilators, the greatest effects in terms of temperature gain were obtained at the first opening degrees; after 10-15 o degrees the effects on inside temperature were greatly reduced, and after 30 o the derivative dT/dx (where x is the sine of the opening angle) was close to zero. As expected, the inside temperature did not vary as a function of external humidity ratio.

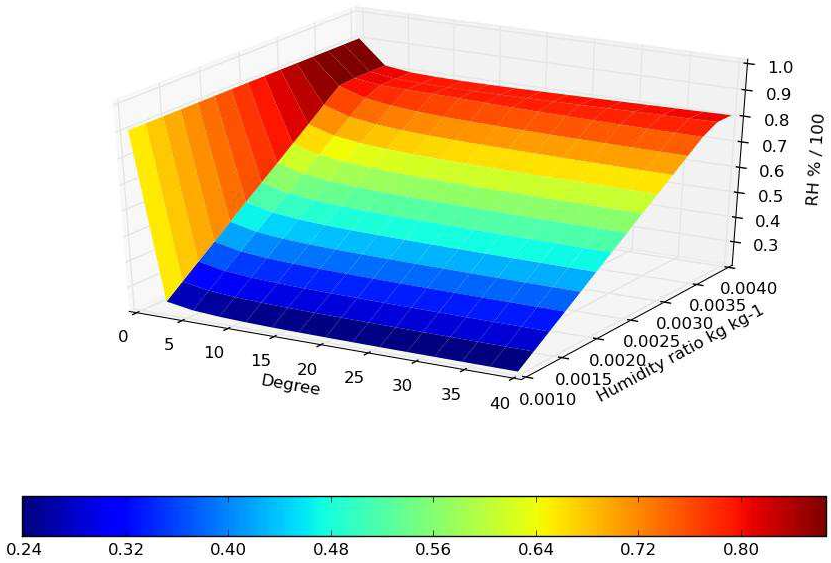

Fig. 5.4. Inside relative humidity for different combinations of ventilator opening angle and external humidity ratio for the case of 256 K equivalent sky temperature and 25 W m^{-2}SHF.

Figure 5.4 shows that the inside relative humidity was always reduced by opening the ventilator; even with an external relative humidity of 85 % (corresponding to outside values of 276 K and 0.004 humidity ratio), there was a drop from the situations of closed greenhouse, which had a relative humidity of almost 90 %. As in the case of temperature (Figure 5.3), most of the effects in terms of RH reduction were obtained within the first 10-15^{o} ventilator opening degrees. As expected, if the outside air had a high humidity, ventilation would reduce the greenhouse RH very little.

From the ES parametric study it can be concluded that in the presence of thermal inversion it is always useful to ventilate. This conclusion agrees with results reported by Baptista (2007).

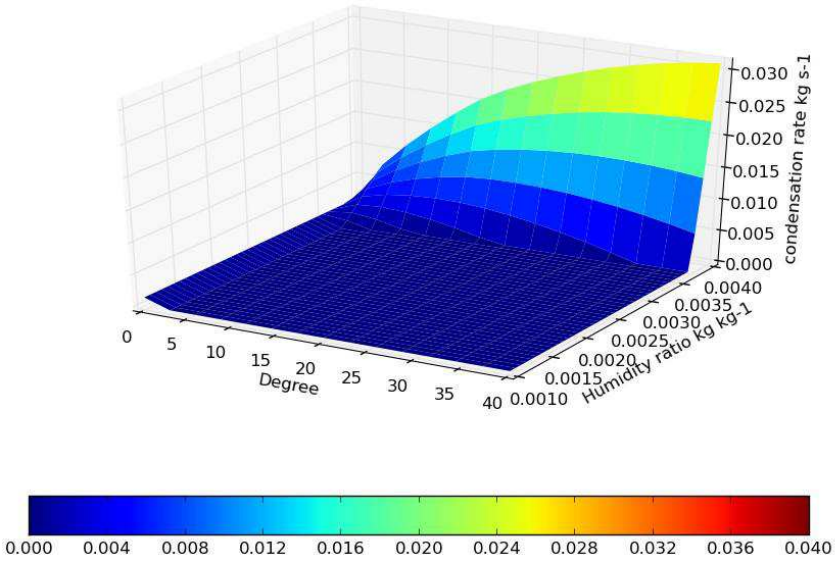

Fig. 5.5. Condensation rate for different combinations of ventilator opening angle and external humidity ratio for the case of 256 K equivalent sky temperature and 25 W m^{-2} SHF.

Figure 5.5 shows the condensation rate as a function of outside air humidity and ventilator opening angle. It can be concluded that ventilation in cases where external humidity ratio is high does not avoid condensation, indeed in some cases it greatly augments it. The presence of high external humidity and high ventilation rate combined with low cover temperature pave the way for a high condensation rate. The condensation rate can be over-predicted by ES model, because of its homogeneity assumption, which makes the ES condense all the humidity excess present in the greenhouse at each time step, this behaviour is different from the CFD model, where only the water vapour in contact to the cold surface condenses while in the ES model all the vapour condenses until the vapour pressure has decreased to the saturated vapour pressure at the condensing surface.

5.5.3.2 Intermediate case: 273 K equivalent sky temperature and 25 W m^{-2}soil heat flux

The cloud covered sky scenario presents an important difference to the clear sky case. Under covered skies thermal inversion does not occur, because the equivalent sky temperature is higher and can be similar to the outside air temperature, the difference is related to the humidity level that the greenhouse air can attain.

Situations which fall in this category are more difficult to handle, since possible gains of bringing in lower humidity air could be offset by the loss of warm air from the greenhouse and lower cover and air temperatures.

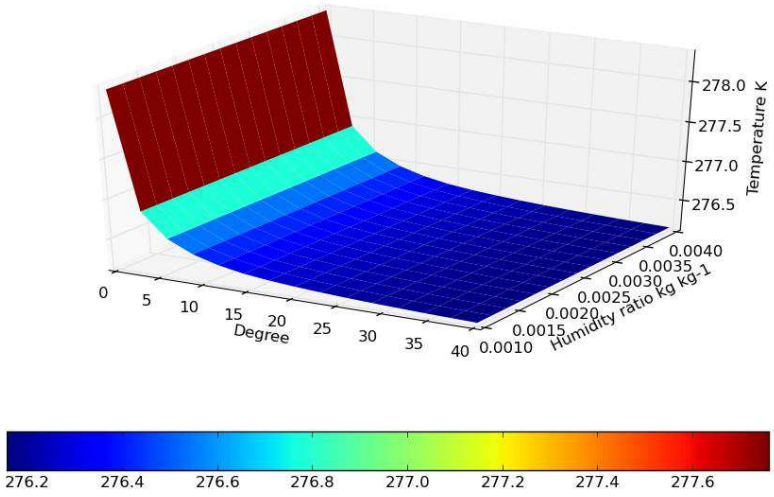

Fig. 5.6. Inside temperature for different combinations of ventilator opening angle and external humidity ratio for the case of 273 K equivalent sky temperature and 25 W m^{-2} SHF.

Figure 5.6 shows that from a point of view of heat conservation, opening the ventilator always implies a drop of temperature regardless the humidity ratio of the outside air. Moreover the air exchange with only a 5^{o} opening angle had a relevant impact on overall greenhouse temperature.

Figure 5.7 shows that in most cases relative humidity diminished when opening the vents slightly. The drawback of opening vents in this scenario is that the inside temperature is reduced, as cooler air flows into the greenhouse. As a conclusion, in term of humidity it is suggested ventilating in all cases but when outside humidity is higher than 85 %, which is the

threshold value given by Campen(2009) to avoid excessive humidity problems on the crop. With an opening angle between 10 ^{o} and 15 ^{o} in most cases RH can be reduced enough without loosing too much heat.

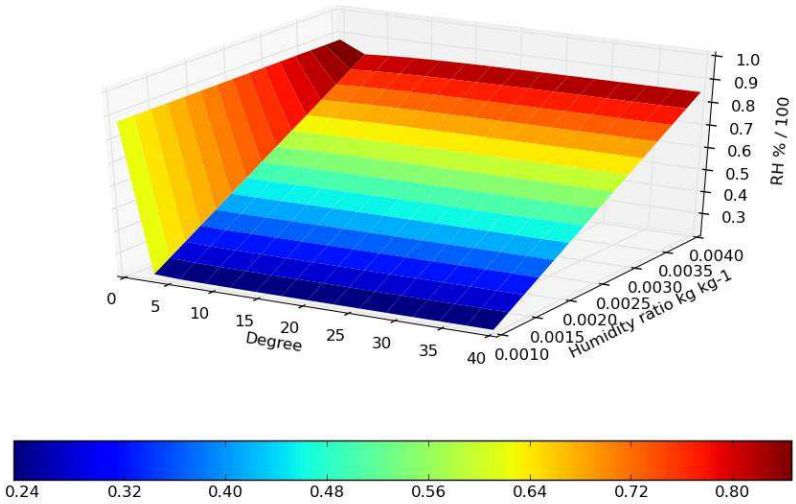

Fig. 5.7. Inside RH for different combinations of ventilator opening angle and external humidity ratio for the case of 273 K equivalent sky temperature and 25 W m^{-2} SHF.

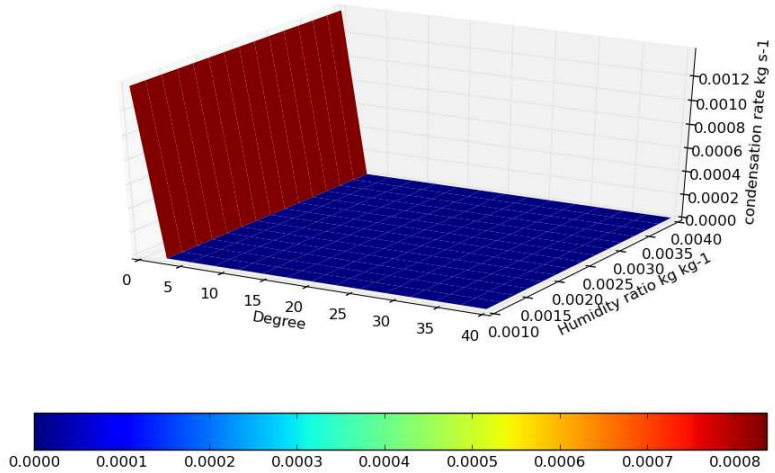

Fig. 5.8. Condensation rate for different combinations of ventilator opening angle and external humidity ratio for the case of 273 K equivalent sky temperature and 25 W m^{-2} SHF.

Regarding the condensation rate under covered skies, from Fig. 5.8 it can be seen that condensation will be avoided by opening the ventilator, this is due to the fact the humidity content of 0.004 kg kg^{-1} is below the value obtained by computing the humidity ratio at the saturation point imposed by the cover temperature.

5.6 Discussion

This paper introduces a novel way of using CD and ES models to study the greenhouse climate, the idea is that rather than being exclusive, the two models can be collaborative. In this case the collaboration was based on the provision of CFD calculated convective coefficients and ventilation rates to the ES model. The coupled ES model then has the advantage of being independent of empirical coefficients, making it more robust.

The coupling approach presented here can be strengthen by carrying out a single larger CFD parametric study , instead of two separate studies, from which both convective coefficients and the ventilation rate can be extracted. This approach requires more computational cost, but it provides a ventilation rate which takes into account the air exchange caused by the combined effects of wind and buoyancy.

This study considered a subset of all possible scenarios, as the convective coefficients applied only to an unheated greenhouse and it considered only one wind speed and direction. Nevertheless the approach is modular, and the application to heated greenhouses with all or part of the spectra of wind directions and speeds.

Nevertheless taking into account more parameters and scenarios greatly increases the number of CFD simulations required. To cope with this requirement, the reconsideration of the design of experiment techniques could be a useful approach; the aim would be to create an experimental design which can sample a high-dimensional space in a representative way with the minimum number of samples.

Classical examples of design of experiment are the central composite design (Giunta, Wojtkiewicz ,& Eldred, 2003) which requires $1+2*Num\_\mathrm{var}+2^{Num\_\mathrm{var}}$ samples or the Box-Behenken design which needs $1+4*Num\_\mathrm{var}+(Num\_\mathrm{var}-1)/2$ samples.

Validation is a fundamental part of a simulation model, but it was not included in this paper since suitable experimental data were not available, moreover it is difficult to accurately

measure greenhouse ventilation rate (three techniques are commonly used, the heat balance, the mass balance or tracer gas technique and the decay method using nitrous oxide, a full review is given by Roy et al. (2002)). A possible alternative or complementary action, can be represented by validating the CFD-ES coupled model against a stand-alone CFD model, as proposed by Mirsadeghi (2011) , the aim is to not only comparing the greenhouse variable output results but also the computational performancesThe ES model can be seen as a form of surrogated model of the CFD model (Eldred, Giunta, & Collis, 2004), which can quickly include the CFD predictions but respond on a much shorter time scale. In this perspective, the ES represents a way of making the CFD results available outside the CFD framework.

ES model can be easily used by a wider audience such as growers, indeed a website or an application can easily wrap an ES model and provide in this way quick answers to user queries.

In the future, the ES model can be enhanced by coupling it to a plant response model; in this way it will be possible to link the effects of different ventilation strategies directly to plant production outputs. This further step goes in the same direction as the one proposed by Vanthoor (2011), which presented a global design model which took into account energy, plant response and economic returns.

The CFD model did not take into account explicitly the air leakage. In CFD modelling it is difficult to consider infiltration loses, since this would require the definition of the location and geometry of the openings through which the greenhouse air could exit, information which is not usually available.

If an air leakage value of 1.34 V h^{-1} (Baille, Lopez, Bonachela, Gonzalez-Real, & Montero, 2006; López, Pérez, Montero, & Antón, 2001) would be considered for a wind speed of 2 m s^{-1}, then the air leakage corresponded to a ventilation rate of 0.04 kg $s^{-1}m^{-1}$, much lower than the ventilation rate provided by a 5º ventilator opening (0.3 kg s^{-1}) .

Based on the analysis and for the scenarios taken into account, ventilation is suggested at night under both clear and overcast sky conditions; this conclusion agrees with Baptista (2007). Moreover another advantage of night-time ventilation is that it causes a significant reduction of *Botrytis cinerea* disease appearance (Baptista,2012).

As stated earlier, only the unheated greenhouse case was studied, because the aim of this research was to study Mediterranean based greenhouses. Nevertheless according to Piscia et al. (2011), in a greenhouse with a SHF greater than 50 W m^{-2} the climate cannot be improved by ventilation, indeed the temperature was higher than outside and the relative humidity level was below the upper limit of 85 %. These results may seem controversial since it is common practise to combine heating and ventilation in Central European greenhouses or introduce

preheated external air for humidity control (Campen, 2009). This apparent discrepancy may be due to the fact that night time transpiration was taken from a previous study of an unheated greenhouse and was considered as constant. Probably the night time transpiration is higher in heated greenhouses, and so the results from the ES and CFD models may differ from the aforementioned data of Piscia et al. (2011).

5.7 Conclusions

A new approach for greenhouse climate simulation was introduced. The method was based on the coupling of an ES model with a CFD model. This technique was applied to study the effect of ventilation on greenhouse temperature, humidity and condensation.

Two CFD parametric studies were carried out in order to compute the ventilation rates and convective coefficients. The first study computed the ventilation rate for different combination of wind speed and ventilator opening angle. The results showed a strong linearity between ventilation rate and ventilator opening angle and were included in the ES model by means of a quadratic spline. The second study computed the convective coefficients for different external conditions. The CFD predictions showed that the convective coefficients depended strongly on ventilation rate.

This work analysed the effects of ventilation on greenhouse climate under two scenarios. The first represented the clear sky and the second the overcast sky combined with unheated situation (SHF of 25 W m^{-2}).

Under clear sky conditions the coupled ES model indicated that ventilation is always advisable but only a minor opening of roof ventilators was required.

Under overcast sky conditions ventilation is suggested in most cases. Only when outside air humidity is above 85% ventilation can be unnecessary.

5.8 Appendix

A. ES model equations

The energy balance of greenhouse air (Eqn. 5.4) can be written also in this way:

$$\frac{V\rho_{air}(c_{p,a}+w_{air}c_{p,w})\partial T_{air}+w_{air}h_e}{\partial t}=A_{soil}\cdot q_{conv,soil}+A_{sid\_in}q_{conv,sid}+A_{cov\_in}q_{conv,cov}+$$
$$+\Phi((c_{p,a}T_{air}+w_{air}h_w(T_{air})-(c_{p,a}T_{air\_out}+w_{air\_out}h_w(T_{air\_out})) \quad [W] \quad (A\ 5.1)$$

Where $h_w(T)=c_{p,w}T+h_e$ is water vapour enthalpy,

B. Quadratic spline

The ventilation rate values obtained by the CFD parametric study are embedded into the ES model by using the following quadratic spline.

Φ = 19.3941877273305 +15.0399995903575*BF1 -22.5664934534249*BF2 -
4.50069762381828*BF3 +9.85686151491185*BF4 -14.6458277948187*BF5
+19.1931416709916*BF6 -19.418993497707*BF7 -15.074984018779*BF8
+16.4915503604416*BF9 [kg s^{-1} m^{-1}] (B 5.2)

BF1 = max(0, $\sin(\Lambda)$ -0.258690844053802)

BF2 = max(0, 0.258690844053802 - $\sin(\Lambda)$)

BF3 = BF1 * max(0, u_{wind} -2)

BF4 = max(0, u_{wind} -2)

BF5 = max(0, 2 - u_{wind})

BF6 = BF4 * max(0, $\sin(\Lambda)$ -0.499770102643102)

BF7 = BF4 * max(0, 0.499770102643102 - $\sin(\Lambda)$)

BF8 = max(0, 0.865759839492344 - $\sin(\Lambda)$)

BF9 = BF8 * max(0, 2 - u_{wind})

5.9 References

Ansys (2012). User guide 13.0. Lebanon, NH, USA.

Baptista, F. J. F. (2007). Modelling the climate in unheated tomato greenhouses and predicting Botrytis cinerea infection. Ph.D. thesis, Univerisade de Evora, Portugal.

Baptista, F.J.,Bailey, B.J. ,& Meneses,J.F. (2012). Effect of nocturnal ventilation on the occurrence of *Botrytis cinerea* in Mediterranean unheated tomato greenhouses. Crop Protection, 32,144-149.

Beausoleil-Morrison, I.(2000). The adaptive coupling of heat and air flow modelling within dynamic wholse-building simulation. Ph.D. thesis, University of Strathclyde.

Baille, A. , Lopez, J. C., Bonachela, S. ,Gonzalez-Real, M. M.,& Montero, J.I. (2006). Agricultural and forest meteorology. 137(1), 107-118.

Boulard, T., & Wang, S. (2000). Greenhouse crop transpiration simulation from external climate conditions. Agricultural and Forest Meteorology, 100(1), 25-34.

Bournet, P., Ould Khaoua, S., & Boulard, T. (2007). Numerical prediction of the effect of vent arrangements on the ventilation and energy transfer in a multi-span glasshouse
using a bi-band radiation model. Biosystems Engineering, 98(2), 224-234.

Campen, J.B. (2009). Dehumidification of Greenhouses. Ph.D. thesis, Agricultural University of Wageningen.

De Halleux, D. (1989). Dynamic model of heat and mass transfer in greenhouses: theoretical and experimental study. PhD Thesis, Gembloux, Belgium.

Eldred, M. S., Giunta,A. A., & Collis, S. S.(2004). Second-order corrections for surrogate-based optimization with model hierarchies. In Proceedings of the 10th AIAA/ISSMO Multidisciplinary Analysis and Optimization Conference, Albany, NY,, Aug. 30–Sept. 1, 2004. AIAA Paper 2004-4457.

Giunta, A.A., Wojtkiewicz, S.F., Jr., & Eldred, M.S. (2003). Overview of Modern Design of Experiments Methods for Computational Simulations . Proceedings of the 41st AIAA Aerospace Sciences Meeting and Exhibit, Reno (USA).

Hand, J.W., & Arch, M. (2010), The ESP-r Cookbook. University of Strathclyde, Glasgow, Scotland.

Jong, T. (1990). Natural ventilation of large multi-span greenhouses. Ph.D. thesis, Agricultural University of Wageningen.

Launder, B. E., & Spalding, D. B. (1972). Lectures in Mathematical Models of Turbulence. Academic Press, London.

López, J.C., Pérez, J., Montero, J.I. and Antón (2001). Air infiltration rate of Almeria "parral type" greenhouses. Acta Horticulturae, 559 (1) , 229–232

Mirsadeghi, M. (2011). Co-simulation of building energy simulation and computational fluid dynamics for whole-building heat, air and moisture engineering. Ph.D. thesis, Technische Universiteit Eindhoven.

Negrao, C.O.R. (1995). Conflation of computational fluid dynamics and building thermal simulation. . Ph.D. thesis, University of Strathclyde.

Richards, P. J., & Hoxey, R. P. (1993). Appropriate boundary conditions for computational wind engineering models using the k-ϵ turbulence model. Journal of Wind Engineering and Industrial Aerodynamics, 46, 145-153.

Roy, J.C., Boulard, T., Kittas ,C., & Wang , S. (2002). PA—Precision Agriculture: Convective and Ventilation Transfers in Greenhouses, Part 1: the Greenhouse considered as a Perfectly Stirred Tank. Biosystems Engineering, 83(1), 1-20.

Papadakis G; Frangoudakis A; & Kyritsis, S. (1992). Mixed, forced and free convection heat transfer at the greenhouse cover. Journal of Agricultural Engineering Research, 51, 191–205.

Piscia, D., Montero, J.I., Baeza, E., & Bailey, B.J. (2011). A CFD greenhouse night-time condensation model. Biosystems Engineering, 111(2),141-154.

Stoffers J. A. (1985). Energy fluxes in screened greenhouses. Communication presented in the Agricultural Engineering Conference of Cambridge, England, unpublished.

Van Doormaal, J.P. ,& Raithby, G.D. (1984). Enhancements of the SIMPLE method for predicting incompressible fluid flows. Numerical heat transfer, 7(2), 147-163.

Vanthoor, B. (2011). A model-based greenhouse design method. Ph.D. thesis, Agricultural University of Wageningen.

Walton, G.N.,& Dols, W.S. (2005). CONTAM 2.4 user guide and program documentation. National Institute of Standards and Technology, NISTIR.

Wang, L. (2007). Coupling of multizone and CFD programs for building airflow and contaminant transport simulation. Ph.D. thesis, Purdue university.

Zhai, Z.J., & Chen, Q.Y.(2005). Performance of coupled building energy and CFD simulations. Energy and buildings, 37(4), 333-344.

Zhang, R. , Lam, K.P. , Yao, S.C. ,& Zhang, Y.(2012). Coupled EnergyPlus and Computational Fluid Dynamics Natural Ventilation Simulation. Proceedings of 5th National SimBuild Conference,Madison (USA).

6 Conclusions

6.1 Final conclusions

As stated in the introduction, the objectives of this work can be grouped into two interrelated categories. On the one hand, the research aimed to study and propose solutions to night-time greenhouse climate issues such as condensation, high humidity and low temperature. On the other, it aimed to develop and propose improvements to the simulation approaches previously used to study greenhouse climate: the CFD, ES coupling and optimization techniques.
Following the same scheme, the conclusions are presented in relation to the objectives proposed.

- **To study night–time greenhouse climate in terms of temperature, humidity and condensation in order to establish a reference situation**

In **Chapter 2** the CFD model simulated different night-time scenarios. These scenarios included different equivalent sky temperature values (256, 263, 273 and 276 K) and different soil heating powers (25, 50 and 100 W m^{-2}). The simulations showed that there was a strong correlation between roof temperature and greenhouse humidity ratio for the twelve combinations of sky temperature and SHF considered in this study. In addition, it was found that RH depended on the SHF more than on the roof temperature. The condensation rate curve was successfully modelled by a logistic function and it was observed that the greenhouse condensation rate could be represented by a single logistic curve for all combinations of the boundary conditions.

- **To study the influence of using a thermal screen in terms of temperature, humidity and condensation**

In **Chapter 3**, thermal screen solution was simulated, which is a widely used solution to low night-time temperature. Simulated and experimental results showed linear correlations between cover temperature, air temperature and air humidity, and external conditions. A comparison between CFD results obtained using a single-layer and a screened greenhouse was presented; it showed significant advantages in terms of temperature gains. The condensation rate curve for the screened greenhouse was also modelled using a logistic curve, but its parameters differed from those of the single-layer greenhouse.

- **To study the effects of the thermal radiation properties of greenhouse cover in terms of temperature, humidity and condensation**

In **Chapter 4**, the main conclusion was that for the optimal material for covering a greenhouse would reflect as much thermal radiation as possible. With such a cover, the potential improvements in terms of temperature gains and reductions in humidity would be significant.
The study highlighted that the temperature gains from using the optimal cover material (as opposed to the reference material) would increase linearly when the sky temperature decreased and would decrease when SHF decreased. The formation of condensation on the cover could be delayed by approximately 2 hours by using the optimal cover material.

- **To study the effects of nocturnal ventilation on greenhouse climate variables**

This work (**Chapter 5**) analysed the effects of ventilation on greenhouse climate under different conditions; two different scenarios were studied. The first represented a clear sky and the second an overcast sky combined with an unheated situation.
Ventilation proved useful in both of the scenarios considered. The proposed solutions are not to be taken as an imperative strategy, but rather as guidelines that could be used to orientate growers.
A CFD parametric study reported that the ventilation rate was linearly related to the sine of the opening angle of the ventilator.

- **To propose an optimization process based on ES and CFD**

A new optimization methodology for greenhouse design was proposed and tested. The new method involved three modules: the first involved optimization algorithms; the second was the ES model; and the third was the CFD model. It was shown that this methodology combines the advantages of ES models with those of CFD, offering a coupled approach to optimize greenhouse design.

- **To couple ES and CFD by exchanging ventilation and convective heat transfer coefficients**

A new approach for greenhouse climate simulation was proposed. The method is based on the coupling of the ES and a CFD model. Two CFD parametric studies were carried out in order to compute the ventilation rates and convective coefficients. The CFD results were embedded into the ES model by means of a quadratic spline (for the ventilation rate) and linear interpolation (for the convective coefficients).

6.2 General conclusion

The CFD proved to be effective and accurate in its climate predictions. Condensation was successfully included in the model and its addition made it possible to take into account a physical phenomenon that plays an important role in the characterisation of night-time climate.

An ES model was also used and it was clearly shown that it could be used in a way that complemented CFD. This approach had been widely used in building-related climate research, but it was not a method that had been explored by those researching into greenhouse climate.

One of the aims of studying greenhouse climate is to improve the energy efficiency of greenhouses or, in other words, to produce a better climate for crop growth using the same inputs.

The last task was efficiently completed using an optimization algorithm. Within this framework, **Chapter 4** proposes the combined use of two algorithms applied to an ES model. The ES model results were then passed to the CFD model. This approach offered computational savings without losing accuracy. However, further study is required to implement a correction method/feedback between the ES and CFD models. This deeper connection is needed when the optimization is applied within a more complex scenario.

The coupling between CFD and ES could also be strengthened by an interchange of information; CFD was able to provide ES with valuable and accurate information, specifically with regard to the convective coefficients and ventilation rates. This information is normally computed using semi-empirical formulas which can fail to capture the right information if conditions differ. **Chapter 5** proposes and analyses an external-static coupling.

Some of the research findings presented here could be used for greenhouse climate management; for example, the equations relating humidity to external conditions could be embedded into the climate controller. One possible focus of such a controller could be preventing the formation of excess humidity formation and reducing the rate of condensation. The latter aspect is particularly crucial in the case of traditional greenhouses, such as the multi-tunnel, whose curved roof shape favours condensation dripping.

The results of the optimization study, which indicate that the cover material should be as reflective as possible, could be used as a guideline for the future development of plastic components. These results do not, however, support the recent interest of greenhouse cover manufacturers in the use of ultra-thermic plastic film.

Finally, the study of ventilation provided useful information about controlling humidity and temperature by means of ventilation; especially in unheated situations, ventilation appears to offer advantages in the majority of situations.

6.3 Additional comments

From the point of view of simulation methodology, open-source tools such as OpenFOAM (as CFD tool), esp-r, Energyplus and Contam (as energy balance simulation tools) are gaining prestige within the building research community as useful tools for climate simulation. It would also be useful for the greenhouse research community to begin using these tools and to collaborate with those carrying out research in the building community.

This thesis focuses on ways of improving the performance of unheated plastic greenhouse covers. They are representative of most of the greenhouses used in the Mediterranean area and for this reason the solutions studied and proposed are predominantly passive and require low investment. There are also other solutions, such as mechanical ventilation and dehumidification devices, but these were not included in this study because it was considered that they were not suited to the passive greenhouse model.

6.4 Directions for future work

This thesis should contribute to the study and further development of semi-closed greenhouses. The semi-closed greenhouse approach aims to keep greenhouses as closed as possible in order to minimise heat losses. Future work should also examine CO_2 enrichment in semi-closed greenhouses and could also study ways of increasing the role of greenhouse soil in storing thermal energy during the day and releasing heat at night, particularly as the soil is the only source of energy in unheated greenhouses at night

The research presented here only focuses on night-time climate; a natural extension to this work would be to also consider the day time regime in future studies. Problems of condensation and related humidity may also occur during the early hours of the morning. When carrying out a study during the early hours of the day, the effect of crop transpiration as a function of greenhouse climate should also be included. Future CFD models should look more cloely at the role of nocturnal crop transpiration and extend this study to other crops and other conditions.

The aim of studying greenhouse climate is to improve crop conditions. In this context, linking a crop response model to an energy model should provide more information about the gains (in terms of crop growth) obtained from different energy solutions.